

**UNIVERSITY OF NINEVAH  
COLLEGE OF ELECTRONICS ENGINEERING  
COMMUNICATION ENGINEERING DEPARTMENT**



**Investigation of the Performance of the Next  
Generations of Wireless Communications over  
mmWave Channels**

By

**Reyam Hafidh Ali-Al Ashou**

**M.Sc. Thesis**

**In**

**Communication Engineering**

Supervised by

**Dr. Mahmood A. Al Zubaidy & Dr. Mohamad A. Al Habbar**

---

**2021 A.D.**

**1442 A.H.**

# **Investigation of the Performance of the Next Generations of Wireless Communications over mmWave Channels**

Thesis Submitted

By

**Reyam Hafidh Ali-Al Ashou**

To

The Council of the College of Electronic Engineering

Ninevah University

As a Partial Fulfillment of the Requirements

For the Degree of Master of Science

In

Communication Engineering

Supervised by

**Dr. Mahmood A. Al Zubaidy & Dr. Mohamad A. Al Habbar**

---

2021 A.D.

1442 A.H.

بِسْمِ اللَّهِ الرَّحْمَنِ الرَّحِيمِ

نَرْفَعُ دَرَجَاتٍ مَّنْ نَّشَاءُ وَفَوْقَ كُلِّ ذِي  
عِلْمٍ عَلِيمٌ

صَدَقَ اللَّهُ الْعَظِيمُ

سورة يوسف

الآية (76)

### **Supervisor's Certification**

I certify that the dissertation entitled (**Investigation of the Performance of the Next Generations of Wireless Communications over mmWave Channels**) was prepared by **Reyam Hafidh Ali Al Ashou** under my supervision at the Department of Communication Engineering, University of Ninevah, as a partial requirement for the Master of Science Degree in Communication Engineering.

**Signature:**

**Name: Dr. Mahmood A. Al Zubaidy & Dr. Mohamad A. Al Habbar**

Department of Communication Engineering

**Date:    /    /2021**

### **Linguistic Advisor Certification**

I certify that the linguistic evaluation of this thesis entitled "**Investigation of the Performance of the Next Generations of Wireless Communications over mmWave Channels**" was carried out by me and it is accepted linguistically and in expression.

**Signature:**

**Name:**

**Date:    /    /2021**

### **Post-Graduate Committee Certification**

According to the recommendations presented by the supervisor of this dissertation and the linguistic reviewer, I nominate this dissertation to be forwarded to discussion.

**Signature:**

**Name: Assistant Prof. Dr. Younis M. Abbosh**

### **Department Head Certification**

I certify that this dissertation was carried out in the Department of Communication Engineering. I nominate it to be forwarded to discussion.

**Signature:**

**Name: Assistant Prof Dr. Younis M. Abbosh**

**Date:    /    /2021**

## ***Committee Certification***

We the examining committee, certify that we have read this dissertation entitled **(Investigation of the Performance of the Next Generations of Wireless Communications over mmWave)** and have examined the postgraduate student **(Reyam Hafidh Ali)** in its contents and that in our opinion; it meets the standards of a dissertation for the degree of Master of Science in Communication Engineering.

Signature:

Name:

Head of committee

**Date:     /     /2021**

Signature:

Name:

Member

**Date:     /     /2021**

Signature:

Name:

Member

**Date:     /     /2021**

Signature:

Name:

Member and Supervisor

**Date:     /     /2021**

The college council, in its ..... meeting on     /     /2021, has decided to award the degree of Master of Science in Communication Engineering to the candidate.

Signature:

Name:

Dean of the College

**Date:     /     /2021**

Signature:

Name:

Council registrar

**Date:     /     /2021**

**Publications: -**

Some of the important results obtained in this work have appeared in the following publication: -

- [1] Reyam H. Ali, Mahmood A. Mahmood, and Mohamad A. Ahmed, "On the Performance of Cooperative Relaying with Maximum-Ratio Combination (MRC) for mmWave Systems," IOP Conf. Ser. Mater. Sci. Eng., vol. 1152, no. 1, p. 012007, 2021, doi: 10.1088/1757-899x/1152/1/012007.

## **ACKNOWLEDGEMENTS**

"Praise be to ALLAH, Lord of the whole creation"

I would like to express my sincere gratitude and thanks to my supervisor, **Dr. Mahmood A. Al Zubaidy & Dr. Mohamad A. Al Habbar** for their continuous guidance, helpful suggestions and constant encouragement throughout this work.

Thanks are due to the Dean of the Electronics Engineering College for his valuable assistance. My appreciation is extended to the Head and all members of the communication Engineering Department for their support and assistance.

Finally, I would like to extend my sincere appreciation to all my family for their encouragement, support and patience throughout the duration of my graduate study.

**Researcher**

**Reyam Hafidh**

**2021**

## **Abstract**

Due to extremely high data rate demands and microwave band spectrum scarcity, the millimeter wave (mmWave) band is a possible alternative for meeting high data rate demands in wireless networks. The availability of enormous bandwidth is the primary benefit of moving to the mmWave frequency. However, because of the propagation losses introduced at high frequencies, mmWave networks are known to have a short coverage reach. To address the transmission issues, proposed solutions include the use of large arrays with greater directivity, the use of smaller cells, and the use of cooperative relaying networks to extend the mmWave link and avoid shadowing areas.

In this dissertation, cognitive radio with two-way relaying networks (TWRN) is considered and proposed over mmWave channels for the next generation of wireless communication. Two types of TWRNs are investigated which are relaying via amplify-and-forward (AF) and decode-and-forward (DF) techniques.

Millimeter-wave (mmWave) channels with different frequency bands are investigated and characterized, in which the data transmitted from a source to destination via this cooperative communication system either by using AF or DF relays to enhance the diversity gain and to overcome the path-loss existed in the band under consideration.

Binary phase-shift keying (BPSK) modulation schemes are utilized to represent the transmitted data in this project over this channel and in the presence of an additive white Gaussian channel (AWGN).

Several simulations scenarios are taken into account in this research, which is achieved by using Matlab programming, where the bit-error rates (BER)'s and the system throughput against different values of signal-to-noise ratio (SNR) are obtained for the sake of comparison

between these two types.

The results show outperforming of AF relaying over DF relaying in the error probability performance metric while relaying by using the DF technique has better throughput than the AF relay.

## TABLE OF CONTENTS

Subject	Page
Acknowledgments	I
Abstract	II
Table of Contents	IV
List of Figures	VI
List of Tables	IX
List of abbreviations	X
<b>Chapter One – Introduction</b>	
<b>1.1. Overview</b>	1
<b>1.2. Literature Review</b>	5
<b>1.3. Research objectives</b>	10
<b>1.4. Thesis Layout</b>	11
<b>Chapter Two – Theory of cooperative communication systems over mm-wave channels</b>	
<b>2.1. Mm wave Spectrum.</b>	12
<b>2.2. Millimeter Wave Propagation Characteristics.</b>	15
<b>2.2.1. Free Space Path Loss.</b>	16
<b>2.2.1.1. Large-Scale Path Loss Models.</b>	18
<b>2.2.2. Environmental Effects.</b>	23
<b>2.3. Cooperative Communication.</b>	24
<b>2.3.1. Relaying Protocols.</b>	26
<b>2.3.1.1. Amplify and Forward (AF) Protocol.</b>	26
<b>2.3.1.2. Decode and Forward (DF) Protocol.</b>	27
<b>2.4. Dual-hop Relay Network.</b>	28
<b>2.4.1. Dual-hop AF Relay Assisted mmWave Channel.</b>	29
<b>2.4.2. Dual-hop DF Relay Assisted mmWave Channel.</b>	32
<b>2.5. Dual-hop Two Parallel Relays Network</b>	33

2.5.1. Dual-hop Parallel AF Relays Assisted mmWave Channel.	34
2.5.2. Dual-hop Parallel DF Relays Assisted mmWave Channel.	36
2.6. Characterization of Millimeter Wave Channels.	38
2.6.1. Indoor mmWave Channel Characteristic.	38
2.6.2. Outdoor mmWave Channel Characteristic	40
<b>Chapter Three – Modeling of Indoor mmWave Channels</b>	
3.1. Introduction.	41
3.2. Comparison of the simulation results of dual-hop AF and DF relays systems over mm-wave frequencies (28 GHz, 38 GHz, 60 GHz, 73 GHz).	43
3.3. Comparison of the simulation results of dual-hop systems using two parallel AF and DF relays over mm-wave frequencies (28 GHz, 38 GHz, 60 GHz, 73 GHz).	51
3.4. Comparison of the simulation results for the dual-hop systems that are using one and two parallel AF and DF relay over 28 GHz.	60
<b>Chapter Four – Modeling of outdoor mmWave Channels</b>	
4.1. Introduction.	62
4.2. Comparison of the simulation results of dual-hop AF and DF relay systems over mm-wave frequencies (28 GHz, 38 GHz, 73 GHz).	63
4.3. Comparison of the simulation results of dual-hop systems using two parallel AF and DF relays over mm-wave frequencies (28 GHz, 38 GHz, 73 GHz).	75
4.4. Comparison of the simulation results for the dual-hop systems that are using one and two parallel AF and DF relay over 28 GHz.	84

<b>Chapter Five – Conclusions and Future Work</b>	
<b>5.1. Conclusions.</b>	86
<b>5.2. Future Work.</b>	87
<b>REFERENCES</b>	
References	88- 98

### **LIST OF FIGURES**

<b>Figure</b>	<b>Title</b>	<b>Page</b>
<b>(2.1)</b>	The electromagnetic spectrum.	12
<b>(2.2)</b>	Millimeter-wave sub-bands and regulation.	13
<b>(2.3)</b>	Frequency bands proposed by the ITU at WRC–2015.	14
<b>(2.4)</b>	MmWave propagation characteristics.	15
<b>(2.5)</b>	Received power at mmWave frequencies, when $P_t=10$ dBm and the antenna gain is 10 dBi.	17
<b>(2.6)</b>	Free space loss at mmWave frequencies.	17
<b>(2.7)</b>	Models of path loss for mmWaves.	19
<b>(2.8)</b>	Specific attenuation curves of O <sub>2</sub> , H <sub>2</sub> O and rain at sea level. The term $\rho$ refers to the density of H <sub>2</sub> O in grams per meter <sup>3</sup> .	23
<b>(2.9)</b>	Basic cooperative relay network.	25
<b>(2.10)</b>	Amplify and forward method.	27
<b>(2.11)</b>	Decode and forward method.	27
<b>(2.12)</b>	Basic structure of a cooperative relay network with two phases.	28
<b>(2.13)</b>	mmWave channel assisted with one AF relay.	29
<b>(2.14)</b>	mmWave channel assisted with one DF relay.	32
<b>(2.15)</b>	mmWave channel assisted with two AF relays.	36

<b>(2.16)</b>	mmWave channel assisted with two DF relays.	37
<b>(3.1)</b>	The proposed model for the dual-hop network.	42
<b>(3.2)</b>	BER vs. SNR for cooperative relaying for mmWaves using one AF and DF relays over 28 GHz in the presence of the direct path at distance ( $r_{SD}$ )10 m.	44
<b>(3.3)</b>	BER vs. SNR for cooperative relaying for mmWaves using one AF and DF relays over 38 GHz in the presence of the direct path at distance ( $r_{SD}$ )10 m.	45
<b>(3.4)</b>	BER vs. SNR for cooperative relaying for mmWaves using one AF and DF relays over 60 GHz in the presence of the direct path at distance ( $r_{SD}$ )10 m.	46
<b>(3.5)</b>	BER vs. SNR for cooperative relaying for mmWaves using one AF and DF relays over 73 GHz in the presence of the direct path at a distance ( $r_{SD}$ )10 m.	47
<b>(3.6)</b>	BER vs SNR for AF relay with a direct path over different frequencies at a distance of 10 m.	48
<b>(3.7)</b>	BER vs SNR for DF relay with a direct path over different frequencies at a distance of 10 m.	49
<b>(3.8)</b>	BER vs. SNR for cooperative relaying for mmWaves using one AF and DF relays over 28 and 73 GHz in the presence of the direct path.	51
<b>(3.9)</b>	BER vs SNR for cooperative relaying for mmWaves using two AF and DF relays in parallel with the direct path over 28 GHz frequency at a distance ( $r_{SD}$ )10 m.	53
<b>(3.10)</b>	BER vs. SNR for cooperative relaying for mmWaves using two AF and DF relays in parallel with the direct path over 38 GHz frequency at distance ( $r_{SD}$ )10 m.	54
<b>(3.11)</b>	BER vs. SNR for cooperative relaying for mmWaves using two AF and DF relays in parallel with the direct path over 60 GHz frequency at a distance ( $r_{SD}$ )10 m.	55
<b>(3.12)</b>	BER vs SNR for cooperative relaying for mmWaves using two AF and DF relays in parallel with the direct path over 73 GHz frequency at a distance ( $r_{SD}$ )10 m.	56
<b>(3.13)</b>	BER vs. SNR for two AF relays with direct path over different frequencies at distance 10 m.	57

(3.14)	BER vs. SNR for two DF relays with direct path over different frequencies at distance 10 m.	58
(3.15)	BER vs. SNR for cooperative relaying for mmWaves using two AF and DF relays with the direct path over 28 and 73 GHz at distance 10 m.	59
(3.16)	BER vs. SNR for cooperative relaying for mmWaves using one and two parallel AF and DF relays over 28 GHz in the presence of the direct path at a distance 10 m.	61
(4.1)	BER vs. SNR for cooperative relaying for mmWaves using one AF and DF relays over 28 GHz in the presence of the direct path at a distance ( $r_{SD}$ )200 m.	64
(4.2)	BER vs. SNR for cooperative relaying for mmWaves using one AF and DF relays over 38 GHz in the presence of the direct path at a distance ( $r_{SD}$ )200 m.	65
(4.3)	BER vs. SNR for cooperative relaying for mmWaves using one AF and DF relays over 73 GHz in the presence of the direct path at a distance ( $r_{SD}$ )200 m.	67
(4.4)	BER vs. SNR for AF relay with a direct path over different frequencies at a distance of 200 m.	68
(4.5)	BER vs. SNR for DF relay with a direct path over different frequencies at a distance of 200 m.	69
(4.6)	BER vs SNR for the direct path without relay over different frequencies at a distance of 200 m.	70
(4.7)	BER vs SNR for the two cooperative relaying systems for mm Waves using one AF and DF relays over 28 at a distance 100 m and 200 m.	71
(4.8)	BER vs SNR for cooperative relaying for mmWaves using one AF and DF relays over 28 and 73 GHz at a distance 200 and 100 m, respectively.	72
(4.9)	Channel capacity of cooperative diversity protocols at 28 GHz.	74
(4.10)	Comparison of channel capacity of one AF, one DF relay, and direct path over mm-wave frequencies 28 GHz and 73 GHz.	75

(4.11)	BER vs. SNR for cooperative relaying for mmWaves using two AF and DF relays in parallel with the direct path over 28 GHz frequency at a distance 200 m.	77
(4.12)	BER vs. SNR for cooperative relaying for mmWaves using two AF and DF relays in parallel with the direct path over 38 GHz frequency at a distance 200 m.	78
(4.13)	BER vs. SNR for cooperative relaying for mmWaves using two AF and DF relays in parallel with the direct path over 73 GHz frequency at a distance 200 m.	79
(4.14)	BER vs SNR for two AF relay with a direct path over different frequencies at a distance of 200 m.	80
(4.15)	BER vs SNR for two DF relay with a direct path over different frequencies at a distance of 200 m.	81
(4.16)	BER vs. SNR for cooperative relaying for mmWaves using two AF and DF relays with the direct path over 28 and 73 GHz at a distance 200 m.	82
(4.17)	BER vs SNR for cooperative relaying for mm Waves using two AF and DF relays with the direct path over distance ( $r_{SD}$ ) 100 m and 200m.	83
(4.18)	BER vs. SNR for cooperative relaying for mmWaves using one and two parallel AF and DF relays over 28 GHz in the presence of the direct path at a distance 200 m.	85

## LIST OF TABLES

Table	Title	Page
(2.1)	Path loss levels at microwave, WLAN, and mmWave frequencies.	41
(2.2)	Summarized the path loss exponent ( $n$ ) and standard deviations ( $\sigma$ ) of the shadowing factor ( $X_\sigma$ ) for the frequencies 28 GHz, 38 GHz and 60 GHz at $d_0 = 5m$ .	45

(2.3)	Summarized the path loss exponent ( $n$ ) and standard deviations ( $\sigma$ ) of the shadowing factor ( $X_\sigma$ ) for the frequencies 28 GHz, 38 GHz, 60 GHz, and 73GHz at $d_0 = 1\text{m}$ .	49
-------	--	----

### LIST OF ABBREVIATIONS

Abbreviation	Name
<b>1G</b>	1st generation
<b>2D</b>	Two Dimensional
<b>2G</b>	2nd generation
<b>3D</b>	Three Dimensional
<b>3G</b>	3rd generation
<b>4G</b>	4th generation
<b>5G</b>	5th generation
<b>6G</b>	6th generation
<b>AF</b>	Amplify and Forward
<b>AWGN</b>	Additive White Gaussian Noise
<b>AoA</b>	Angle of Arrival
<b>BER</b>	Bit Error Rate
<b>BPSK</b>	Binary Phase Shift Keying
<b>BS</b>	Base Station
<b>CF</b>	Compress and Forward
<b>CDMA</b>	Code Division Multiple Access
<b>CRAN</b>	Cloud Radio Access Networks
<b>CR</b>	Continuous Route
<b>CRC</b>	Cyclic Redundancy Rheck
<b>CSI</b>	channel state information

<b>CI</b>	Close-In
<b>DOA</b>	Direction of Arrival
<b>DBPSK</b>	Differential Phase Shift Keying
<b>D2D</b>	Device to Device
<b>DF</b>	Decode and Forward
<b>DAF</b>	Decode Amplify and Forward
<b>EDGE</b>	Enhanced Data rates for GSM Evolution
<b>FDMA</b>	Frequency Division Multiple Access
<b>FD</b>	Full Duplex
<b>FSPL</b>	Free Space Path Loss
<b>FI</b>	Floating Intercept
<b>GSM</b>	Global System for Mobile
<b>GPRS</b>	General Packet Radio Service
<b>GPS</b>	Global Positioning System
<b>HSDPA</b>	High Speed Downlink Packet Access
<b>HSUPA</b>	High Speed Uplink Packet Access
<b>LOS</b>	Line Of Sight
<b>MMS</b>	Multimedia Messages
<b>MIMO</b>	Multiple Input Multiple Output
<b>mmWave</b>	Millimeter Wave
<b>MS</b>	Mobile Station
<b>MRC</b>	Maximum Ratio Combining
<b>ML</b>	Maximal Likelihood
<b>NLOS</b>	Non Line Of Sight
<b>OP</b>	Outage Probability
<b>OFDMA</b>	Orthogonal Frequency Division Multiple Access
<b>PDA<sub>s</sub></b>	Personal Digital Assistants
<b>PAN</b>	Personal Area Network
<b>P2P</b>	Point to Point

<b>PLE</b>	Path Loss Exponent
<b>QoS</b>	Quality of Service
<b>QPSK</b>	Quadrature Phase Shift Keying
<b>RATs</b>	Radio Access Technologies
<b>RHO</b>	Relay assisted Handover
<b>SISO</b>	Single Input Single Output
<b>SNR</b>	Signal to Noise Ratio
<b>SC</b>	Selection Combining
<b>TDMA</b>	Time Division Multiple Access
<b>UHF</b>	Ultra High Frequency
<b>WAP</b>	Wireless Application Protocol
<b>WLAN</b>	Wireless Local Area Network
<b>WPAN</b>	Wireless Personal Area Networks
<b>WiGig</b>	Wireless Gigabit
<b>ZB</b>	Zettabytes

# Chapter One

## Introduction

### 1.1 Overview

Wireless technologies have experienced preternatural growth. There are many systems in which wireless communication is applicable. Radio and television broadcasting and satellite communication are perhaps some of the earliest successful typical applications[1]. It also encompasses mobile, cellular telephones, Personal Digital Assistants (PDAs), and wireless networking [2].

Nearly every decade, mobile and wireless communications systems witness a new generation [3]. Each generation has some standards, capacities, techniques, and new features which differentiate it from previous generations. Due to these new features, the number of mobile phone subscribers is increasing day by day. Surveys have shown that a new wireless subscriber signs up every 2.5 seconds [4]. However, the recent interest in wireless communication is perhaps inspired mainly by establishing first-generation (1G) cellular phones [1].

The 1st generation (1G) wireless communications systems were introduced in the 1980s. These early systems were characterized by the analog transmission of speech signals, Frequency-Division Multiple Access multiplexing(FDMA) [5], and allowing for communication data rates of 2.4 kbps. However, in addition to their lack of support for data services, such systems presented quite a few disadvantages, including poor battery life, poor voice quality, limited capacity, and poor security [6].

Therefore, the 2nd generation (2G) wireless telecommunication technology was introduced in the late 1980s, and they upgraded to digital

technologies [7].

In comparison to 1st generation systems, the 2nd generation systems employ digital multiple access technologies, including TDMA (time division multiple access) and CDMA (code division multiple access) [4].

Not only have second-generation networks marked the transition from the analog to the digital age of mobile phones, but data services including text and image messaging have also been added [8].

Global System for Mobile Communications (GSM) has been the most successful 2G system, operate at frequency bands include 900 and 1800 MHz. The systems run with a bandwidth of 200 kHz channel with data rates up to 9.6 kbps [6].

General packet radio service (GPRS), also referred to as 2.5G networks, expands the 2G network to launch packet-based services with increased data rates. GPRS supports data rates ranging from 56 Kbps to 115 Kbps and offers services such as Multimedia Messages (MMS), online networking services such as e-mail, and wireless application protocol access (WAP) [7].

Enhanced Data rates for GSM Evolution (EDGE), also referred to as 2.75 G, are evolving technology for the GPRS network to enhance data rates by introducing 8PSK encoding. EDGE can support data rates that reach up to 236.8 Kbps are accomplished by using more advanced coding techniques (8PSK) within current GSM timeslots [9].

The 3rd generation systems (3G) were standardized around the year 2000 [1]; these systems are designed to transmit data at a high rate of speed [8]. The 3G technologies employ TDMA and CDMA to provide more advanced services to users, including video calls, mobile TV, a global positioning system (GPS), wide-related wireless voice telephony, Wireless

Local Area Network(WLAN), Bluetooth [2].

The third-generation evolved into several enhanced technologies such as HSDPA (High-speed downlink packet access) and HSUPA (High-Speed Uplink Packet Access) [9].

Despite the significant advances in data rates from 1G to 3G and beyond, there remained a need for higher transfer speeds. Therefore, the 4th generation (4G) systems emerged in 2010. The signal processing technology in 4G as orthogonal frequency-division multiple access (OFDMA) [10]. The main features of these systems are seamless access, quality of service, high data rates and capacity, and have interoperability with the existing wireless standards [11].

Smartphones and tablets have increased in popularity over the previous several years as apps and services multiplied, creating a staggering increase in mobile data traffic. It is expected by 2030, the total mobile data traffic will reach five zettabytes (ZB) per month, and the individual data rates would exceed 100 Gbps [12]. This growth puts a lot of pressure on the 4G network. It causes increases latency, signal interference, and reduction in data rates, hence the race to develop new technologies to build the 5th generation (5G) wireless systems to overcome these challenges [13].

5th generation wireless systems or mobile networks is a concept that refers to the next big step of mobile telecommunications standards after the existing 4G standard, and it will be available after 2020[14]. The main requirements of 5G would be to increase network capacity while also increasing coverage at a lower cost, support more users, low power consumption, improved data transmission rates reach to 1 Gbps for mobility users and 10 Gbps for static users, low-cost devices, and also can achieve lower latency about 1ms [15]. The key enabling technologies for 5G to fulfil

such requirements, including solutions based on new radio access technologies (RATs) such as massive multiple-input multiple-output (MIMO) systems, full-duplex communications, Small-cells network densification, beamforming, cloud radio access networks (CRAN), and millimeter-wave (mmWave) frequency band [6].

Due to the scarcity of spectrum in traditional microwave bands, millimeter-wave (mm-Wave) bands have garnered considerable interest as a potential additional spectrum band for 5G and 6G cellular networks[16]. The millimeter-wave band is classified as the portion of the electromagnetic spectrum ranging from 30 GHz to 300 GHz corresponding to wavelengths of 10 mm to 1 mm[17]. A mmWave communication system can support multiple gigahertz of bandwidth to enhance the capacity/data rate and can be used for mobile cellular access, indoor wireless communications, or outdoor communications such as wireless mesh networks [18].

Mm-wave frequencies required new antenna architecture concepts for the base station (BS) and mobile station (MS) systems. To achieve an effective beam-steerable phased array antenna, which is a critical component of 5G cellular networks[19]. Due to the short wavelength of mmWaves, mm-wave antennas may be rendered smaller than those used for traditional cellular frequency waves, so this allows the use of a huge number of antenna elements to be packed into small form factors and also enables sharp beamforming or massive MIMO technology [20].

The mmWave spectrum is used predominantly for military applications, short-range wireless personal area networks (WPANs), satellite communications, backhaul communications, and wireless local area networks (WLANs). Other frequency bands, including 28 GHz, 38 GHz, and 72 GHz, offer lower attenuation and are therefore more suited for long-range mobile communications. Furthermore, the recent deployment of combined

analog and digital components in a single chip will allow for the production of cost-effective mmWave equipment [21].

However, to fully exploit the benefits of mm-Wave, it is essentially better to understand the propagation channel characteristics in these bands.

## **1.2 Literature Review**

In 1896, the wireless technology revolution launched when Guglielmo Marconi demonstrated the propagation of a signal through free space without using a physical medium between the transmitter and receiver. Numerous wireless applications have been established as a result of the success of that experiment [22].

Since then, wireless innovations have developed at a breakneck rate. However, interest in wireless communication may have been sparked primarily by introducing first-generation (1G) cellular phones in the early 1980s [23].

Even though mmWaves may represent the available technologies for 5G networks, it is critical to recognize their unique characteristics and conduct adequate analysis to develop a system that incorporates such technologies correctly.

Radoslaw Piesiewicz, et al. in 2005 provided refractive index and absorption coefficient measurements for common building materials and used Fresnel's equations to calculate reflection in order to model the propagation channel accurately for future indoor THz communication systems, including NLOS scenarios [24].

Suiyan Geng, et al. in 2009 analyzed the statistical parameters(number

of paths, the path loss, and the shadowing) of the multipath channels based on 60-GHz propagation channel measurements that are performed in various indoor environments for continuous-route (CR) and direction-of-arrival (DOA) measurement campaigns [25].

V. K. Sakarellos, et al., in 2009, proposed the optimal positioning of radio relays in a two-hop format, using physical prediction models for the overall outage probability. The study included both transparent and regenerative radio relays operating at frequencies greater than 10 GHz and meeting the line-of-sight requirement [26].

Eric Torkildson, et al. in 2010 that propagation geometry at 60 GHz differs significantly from that at lower carrier frequencies. They modeled the space-time channel by a small number of rays so that ray tracing becomes a very effective tool. In addition, they found that can get data rate reaches 10 Gbps on a 1 GHz channel by using spatial multiplexing for indoor environments [27].

In 2011, Eric Torkildson, et al. proposed a MIMO architecture for millimeter-wave carrier frequencies (60 GHz) that use arrays of subarrays to provide spatial multiplexing gains and directivity in an indoor environment [28].

Salam Akoum, et al. in 2012 studied the probability of the coverage and capacity of mmWave cellular systems and showed that the coverage in mmWave systems can rival or even exceed coverage in microwave systems due to the larger bandwidths at mmWave frequencies [29].

In 2013, Theodore S. Rappaport, et al. performed an outage study in New York at 28GHz and in Austin at 38GHz, demonstrating that consistent coverage can be achieved with a distance of 200 meters between the transmitter and the receiver [8].

In 2014, Mustafa Riza Akdeniz, et al. derived comprehensive spatial statistical models of channels operating at 28 GHz and 73 GHz in New York, USA. The channel parameters consist of angular dispersal, number of spatial clusters, outage, and loss of direction. It was discovered that powerful signals might be recognized 100-200 m from possible sites for cells even in NLOS environments. It is possible to provide spatial multiplexing and variance at several Sites of multiple path clusters obtained [30].

Esma Turgut and M. Cenk Gursoy in 2015 studied the energy efficiency of relay-assisted downlink Millimeter-Wave cellular networks by integrating the distinguishing features of Millimeter-Wave communication such as a variety of path loss laws for line-of-sight (LOS) and non-line-of-sight (NLOS) connections into energy efficiency study. Additionally, they demonstrated that wave cellular networks use directional antennas to make them more energy-efficient than microwave Wave cellular networks.

In 2016, Hatem Abbas and Khairi Hamdi proposed Amplify and Forward (AF) full-duplex relays (FD) in mm-wave connections between cells. They updated the sparsity-based algorithm to create hybrid (analog/digital) beamforming and use it at the source, destination, and FD relay to address outside mmWave propagation losses [31].

In 2017, Sungoh Kwon and Joerg Widmer introduced an algorithm of two-hop relay selection for mmWave communications without a direct path. By using geometric analysis, they analyzed the relay blockage probability. They showed that the probability of taking an indirect path is dependent on both the position of relay nodes and the density of obstacles [32].

In 2017, Won-Ik Kim, et al. examined the dynamics of the mmWave channel by simulation experiments based on two blocking scenarios. They then proposed a Relay-assisted Handover (RHO) scheme, which reduces link

disruption due to blockage events even in environments where various blockage types coexist [33].

In 2018, Yan Yan, et al. proposed algorithms for path selection to enable mmWave backhaul networks by identifying high-throughput paths employing amplify and forward relays. They also demonstrated that the pathways generated by these algorithms have a very high probability of being interference-free and presenting an extended technique for handling the rare situations of interference [34].

In 2018, Khagendra Belbase, et al. investigated the potential benefits of establishing two way amplify and forward relays to facilitate bidirectional data flow between two millimeter-wave network end users. They used a homogeneous Poisson point process to represent the locations of prospective relay nodes. Thus, a relay is chosen to optimize the minimum of the end-to-end signal-to-noise ratios of the two users [35].

In 2019, Khagendra Belbase, et al. analyzed the capacity, coverage, and symbol error rates of millimeter-wave multi-hop decode-and-forward (DF) relays in interference-limited and noise-limited scenarios using three types of digital modulation: BPSK (binary phase-shift keying), DBPSK (differential phase-shift keying), and QAM (square-quadrature amplitude modulation), they demonstrated that by utilizing multi-hop relaying, considerable coverage might be achieved in blockage-prone mmWave networks [36].

In 2019, Yuchen Liu and Douglas M. Blough studied blockage effects in roadside relay aided mm-wave backhaul networks and derived blockage probabilities for different blocking types and showed that the change to near-BS topology angles results in a considerable improvement of blockage

robustness [37].

In 2020, Mohamed Ibrahim, et al. suggested a new routing technique called Nth Best Relay Routing Technique to improve the spectral efficiency of mmWave networks. They derived a closed-form for the distance distribution from the destination to the nth best relay using a stochastic framework for modeling LOS relays. The results indicate that the highest spectral efficiency is reached at specific SNR thresholds and varies depending on the best relays selected [38].

In 2020, Durgesh Singh, et al. studied the relay selection problem in mmWave device-to-device (D2D) communication in the presence of a dynamic barrier using a finite horizon partially observable Markov decision process (POMDP) framework[39].

In 2021, Meng Han, et al. evaluated the mixed-structure decode-and-forward (DF) relay system in mmWave massive multiple-input multiple-output (MIMO) systems, and they suggested an efficient sorted serial design method for designing each node's analog beamforming to mitigate inter-user and inner user interference and increasing the number of users in the system [40].

### **1.3 Research objectives**

The main objectives of this research are:

1. Study the need for relays (repeaters) such amplify-and-forward (AF) and decode-and-forward (DF) to assist the mmWave channel and to compensate for attenuation and corruption of signals between the transmitter and receiver.
2. Study and investigate the effects of constraints associated with this new uncongested spectrum as the high attenuation due to path losses of the waves of the designed system, and how to tackle these effects to increase the capacity of the network and reduce the bit-error-rate along with different signal-to-noise ratio and to keep an optimum Quality of Service (QoS).
3. Designing a digital communication system in which BPSK symbols pass-through this mmWave channel to obtain this system's error probability and channel capacity by simulation.
4. Design an equalizer and detector to recover the transmitted signals after affected by the channels.
5. To model the mmWave channels and find the optimum band and the specific frequency to be used in the mmWave technology for indoor/outdoor scenarios and the antenna technology used is single-input single-output (SISO).
6. It uses Monte-Carlo simulations via MATLAB programming to simulate the designed systems, protocols, and techniques associated with mmWave channel modeling.

## **1.4 Thesis Layout**

This thesis includes the following chapters:

Chapter two illustrating the theoretical background of cooperative communication systems over mm-wave channels. And also introduces the spectrum and propagation characteristics of the millimeter-wave technology.

Chapter three presents the modeling of the Indoor mmWave channels-dual-hop networks in different scenarios (one AF and DF relay, two- parallel AF and DF relays), the results of these modeling systems are compared with them and with the direct path in terms of the performance of BER as a function of SNR using Matlab programming.

Chapter four presents the modeling of the outdoor mmWave channels-dual-hop networks in different scenarios (one AF and DF relay, two- parallel AF and DF relays), the results of these modeling systems are compared with them and with the direct path in terms of the performance of BER and channel capacity as a function of SNR using Matlab programming.

Chapter five presents conclusions and suggests trends for future works.

## Chapter Two

# Theory of cooperative communication systems over mm-wave channels

### 2.1 Mm wave Spectrum

Almost all wireless and mobile technologies operate at frequencies less than 6 GHz. Due to the exponential growth of network data traffic, these frequency bands are getting saturated. studies have found that the present sub-6 GHz frequency bandwidth will not be sufficient to supply the capacity necessary for future systems [41]. As a result, a shift toward millimeter-Wave (mmWave) frequency bands, which offer greater frequency bandwidths, is unavoidable.

mmWave frequencies are theoretically between 30 and 300 GHz, which corresponds to wavelengths between 1 and 10 mm. However, wireless researchers typically refer to frequency bands over 6 GHz as mm-Wave bands [6].

The mmWaves are slightly longer than X-rays or infrared waves, but shorter than radio waves or microwaves as shown in Figure 2.1 [42].

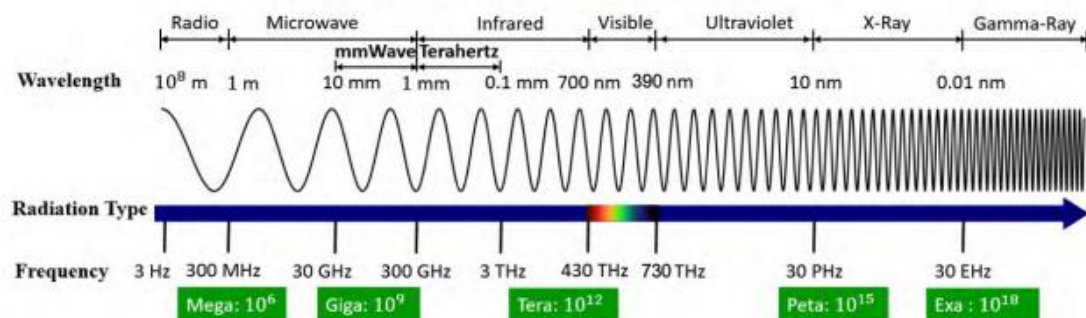


Figure 2.1 The electromagnetic spectrum [42].

Additionally, the extremely short wavelengths of mmWave enable the integration of a large number of miniaturized antennas into a comparatively small area. These multiple antenna systems can be employed to create extremely high gain electrically steerable beams at the base station, mobile station, or even on a chip [3].

Actually, an extensive review of the literature indicates that there are three main attractive bands in general. First, one has the spectrum around 60 GHz, the [57 GHz-64 GHz] band, the so-called V-band. Second, the second bands in the 70/80 GHz are [71 GHz-76 GHz] and [81 GHz-86 GHz], the so-called E-band. Both are under the focus due to the large available bandwidth to support higher data rates. Third, the bands around 90 GHz are [92 GHz-94 GHz] and [94.1 GHz-95 GHz]. Note that [94 GHz-94.1 GHz] is reserved for military applications. Therefore, in this last case, although there is significant bandwidth to exploit, its uneven allocation and the proximity to the military bands may suppose a handicap in future use[43]. These bands are depicted in Figure 2.2 [44]

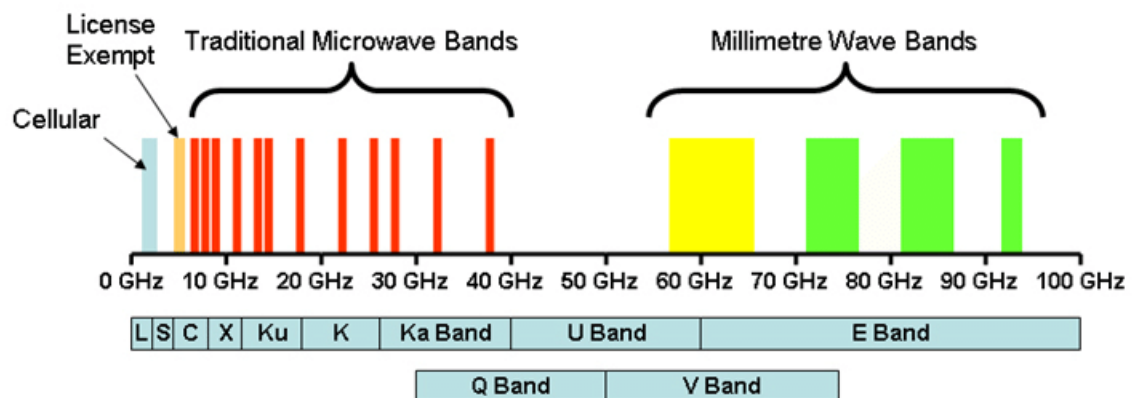


Figure 2.2 Millimeter-wave sub-bands and regulation [44].

The 5G tech is expected to exploit these bands and step up the current traffic requirements and system capacity shortage one step ahead. Several industrial standards tried to recommend different bandwidth for 5G networks with respect to coexistence with it and achieving better coverage and performance.

The simplified frequency spectrum chart represented in Figure 2.3 [45] highlights the frequency bands proposed by the ITU at WRC–2015. These frequency bands include 24.25 – 27.5 GHz, 31.8 – 33.4 GHz, 37 – 43.5 GHz, 45.5 – 50.2 GHz, 50.4 – 52.6 GHz, 66 – 76 GHz and 81 – 86 GHz [45].

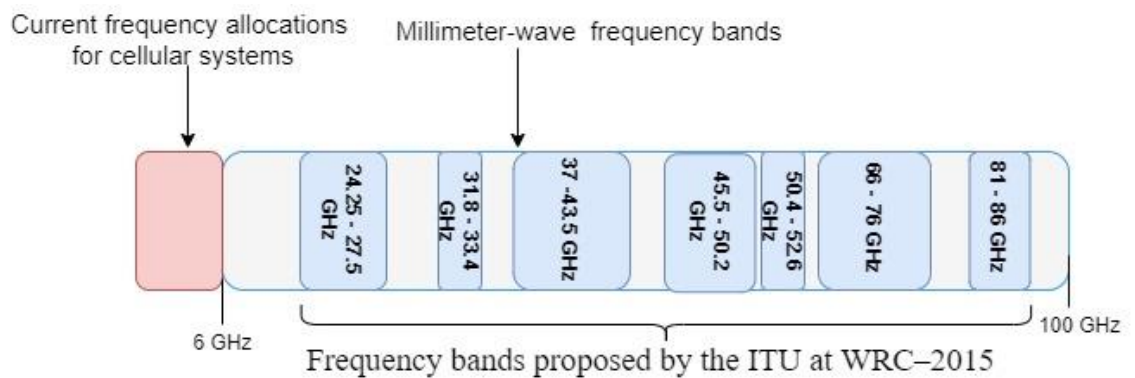


Figure 2.3 Frequency bands proposed by the ITU at WRC–2015.

These frequency bands are wide so that they can accommodate a huge amount of data flow, and as such, the mmWave technology can easily achieve 10 Gbps data rate for communication [45].

MmWave technology is well suited for modern smart devices and mobile phones, which are supposed to be efficient and small in size due to its tiny component size [45].

## 2.2 Millimeter Wave Propagation Characteristics

The mmWave band's propagation properties are distinct from those of lower frequency band conventional communication networks, requiring additional modeling and design efforts for communication systems, their power requirements, and the length of wireless links [46].

The propagation of the signal is directly affected by the frequency band of operation. The short wavelength of the mmWaves makes ordinary objects like trees and light posts obstacles that might likely block the signal. The short distance after which the signal dropped below the thermal noise level allowed the short-range communications, which is also known as "whisper radio" communications. For longer-range communications, rain and other weather factors are principal components in determining the cell size [21].

The major propagation characteristics of mmWaves are shown in Figure 2.4 [47], including free-space path loss, atmospheric attenuation, rain-induced fading, foliage attenuation, material penetration, propagation mechanisms (reflection, diffraction, multipath, scattering, refraction). we explain only a few examples of these characteristics in the context of this dissertation [47].

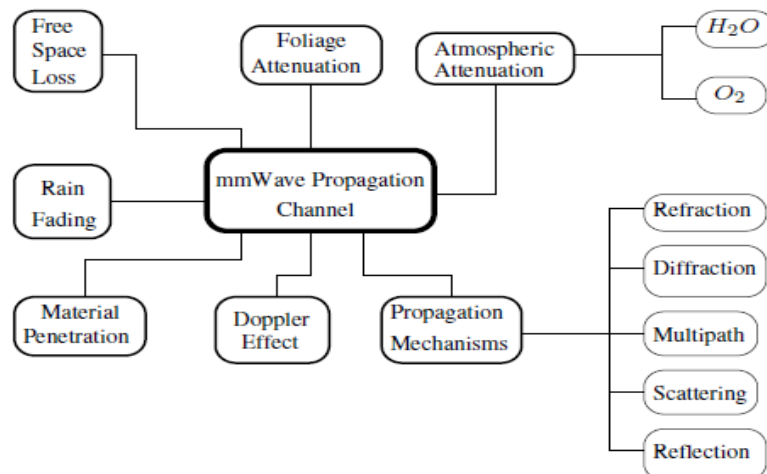


Figure 2.4 MmWave propagation characteristics [47].

### 2.2.1 Free Space Path Loss

The free space path loss (FSPL) can be defined as the attenuation of energy between two radiators in free space. The FSPL between two communicating isotropic antennas separated by a distance  $d$  is given by the Friis transmission formula [48]:

$$PL = \frac{1}{G_{TX}G_{RX}} \left( \frac{4\pi df}{c} \right)^2 \quad (2.1)$$

Where  $f$  is the frequency of the transmitted signal,  $c$  is the speed of light and  $G_{TX}$  and  $G_{RX}$  are the transmit and receive antenna gains, respectively. In the case of isotropic transmission (i.e.  $G_{TX} = G_{RX} = 1$ ), we can see in the above equation  $PL \propto f^2$ , thus coming to the conclusion that at high frequencies of the mm-Wave signal, the path loss is significantly higher than that of lower frequency signals when all other conditions are the same; one of these conditions is antenna gains. [48].

The received power over the sub-100 GHz mmWave band at three different distances are illustrated in Figure 2.5 [47].

Furthermore, the FSPL obtained at the 28 GHz, 40 GHz, 60 GHz, 100 GHz, 200 GHz and 300 GHz frequencies are depicted in Figure 2.6 [47], where it shows that an additional loss of 24 dB, 27 dB, and 32 dB added in the 28 GHz, 38 GHz, and 73 GHz bands compared to the 1.8 GHz GSM band at any given separation distance [47].

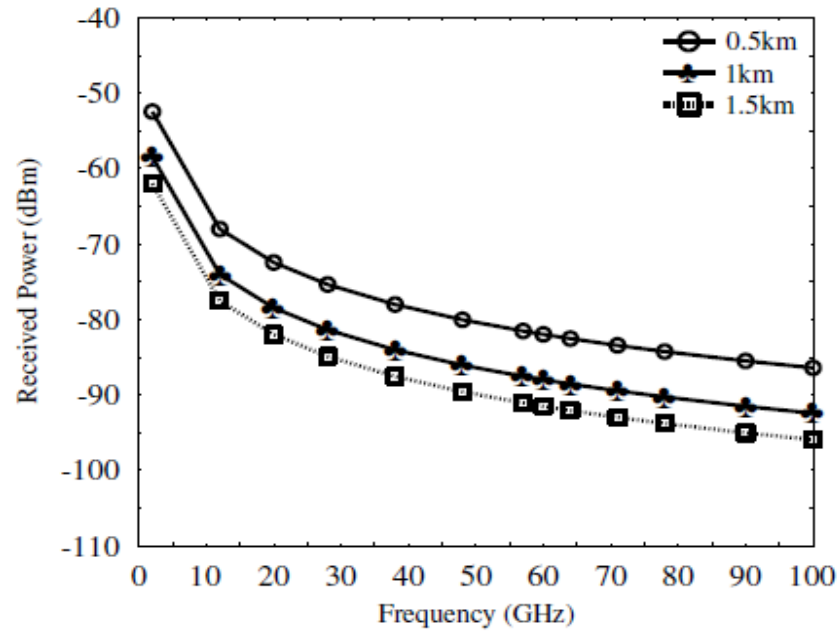


Figure 2.5 Received power at mmWave frequencies, when  $P_t=10$  dBm and the antenna gain is 10 dBi [47].

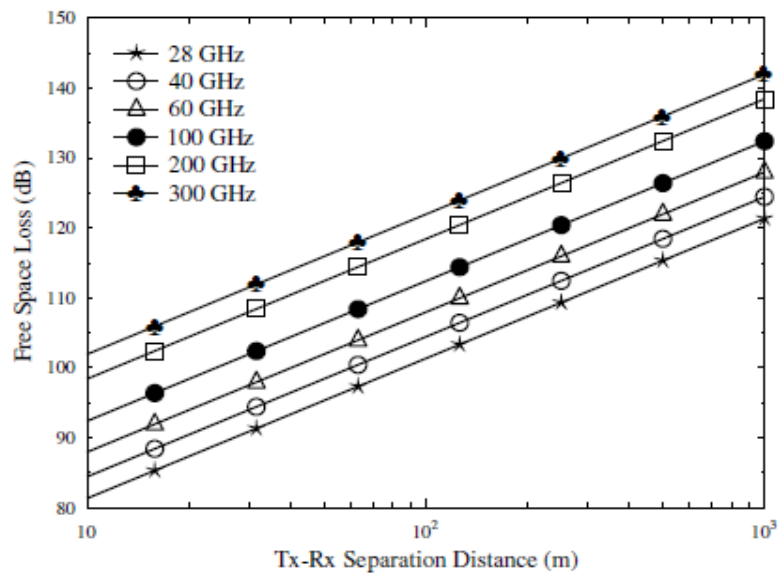


Figure 2.6 Free space loss at mmWave frequencies [47].

Table 2.1 [49] summarizes free-space path loss values for commercial ultra-high frequency (UHF) microwave cellular bands (1.8 GHz), WLAN bands (2.4 GHz), and licensed/unlicensed mmWave bands (28, 38, and 73 GHz) for 100 m and 200 m separation distances.

Table 2.1 Path loss levels at microwave, WLAN, and mmWave frequencies [49]

Frequencies	FSPL at distance 100 m	FSPL at distance 200 m
1.8 GHz	67.55 dB	73.57 dB
2.4GHz	70.04dB	76.06dB
28 GHz	91.38 dB	97.40 dB
38 GHz	94.04 dB	99.71 dB
73 GHz	100.1 dB	105.7 dB

### 2.2.1.1 Large-Scale Path Loss Models

Large-scale propagation properties characterize the variations due to path loss and shadowing as the transmitter and the receiver becomes separated over long distances, from meters to hundreds or thousands of meters [50].

As previously stated, due to frequency-dependent differences, the existing propagation models utilized at lower frequency bands are insufficient and cannot be used for path loss modeling or channel modeling.

Characteristics for millimeter wave (mmWave) bands. Thus, extensive studies on channel characterization and path loss modeling are required to develop general and appropriate channel models that can be suitable for a wide range of mmWave frequency bands.

There are several types of path loss models based on comprehensive measurements carried out for the 28 GHz, 38 GHz, 60 GHz, and 73 GHz frequency bands, some of them are: Reference Path Loss [47] or "close-in free space reference distance (CI) model"[51], the floating intercept (FI) model, the dual-slope model [51], and the parabolic model [47], which are shown in Figure 2.7 [47], would be discussed only the first and second models.

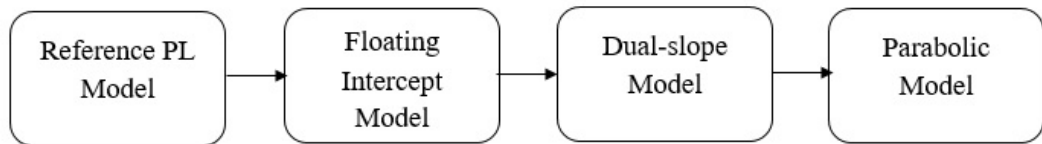


Figure 2.7 Models of path loss for mmWaves.

- Floating Intercept (FI) Model

The floating-intercept (FI) path loss model of equation (2.2) has three parameters:  $\alpha$  represents the floating-intercept in dB,  $\beta$  is the slope of the line, and  $\sigma$  is the standard deviation of the linear fit line. Neither  $\alpha$  nor  $\beta$  necessarily have any physical basis but are simply the result of a linear fit of path loss in dB to the logarithm of distance. The FI model equation is as follows:

$$PL^{FI}(d)[\text{dB}] = \alpha + 10 \beta \log_{10}(d) + X_{\sigma}^{FI} \quad (2.2)$$

Shadowing is represented by the zero-mean (usually assumed Gaussian) random variable  $X_{\sigma}^{FI}$  with a standard deviation of  $\sigma$  dB.

- Close-In Free Space Reference Distance (CI) Model

The close-in free space reference distance (CI) model (reference path loss model) is the simplest model from the models of the path loss that is shown in Figure 2.7, it is used for describing the path-loss and shadowing effects at mmWaves [52].

In the past, models in the ultra-high frequency (UHF) and microwave bands used a close-in reference distance of 1 km or 100 meters [53], since base station towers were tall without any nearby obstructions, and cell size was on the order of many kilometers. In mmWave CI models, typically  $d_0 = 1$  meter since base stations will be at lower heights or mounted indoors, and closer to obstructions [53], and link distances will be shorter, up to a few hundred meters. The CI 1-meter reference distance is a conveniently suggested standard that ties the true transmitted power or path loss to a convenient close in a distance of 1 m, as suggested in [51][54]:

$$PL^{CI}(d)[\text{dB}] = \text{FSPL}(d_0) + 10 n \log_{10} \left( \frac{d}{d_0} \right) + X_{\sigma}^{CI} \quad (2.3)$$

where  $d_0 = 1\text{m}$ ,  $d \geq d_0$ ,  $n$  is the path loss exponent (PLE) which characterizes how quickly the PL increases with respect to Tx-Rx distance[21],  $X_{\sigma}^{CI}$  is a zero-mean Gaussian random variable with  $\sigma$  is the standard deviation in dB, also called the shadow factor, reflecting wide-scale signal fluctuations due to wireless channel obstructions caused by shadows [21]. It considers how the PL is affected not only by distance but also by the propagation environment and the Tx and Rx positions[54]. The  $\text{FSPL}(d_0)$  denotes free space path loss in dB, calculated using equation (2.4) [21].

$$FSPL(d_0) = 20 \log_{10} \left( \frac{4\pi d_0}{\lambda} \right) \quad (2.4)$$

The PLE is determined by the scenario being considered, which may include both LOS and NLOS scenarios for two cases of close-in free-space reference distance, the first case set  $d_0 = 1\text{m}$  and the second  $d_0 = 5\text{m}$ . In this work we have modeled the channel only for the LOS scenario for the frequencies 28 GHz, 38 GHz, 60 GHz, and 73 GHz, the  $n$  and  $\sigma$  is produced empirically from measurements [47] on the various frequency bands and their values at  $d_0 = 1\text{m}$  and  $d_0 = 5\text{m}$  are summarized in the following tables [21][47][55][56].

Table 2.2 summarized the path loss exponent ( $n$ ) and standard deviations ( $\sigma$ ) of the shadowing factor ( $X_\sigma$ ) for the frequencies 28 GHz, 38 GHz and 60 GHz at  $d_0 = 5\text{m}$ .

Ref.	Frequency (GHz)		LOS		NLOS	
			$n$	$\sigma[dB]$	$n$	$\sigma[dB]$
[47]	28GHz	$G_{Tx}=24.5$ dBi	2.55	8.66	5.76	9.02
[55]		$G_{Rx}=24.5$ dBi				
[56]						
[47]	38GHz	$G_{Tx}=25$ dBi	2.20	10.3	3.88	14.6
[55]		$G_{Rx}=25$ dBi				
[56]	38GHz	$G_{Tx}=25$ dBi $G_{Rx}=13$ dBi	2.21	9.40	3.18	11.0
[47]	60 GHz (MiWEBA)		-	-	2.36	-

Table 2.3 summarized the path loss exponent ( $n$ ) and standard deviations ( $\sigma$ ) of the shadowing factor ( $X_\sigma$ ) for the frequencies 28 GHz, 38 GHz, 60 GHz, and 73GHz at  $d_0 = 1m$  .

Ref.	Frequency (GHz)		LOS		NLOS	
			n	$\sigma$ [dB]	n	$\sigma$ [dB]
[21]	28GHz	$G_{Tx}=24.5$ dBi $G_{Rx}=24.5$ dBi	n	$\sigma$ [dB]	n	$\sigma$ [dB]
			1.9	1.1	4.5	10.0
[21]	38GHz	$G_{Tx}=25$ dBi $G_{Rx}=25$ dBi	1.9	4.6	3.3	12.3
	38GHz	$G_{Tx}=25$ dBi $G_{Rx}=13$ dBi	1.9	3.5	2.8	10.3
[47] [57]	60 GHz (hall)		2.17	0.88	3.01	1.55
[47]	60 GHz (room)		1.92	1.72	-	-
[47]	60 GHz(PTP)		2.25	2	4.22	10.12
[21]	73GHz at $h_{TX} = 7; 17m, h_{TX}=4.06m$ $G_{Tx}=27$ dBi $G_{Rx}=27$ dBi		2.4	6.3	4.7	12.7

## 2.2.2 Environmental Effects

In addition to the FSPL, environmental factors such as atmospheric absorption by gases such as oxygen and water vapor and rainfall as seen in Figure 2.8 [47] also play a significant role in the mm-Wave signal propagation.

The intensity of gaseous absorption depends on several factors, such as temperature, pressure, altitude, and most importantly the operating carrier frequency [47].

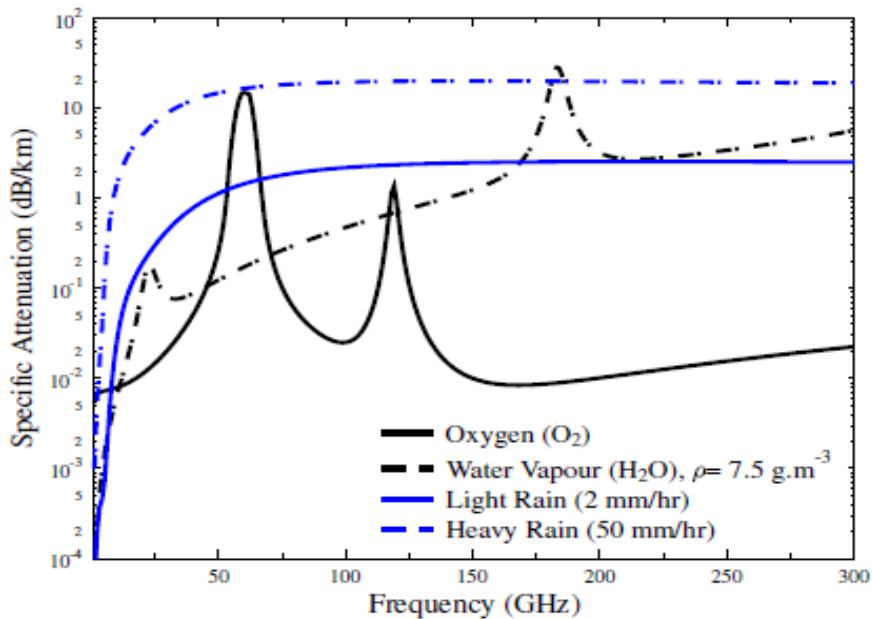


Figure 2.8 Specific attenuation curves of O<sub>2</sub>, H<sub>2</sub>O and rain at sea level. The term  $\rho$  refers to the density of H<sub>2</sub>O in grams per meter<sup>3</sup> [47].

The figure above shows that the attenuation due to environmental factors (usually measured in [dB/km]) is frequency-dependent. The O<sub>2</sub> absorption curve maxima are observed at the 60 GHz and 119 GHz frequencies, at a record of 15 dB/km and 1.4 dB/km loss, respectively.

However, by operating at short distances the oxygen absorption loss can be further reduced. For example, by reducing the cell range from 1 km to 100 m, the O<sub>2</sub> absorption at 60 GHz and 119 GHz drops to only 1.5 dB and 0.14 dB, respectively. Consequently, there is a huge interest in these frequencies, generally for short-range high data rate communications [48].

On the other hand, the frequency bands [28 GHz-38 GHz] and [70 GHz-110 GHz] have the lowest atmospheric propagation losses. Consequently, they are projected for outdoor applications, including mobile communications, Point-to-Point (P2P) high data rate links, vehicular radars (mainly planned at  $f = 77$  GHz), radiometry (often using the minimum of absorption at  $f = 94$  GHz), or imaging (also taking advantage of the atmospheric properties at  $f = 94$  GHz) [43]. Furthermore, it is depicted in Figure 2.8 that H<sub>2</sub>O molecules can resonate at 23 GHz, 183 GHz, and 323 GHz, which are associated with a loss of 0.18 dB/km, 28.35 dB/km and 38.6 dB/km, respectively [47].

Both light and heavy rain attenuation losses are illustrated in the Figure above at 2 mm/hr and 50 mm/hr rain rates. The attenuation curves of rain rates ranging between 2 mm/hr and 50 mm/hr exist between the light and heavy rain curves in Figure 2.8 [47].

### **2.3 Cooperative Communication**

There are different challenges faced by a mm-wave channel that reduce the performance and efficiency of the mm-wave networks. The main challenges are high propagation loss, high absorption loss, and limited coverage area etc. [58]. Cooperative communication is one of the most trustworthy options for overcoming these challenges in terms of size, achieving high channel capacity, providing optimal power, and cost [58][59].

Additionally, it has the potential to considerably improve the communication network's effective quality of service. This can be quantified in terms of bit error rate (BER) or outage probability (OP), which measures the robustness of the communication process to fading based on the SNR [60]. The cooperative communication technique requires relay nodes to transmit signals to the destination in order to enhance the link's range and margin [50].

One of the leading motives behind the use of cooperative communications lies in utilizing the spatial diversity provided by the network nodes.

A simple scenario for cooperative communications is demonstrated in Figure 2.9, consists of a source (S), a relay (R) and a destination (D) [61], The signal ( $x$ ) is transmitted by the source (S) to the destination (D) as well as the relay node (R). The relay then processes the received signal ( $x$ ) using various relaying protocols before forwarding it to a destination with noise added ( $n$ ). Consequently, at the destination, various strategies for combining the received signals can be employed to produce power gain and diversity gain [43]. One of these strategies that have been employed in this work is Maximum Ratio Combining (MRC).

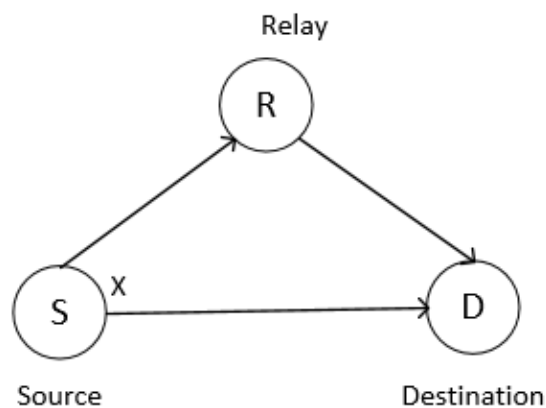


Figure 2.9 Basic cooperative relay network [61].

Relays process the received signal using multiple protocols before forwarding it to the destination. Between the source and the destination, a single or several relays might be deployed. Typically, if the distance is not too great, a two-hop relay network is utilized; otherwise, a multi-hop relay network is employed.

### **2.3.1 Relaying Protocols**

Relaying protocols are classified in cooperative wireless communication according to the process occurring at the relay terminal. Some of these protocols are: amplify and forward (AF) [62], decode and forward (DF) [62], compress and forward (CF) [63], decode amplify and forward (DAF) [64]. The amplify-and-forward (AF) and decode-and-forward (DF) have been utilized in this work.

#### **2.3.1.1 Amplify and Forward (AF) Protocol**

The Amplify and Forward (AF) is a simple relay scheme in which the relay simply amplifies the received signal with a gain factor and forwards a resulting signal to the destination. The advantage of this technique is its simplicity, as it eliminates the requirement for signal encoding and decoding at the relay node. Apart from its simplicity and low cost, noise amplification at the relay is a significant disadvantage [65]. The process of amplification and forwarding is depicted in Figure 2.10 [58].

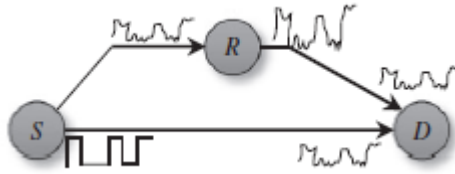


Figure 2.10 Amplify and forward method [58].

### 2.3.1.2 Decode and Forward (DF) Protocol

In decode and forward (DF), a relay decodes the signal received from the source before forwarding it to the destination. Following that, error detection is employed, such as a cyclic redundancy check (CRC), to ensure the estimated sequence does not contain errors [66]. The relay re-encodes the correctly decoded estimates and forwards them to the destination, while it discards the incorrectly decoded estimates to avoid error propagation [66].

In comparison to the AF relaying protocol, the DF relaying protocol is more complicated and progressive, and it forwards just the useful signal to the destination with additional time processing [65]. The procedure of decoding and forwarding is illustrated in Figure 2.11 [58].

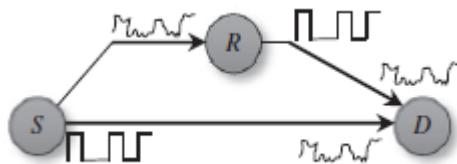


Figure 2.11 Decode and forward method [58].

## 2.4 Dual-hop Relay Network

The transmission process of a dual-hop relay is divided into two orthogonal phases. The source transmits its signal to the relay and destination during the first phase, while the relay processes the signal received from the source and delivers the result to the destination during the second phase as shown in Figure 2.12 [61].

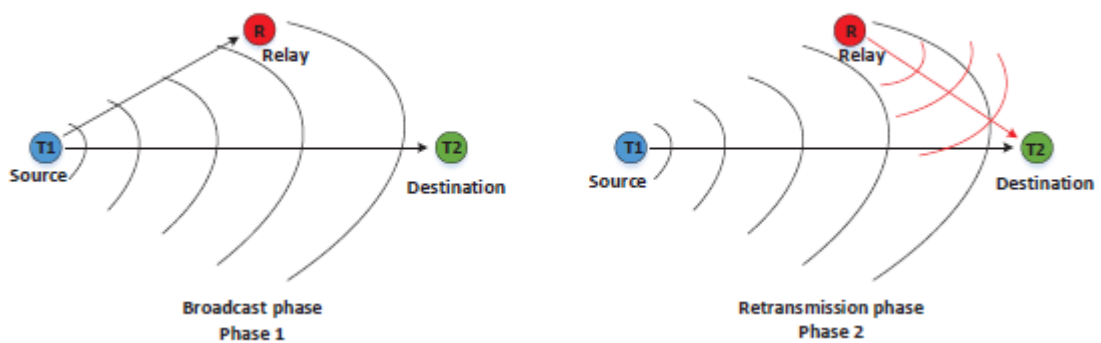


Figure 2.12 Basic structure of a cooperative relay network with two phases [61].

Network design incorporates various possible scenarios in order to create it. For the first approach, the network uses AF relays, and for the second, DF relays are employed. Additionally, the equations will be derived at each node of the network.

### 2.4.1 Dual-hop AF Relay Assisted mmWave Channel

As illustrated in Figure 2.13, a dual-hop system with an AF relay node has been assumed. In Phase 1, the source transmits the BPSK symbol through the mmWave channels to the destination and the AF relay. As a result, the signals received at the relay node and destination can be written as follows:

$$y_{sd} = h_0x + n_0 \quad (2.5)$$

$$y_{sr} = h_1x + n_1 \quad (2.6)$$

where  $h_0$ ,  $h_1$  the amplitude of the mmWave channel gain between S and D, S and R, respectively.  $x$  is the transmit symbol by the source, and according to BPSK modulation  $x = \pm 1$ , also,  $n_0$ ,  $n_1$  the complex additive white Gaussian noise (AWGN) added to the signal at the receiver antenna of both nodes.

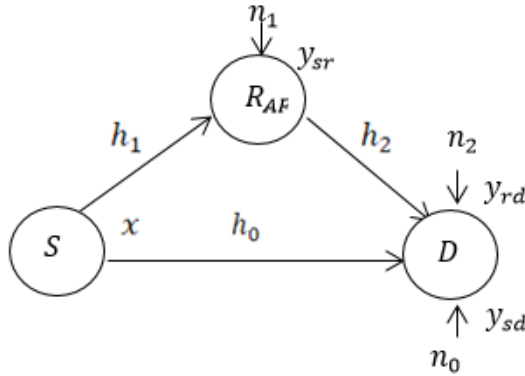


Figure 2.13 mmWave channel assisted with one AF relay.

Subsequently, the received signal from the source is amplified by a gain factor  $G$  and then forwarded the message to the destination.

$$G \leq \sqrt{\frac{p_r}{h_1^2 E[|x|^2] + E[|n_1|^2]}} \quad (2.7)$$

Where:

$G$ : is defined as the amplification factor scaling the power transmitted by the relay.

$p_r$ : is the transmit power of the relay.

$E[|x|^2], E[|n_1|^2]$ : represents the expectation of signal and noise, respectively.

Also, we can write equation (2.7) as

$$G \leq \sqrt{\frac{p_2}{h_1^2 p_1 + \sigma_1^2}} \quad (2.8)$$

Where

$p_2$ : is the transmit power of the relay.

$p_1$ : is the transmit power of the source.

$\sigma_1$ : is a standard of deviation of the  $n_1$  (AWGN).  $\sigma_1^2 = E[|n_1|^2]$  is the variance of the  $n_1$ .

In Phase 2, the scaled signal (signal after amplification) is forwarded to the destination.

The received signal at the destination from the relay link is

$$y_{rd} = h_2 G y_{sr} + n_2 \quad (2.9)$$

Where  $h_2$  is the amplitude of the mmWave channel gain between R and D; and  $n_2$  is the AWGN at the destination.

The received signals from each channel are added together at the received node, which can be written as equations 2.10 and 2.11.

$$y = y_{sd} + y_{rd} \quad (2.10)$$

Also, we can write it as :

$$y = (h_0x + n_0) + (h_1h_2xG + h_2Gn_1 + n_2) \quad (2.11)$$

In (2.10), both signals  $y_{sd}$  and  $y_{rd}$  are received and from a combined cooperative signal ( $y$ ), which leads to better performance. Moreover, different receive diversity techniques can be used at the receiver side.

Diversity strategies such as the Maximal Ratio Combiner (MRC), Selection Combining (SC), and Maximal Likelihood (ML) all have various trade-offs in terms of complexity and performance [58].

The reconstructed signal at the receiver (output of the combiner) can be written as in equation (2.8).

$$\hat{x} = h_0^* y_{sd} + h_1^* h_2^* G^* y_{rd} \quad (2.12)$$

The channel capacity (bit/s/Hz) for the link  $S \rightarrow R \rightarrow D$  link is given by [65]

$$C = \frac{1}{2} \log \left( 1 + \frac{\gamma_1 \gamma_2}{\gamma_1 + \gamma_2 + 1} \right) \quad (2.13)$$

Where  $\gamma_1 = \frac{h_1^2 p_1}{\sigma_1^2}$ , and  $\gamma_2 = \frac{h_2^2 p_2}{\sigma_2^2}$ , is the SNR for the links from  $S \rightarrow R$ ,  $R \rightarrow D$ .

Where

$\sigma_2^2 = E[|n_2|^2]$  is the variance of the  $n_2$ .

The factor  $1/2$  in equation (2.13) is necessary because two channels are required to send data from S to D [65].

## 2.4.2 Dual-hop DF Relay Assisted mmWave Channel

DF relay has been considered in the system model that is shown in Figure 2.14.

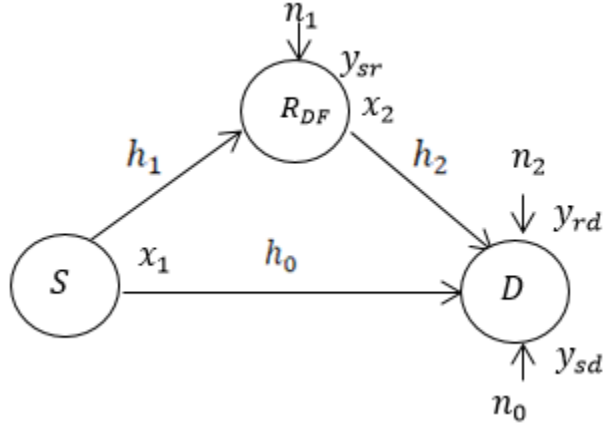


Figure 2.14 mmWave channel assisted with one DF relay.

In phase 1, the source transmits the message to the relay, which decodes it. If decoding is successful, the relay delivers the re-encoded message to the intended recipient. In phase 2, the source sends its message directly to the destination.

The received signals at the destination from the direct path  $y_{sd}$  and at the relay  $y_{sr}$  are given by (2.14) (2.15) respectively.

$$y_{sd} = h_0 x_1 + n_0 \quad (2.14)$$

$$y_{sr} = h_1 x_1 + n_1 \quad (2.15)$$

We utilized the MRC technique in the DF relay to remove the channel effects on the signal and also to restoration of the decoded version ( $\hat{x}_1$ ) of the original signal  $x_1$ .

$$\widehat{x}_1 = h_1^* y_{sr} \quad (2.16)$$

The transmitted symbol, which is denoted as  $x_2 = \widehat{x}_1$  is passed through a mmWave channel  $h_2$  towards the destination.

$$y_{rd} = h_2 x_2 + n_2 \quad (2.17)$$

In this type of relay, AWGN is not accumulated due to the decoding process at the relay [36]. This feature is not found in AF relay so it helps to improve the achievement of the network.

The reconstructed signal at the receiver (output of the maximal ratio combiner) can be written as in equation (2.18).

$$\widehat{x}_1 = h_0^* y_{sd} + h_2^* y_{rd} \quad (2.18)$$

In general, a DF relay network requires knowledge of source-destination and relay-destination channel state information (CSI), whereas an AF relay network just requires knowledge of the source-to-relay link's channel state information[60].

The channel capacity (bit/s/Hz) for the link  $S \rightarrow R \rightarrow D$  link is given by

$$C = \frac{1}{2} \min [\log_2(1 + \gamma_1), \log_2(1 + \gamma_2)] \quad (2.19)$$

## 2.5 Dual-hop Two Parallel Relays Network

When two relays are placed in parallel between the source and destination, the network is referred to as a dual-hop two parallel relays network. The parallel relay transmission is more useful for the outdoor environment to increase robustness against multi-path fading.

The whole transmission consists of two phases: the broadcasting phase, during which the transmitter broadcasts its data to two cooperative relays, as well as direct transmission between the transmitter and the receiver [67].

On the other hand, the relay nodes process the transmitter signals and then forward them to the receiver node during the relaying phase. The receiver then combines the numerous independent copies of the signal received by utilizing different combining techniques, which provide power gain, diversity gain, increase the reliability of the wireless communication link, and expanding link coverage without the need for additional antennas and associated complexity at each node [67].

It is possible to implement many relaying strategies, however mostly utilized AF and DF relays because those are the two most commonly used relaying strategies.

### **2.5.1 Dual-hop Parallel AF Relays Assisted mmWave Channel**

In the example shown in Figure 2.15, two AF relays are set up in a parallel transmission model to enhance the system's overall performance by outage probability, minimizing the error probability, and enhancing the diversity gain. In this scenario the transmitted signal ( $x$ ) is propagated through three paths to reaches the destination, the first is the direct path as illustrated in Eq. 2.5. The two other paths are relaying paths (indirect paths) via AF relays placed in the middle between the source and destination to make them communicates with each other. The use of two relays in the network instead of one relay is to achieve the lowest bit error rate (BER) at the destination. The received signals at the destination node from the relays R1 and R2 can be expressed as:

$$y_{sr1} = h_1 x + n_1 \quad (2.20)$$

$$y_{r1d} = h_2 G_1 y_{sr1} + n_2 \quad (2.21)$$

$$y_{sr2} = h_3 x + n_3 \quad (2.22)$$

$$y_{r2d} = h_4 G_2 y_{sr2} + n_4 \quad (2.23)$$

The received signals in the first and second hop for AF relay are amplified by a gain factor  $G_1$  and  $G_2$  respectively.

$$G_1 \leq \sqrt{\frac{p_{r1}}{h_1^2 E[|x|^2] + E[|n_1|^2]}} \quad (2.24)$$

Where:

$G_1$ : is defined as the amplification factor scaling the power transmitted by the first relay.

$p_{r1}$ : is the transmit power of the first relay.

$h_1$ : is the amplitude of the mmWave channel gain between S and  $R_{AF1}$ .

$E[|x|^2], E[|n_1|^2]$ : represents the expectation of signal and noise, respectively.

$$G_2 \leq \sqrt{\frac{p_{r2}}{h_3^2 E[|x|^2] + E[|n_3|^2]}} \quad (2.25)$$

Where:

$G_2$ : is defined as the amplification factor scaling the power transmitted by the second relay.

$p_{r2}$ : is the transmit power of the second relay.

$h_3$ : is the amplitude of the mmWave channel gain between S and R2.

$E[|x|^2], E[|n_3|^2]$ : represents the expectation of signal and noise, respectively.

As we mentioned in the previous part, the signals that reach the destination are combined and decoded by the MRC decoder to reconstruct the original signal at the receiver as

$$\hat{x} = h_0^* y_{sd} + h_1^* h_2^* G_1^* y_{r1d} + h_3^* h_4^* G_2^* y_{r2d} \quad (2.26)$$

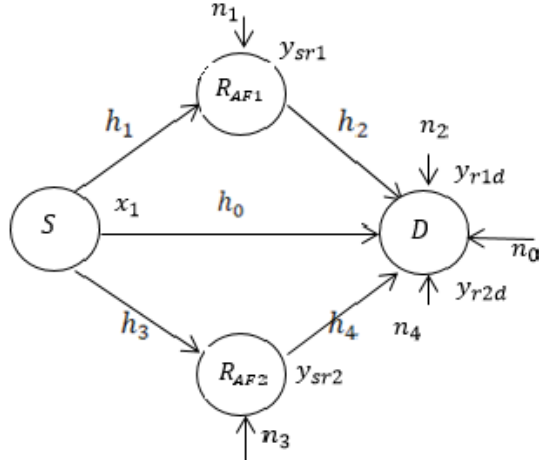


Figure 2.15 mmWave channel assisted with two AF relays.

## 2.5.2 Dual-hop Parallel DF Relays Assisted mmWave Channel

The second example involves paralleling two DF relays in the presence of a direct path, as seen in Figure 2.16. The received signals at the two relays are expressed as:

$$y_{sr1} = h_1 x_1 + n_1 \quad (2.27)$$

$$y_{sr2} = h_3 x_1 + n_3 \quad (2.28)$$

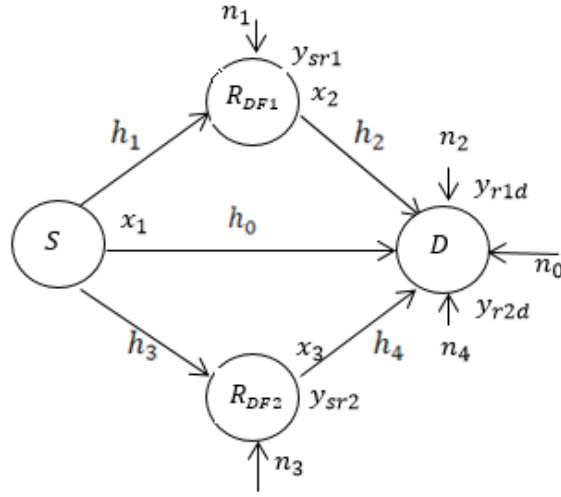


Figure 2.16 mmWave channel assisted with two DF relays.

The signals that reach the destination node from the relays and the source are expressed as:

$$y_{sd} = h_0 x_1 + n_0 \quad (2.29)$$

$$y_{r1d} = h_2 x_2 + n_2 \quad (2.30)$$

$$y_{r2d} = h_4 x_3 + n_4 \quad (2.31)$$

While the reconstructed signal is written as

$$\widehat{x}_1 = h_0^* y_{sd} + h_2^* y_{r1d} + h_4^* y_{r2d} \quad (2.32)$$

## **2.6 Characterization of Millimeter Wave Channels**

The propagation characteristics of mmWave bands are significantly different than those of lower frequency bands. Smaller wavelengths at mmWave frequencies are believed to have more attenuation (because of oxygen absorption and precipitation) via air than the cellular bands of today. As a result, the deployment of mmWave systems is regarded as extremely difficult, especially for outdoor communications [68].

Because of the mmWave channel's diffraction and penetration properties, it's expected that the mmWave channels will have a sparse multipath nature rather than the rich-scattering one seen in traditional microwave channels. As a result, microwave propagation models cannot be easily applied to mmWave systems. A thorough understanding of the properties of mmWave propagation is required for the design and study of future mmWave wireless networks [69].

### **2.6.1 Indoor mmWave Channel Characteristic**

The design of the mmWave indoor wireless channel helps define design factors such as coverage architecture, link budget, and power management.

With the growing interest in increasing data rates for wireless communications during the last decade, substantial experiments in the mmWave band have been undertaken in indoor environments [70].

Various channel models have been developed by the research community, each one tailored to a certain contact circumstance. For example, owing to its wide unlicensed spectral resources for indoor wireless networks, most of the early modeling efforts were carried out in the 60 GHz

band [71], like the Wireless Gigabit (WiGig) and Wireless Local Area Networks (WLAN) devices [72], the unlicensed WirelessHD, and the development of 60-GHz Personal Area Network (PAN) systems [73].

The IEEE published two standards IEEE 802.15.3c and IEEE 802.11ad which operate at 60 GHz frequency (mmWave bands). IEEE 802.15.3c is a 2D model and IEEE 802.11ad is a 3D model[74]. They were designed for a variety of channel scenarios.

The IEEE802.15.3c standard focuses on channel modeling in wireless personal area networks (WPAN) contexts as an office, desktop, library, desktop, residential, and kiosk. The IEEE 802.11ad standard focuses on channel modeling in wireless local areas networks (WLAN) scenarios such as living rooms, conference rooms, and cubicle environments [74].

IEEE 802.15.3c is a model for a single-input multiple-output channel that simply defines the Angle of Arrival (AoA) in the azimuth domain [75]and IEEE 802.11ad a model multi-input multi-output channels (MIMO) which characterizes two-way angle properties [76].

The Line of Sight (LOS) mmWave channel model for indoor environments can be modeled as [1][77][78]:

$$h_\ell = \frac{\lambda}{4\pi R_\ell} e^{-j\frac{2\pi R_\ell}{\lambda}} \quad (2.33)$$

Where  $h_\ell$ denotes all channel paths (the amplitude of the  $\ell$ th mmWave channel gain) from source to destination also the path from source and destination via a relay, i.e.  $h_\ell$  for ( $\ell=0, 1,2,3,\dots, L$ ).  $R_\ell$  is the distance between the transmitter antenna and the receiver antenna.

## **2.6.2 Outdoor mmWave Channel Characteristic**

In comparison to indoor contexts, there has been comparatively little research on mmWave outdoor channels. Knowledge of the outside propagation characteristics will be more essential given the rising interest of 5G communication groups and industry in the wide bandwidth offered by the mmWave. While mmWave interior channels are effectively modeled, the outside mmWave channel model is not yet satisfactory[50].

Most of the latest research emphasizes the characterization of the mmWaves sub-100 GHz domain with interest in the 28 GHz band, 38 GHz band, 60 GHz band, and E-band (71 to 76 GHz and 81 to 86 GHz). These bands are planned to be employed for mobile cellular 5G [80] to fulfill the data rate criteria at the Gbps.

Measurements have been made in a variety of urban areas, including Daejeon, Korea[81] and New York, Manhattan, USA [21][8][82], using the frequency bands 10, 18, 28, 38, 60, 72, and 81-86 GHz.

## Chapter Three

### Modeling of Indoor mmWave Channels

#### 3.1 Introduction

The system model investigated in this thesis is a dual-hop relay-based wireless system with one source (S), one destination (D), and either one or two relays in parallel between the source and the destination in the presence of the direct path. All channels between nodes are considered Line of Sight (LOS) mmWave channels that have been explained in equation (2.33).

The systems model employs AF and DF relaying protocols to aid communication between the source and destination and achieve higher data rates over 28, 38, 60, and 73 GHz waves, in which binary phase-shift keying (BPSK) is employed as a modulation scheme in the proposed systems.

At the destination, a maximum-ratio combination (MRC) was used in this work to combine the received signals from the direct and relaying paths and then to retrieve the original signal from the combined signals obtained from multiple pathways. This technique can be used to equalize mmWave channels and reduce bit error rates (BER).

The error probability performance for the proposed systems shown in Figures (2.13, 2.14, 2.15, 2.16) for the indoor environments are analyzed through simulation by using Monte-Carlo simulations via MATLAB programming.

The proposed model of this dissertation is depicted in Figure 3.1.

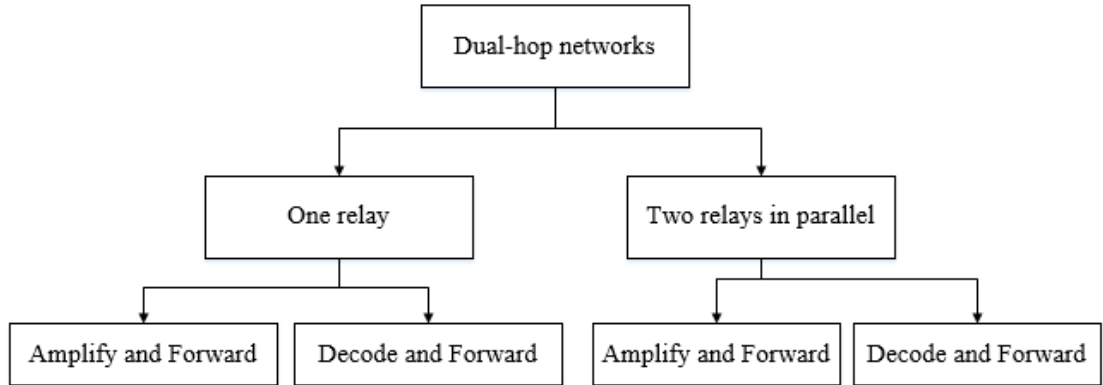


Figure 3.1 The proposed model for the dual-hop network.

The following paragraphs explain the comparison of the simulation results of dual-hop AF and DF relay systems over mm-wave frequencies (28 GHz, 38 GHz, 60 GHz, 73 GHz), comparison of the simulation results of dual-hop systems using two parallel AF and DF relays over mm-wave frequencies (28 GHz, 38 GHz, 60 GHz, 73 GHz), and comparison of the simulation results for the dual-hop systems that are using one and two parallel AF and DF relay over 28 GHz.

### **3.2 Comparison of the simulation results of dual-hop AF and DF relays systems over mm-wave frequencies (28 GHz, 38 GHz, 60 GHz, 73 GHz)**

The error probability of the relaying protocols described in figures 2.13 and 2.14 have been compared in this part, which utilized one relay protocol (AF and DF) placed between the source and destination. Moreover, we assume  $(r_{SD})$   $(r_{SR})$   $(r_{RD})$  are the distances from the source to the destination, the source and relay, and the relay and destination, respectively, where  $(r_{SD})$  is considered to be 10 m, and  $r_{SR}, r_{RD}$  equal 6 m and 6 m respectively.

The error probability results of diversity mmWave systems proposed in Figure 2.13 and Figure 2.14, which use AF and DF relay with the direct path without relay, over the frequencies stated above, are shown in Figures 3.2, 3.3, 3.4, and 3.5.

As illustrated in Figure 3.2, the error probability values for diversity AF relay, diversity DF relay “where diversity refers to the fact that the MRC combiner at the destination combines the relaying and direct paths to generate the diversity gain”, and the direct path without a relay are relatively similar at low SNR ( $< 30\text{dB}$ ), but as SNR increases, the performance of diversity AF relay outperforms both the diversity DF relay and the direct path without a relay. Furthermore, it illustrated that the diversity DF relay and the direct path has nearly identical performances.

The difference in performance between diversity DF relay and the direct path with diversity AF relay performance is almost 22 dB and 24 dB respectively, at BER  $10^{-3}$  when the carrier frequency 28 GHz and distance  $(r_{SD})10$  m.

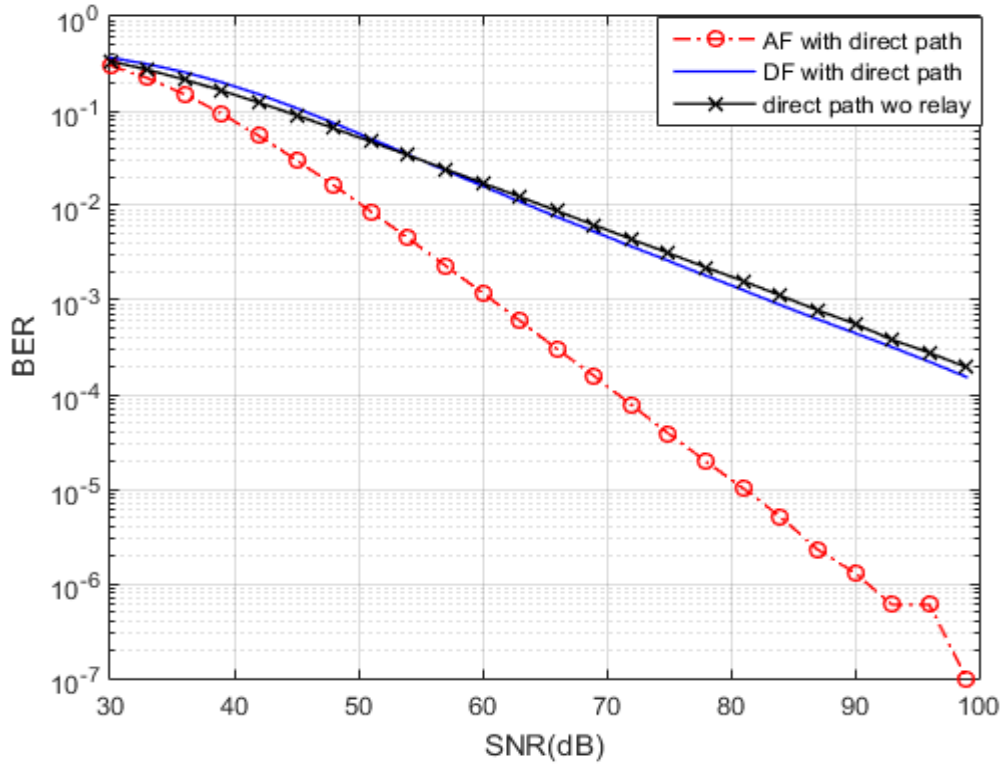


Figure 3.2 BER vs. SNR for cooperative relaying for mmWaves using one AF and DF relays over 28 GHz in the presence of the direct path at distance  $(r_{SD})$  10 m.

The error probability performance results of diversity AF, diversity DF and direct path without relay over carrier frequency 38 GHz and distance 10 m between the source and destination are shown in Figure 3.3.

This Figure demonstrates that in low SNR ( $< 37$ dB), both types of diversity and the direct path have nearly similar error probability performance, but as SNR rises, the diversity AF outperforms the diversity DF and the direct path without a relay while the diversity DF and the direct path have nearly identical performances at all values of SNR. The difference

in performance between diversity DF relay and direct path with AF relay performance is almost 21 dB and 25 dB respectively, at BER  $10^{-3}$ .

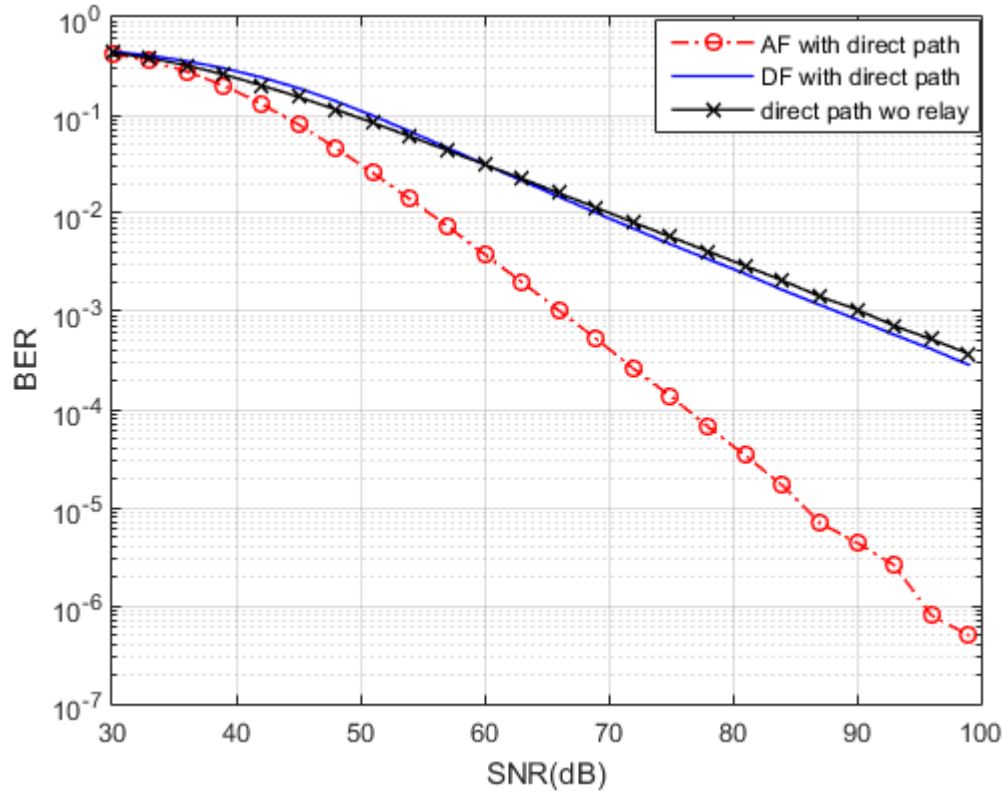


Figure 3.3 BER vs. SNR for cooperative relaying for mmWaves using one AF and DF relays over 38 GHz in the presence of the direct path at distance  $(r_{SD})$  10 m.

The error probability performance results of the three types stated above over carrier frequency 60 GHz and distance 10 m between the source and destination are shown in Figure 3.4.

Before 40 dB SNR, the error probability performance of the two types of relays and the direct path is virtually identical; however, as SNR increases, also the diversity AF outperforms the diversity DF and the direct path

without a relay. Additionally, diversity DF relay and direct path operate nearly identically at all SNR values. The differences in performance between diversity DF and the direct path with diversity AF is approximately 22 dB and 27 dB, respectively at BER  $10^{-3}$ .

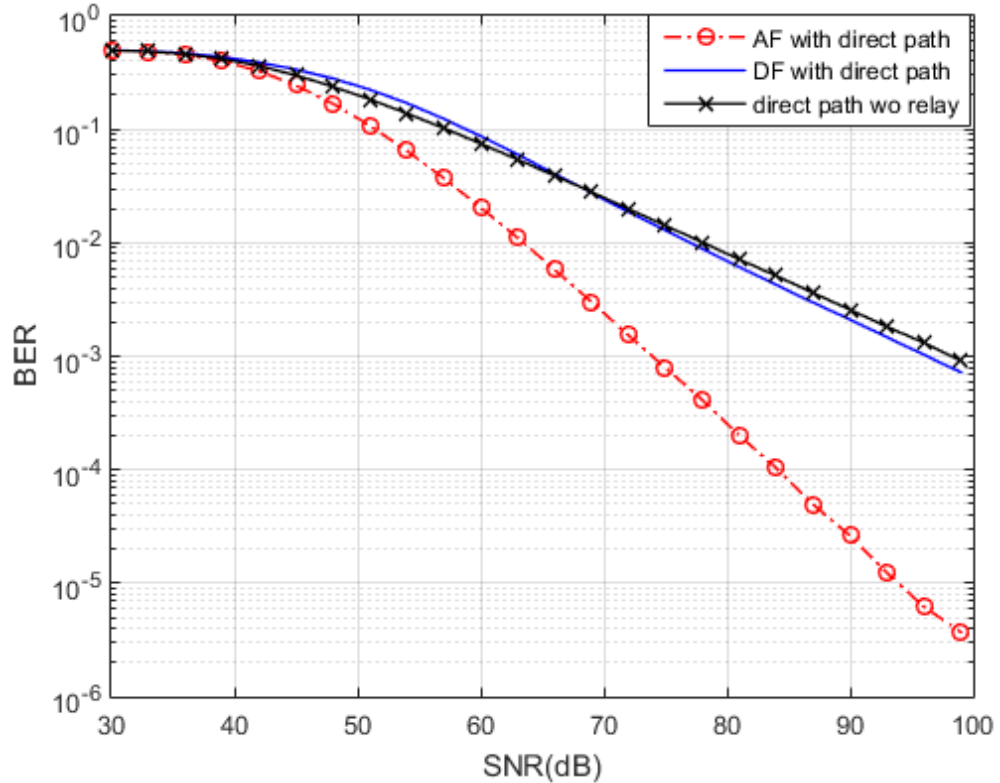


Figure 3.4 BER vs. SNR for cooperative relaying for mmWaves using one AF and DF relays over 60 GHz in the presence of the direct path at distance  $(r_{SD})$  10 m.

Figure 3.5 illustrates the error probability performance for the same types stated above but at carrier frequency 73 GHz and a distance of 10 m between source and destination.

The Figure shows that the performance of three types perform similarly before 45 dB SNR; as SNR increases, the diversity AF outperforms the diversity DF and the direct path without a relay, while the diversity DF relay and the direct path perform nearly identically at all SNR values.

At BER  $10^{-3}$ , the difference in performance between diversities of DF and AF is almost 21 dB.

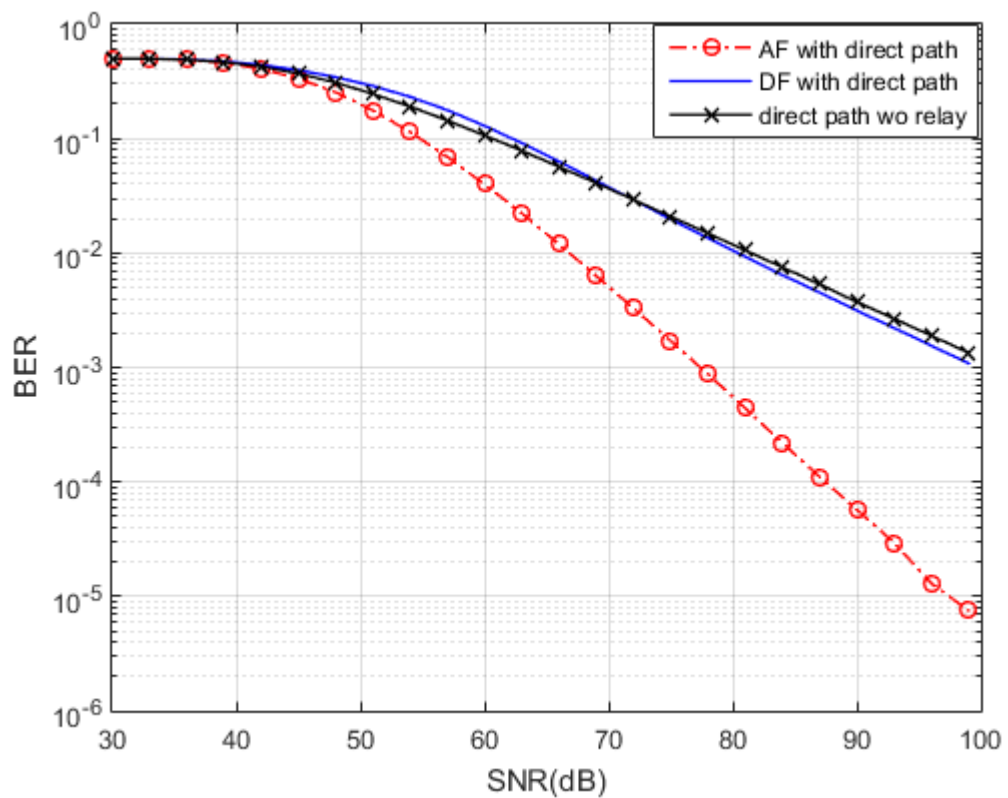


Figure 3.5 BER vs. SNR for cooperative relaying for mmWaves using one AF and DF relays over 73 GHz in the presence of the direct path at a distance ( $r_{SD}$ ) 10 m.

The error probability curves for the diversity AF "to achieve diversity gain" rise with rising frequency due to significant attenuation at high carrier frequencies, as illustrated in Figure 3.6. It demonstrates that at SNR 60 dB, the BER for 28 GHz is  $10^{-3}$ , but it is about  $10^{-1.5}$  for 73 GHz. This indicates that the performance of the 28 GHz frequency is superior to that of the other frequencies mentioned.

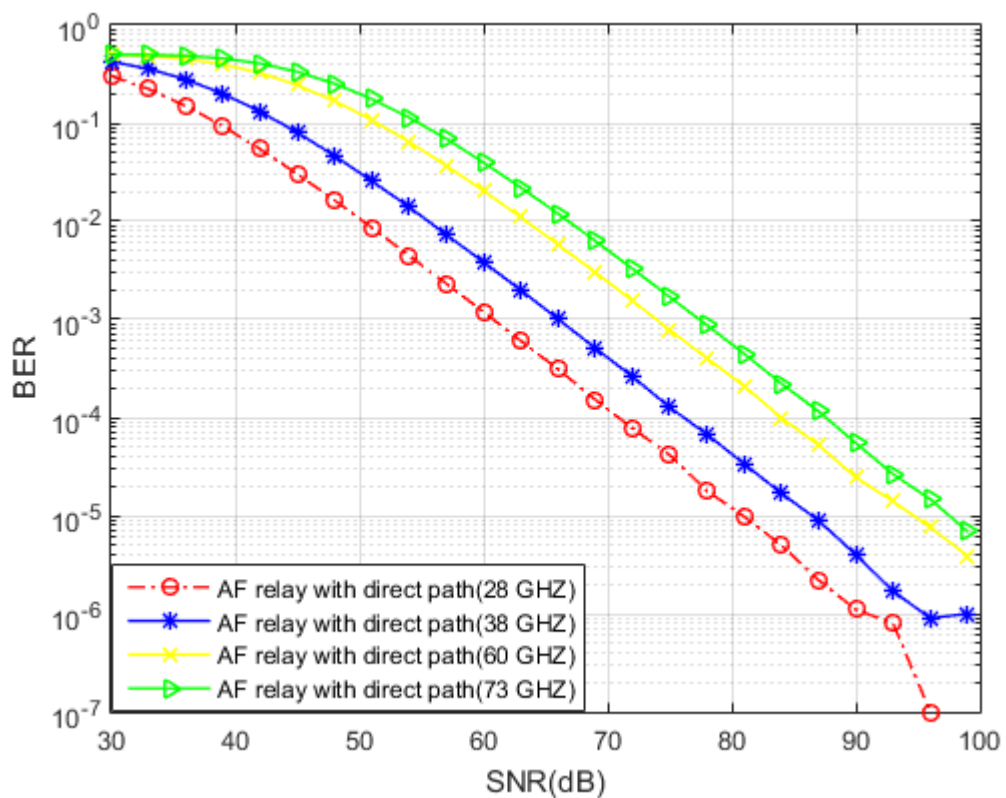


Figure 3.6 BER vs SNR for AF relay with a direct path over different frequencies at a distance of 10 m.

The error probability performance of the diversity DF at four frequencies mentioned above has been compared in figure 3.7. The figure shows at SNR 60 dB the BER for the 28 GHz about  $10^{-2}$ , whereas it is about  $10^{-1}$  for 73 GHz. This means that error probability becomes bad when increasing the carrier frequency.

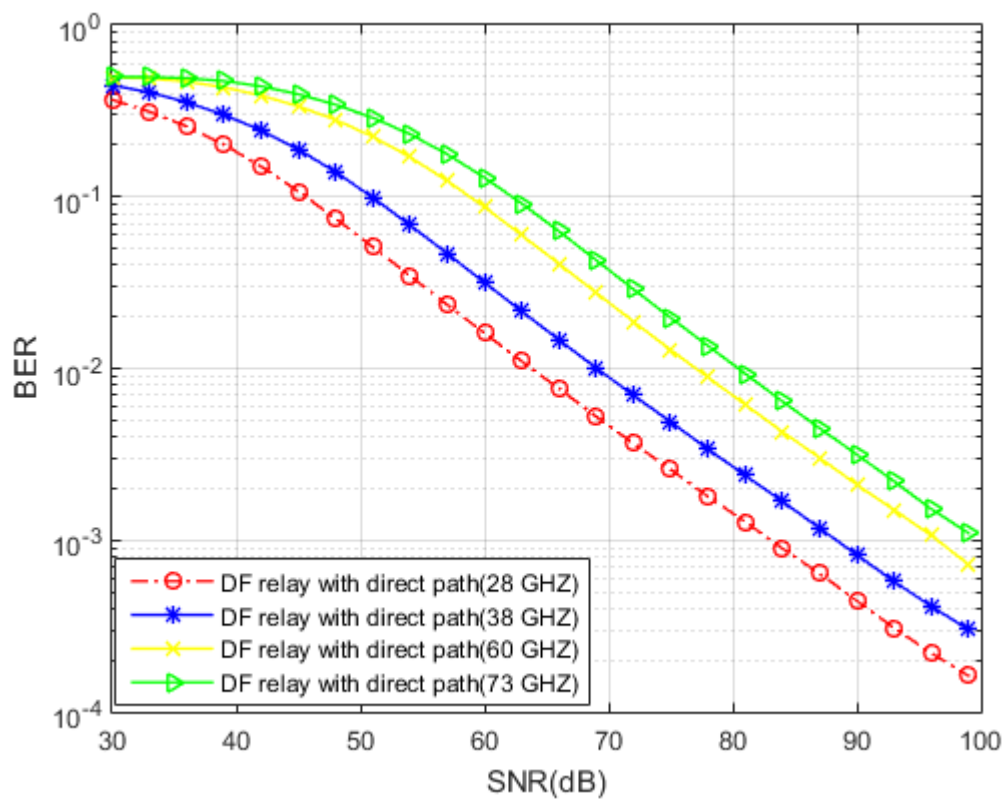


Figure 3.7 BER vs SNR for DF relay with a direct path over different frequencies at a distance of 10 m.

The error probability performance of two cooperative relaying systems (dual-hop AF and DF with direct path) has been compared in figure 3.8; one operates at 28 GHz and the other at 73 GHz; also, the source and destination distances for both systems are considered to be 10 m.

The figure demonstrates two results: first, that the system operating at 28GHz has a better error probability performance than the system operating at 73GHz, and second, that despite noise propagation, the diversity owing to amplified and forward relaying with the direct path is proven to be generally better than that of decoded relaying. This significant and rather unexpected finding is because amplified relaying channels do not suffer from the weakest-link problem that decoded relaying channels do, in which decoding failures on any single-hop propagate along the channel.

Additionally, it shows that at SNR 60 dB, the BER of an diversity AF is  $10^{-3}$  at 28 GHz, but it is about  $10^{-1.5}$  at 73 GHz. The performance difference between 73GHz and 28GHz is approximately 18 dB at BER  $10^{-3}$  for the same type of relaying protocol (AF relay with direct path).

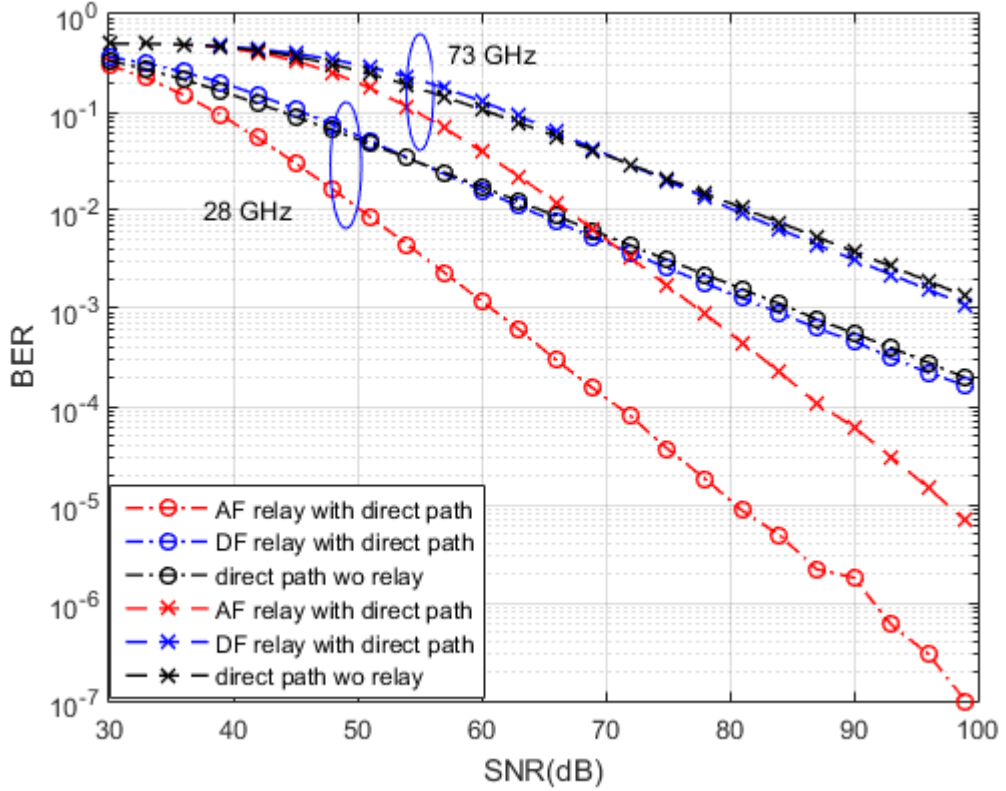


Figure 3.8 BER vs. SNR for cooperative relaying for mmWaves using one AF and DF relays over 28 and 73 GHz in the presence of the direct path.

### 3.3 Comparison of the simulation results of dual-hop systems using two parallel AF and DF relays over mm-wave frequencies (28 GHz, 38 GHz, 60 GHz, 73 GHz)

The error probabilities of cooperative communication systems consisting of two relays located halfway between the source and the destination in parallel with a direct path have been compared in this subsection, as shown in schemes in section 2.5. The relaying protocols are AF and DF, and the distance between the source and destination ( $r_{SD}$ )

assumed to be 10 m, and  $(r_{SR1}), (r_{R1D}), (r_{SR2}), (r_{R2D})$ , have the same distances equal 6 m.

Where  $(r_{SR1}), (r_{R1D}), (r_{SR2}),$  and  $(r_{R2D})$  are the distances from  $S \rightarrow R1, R1 \rightarrow D, S \rightarrow R2,$  and  $R2 \rightarrow D$ , respectively.

The following figures (3.9, 3.10, 3.11, 3.12) show the error probability results for the schemes that are illustrated in Fig. 2.15 and Fig. 2.16, which are used 2 AF relays with the direct path and 2 DF relays with the direct path, respectively, over mm-wave frequencies (28 GHz, 38 GHz, 60 GHz, 73 GHz).

As illustrated in Figure 3.9, the error probability values for two AF relays with direct path (diversity AF), two DF relays with direct (diversity DF), and the direct path without a relay are relatively similar at low SNR ( $< 30\text{dB}$ ), but as SNR increases, the performance of AF relay with direct path outperforms both the DF relay with the direct path and the direct path without a relay.

Furthermore, it illustrated that the curves of the DF relays with direct path and direct path without relays have nearly identical performances at all values of SNR. The difference in performance between two DF relays with two AF relays performance is almost 20dB at BER  $10^{-2}$  when the carrier frequency 28 GHz and distance  $(r_{SD})$  10 m.

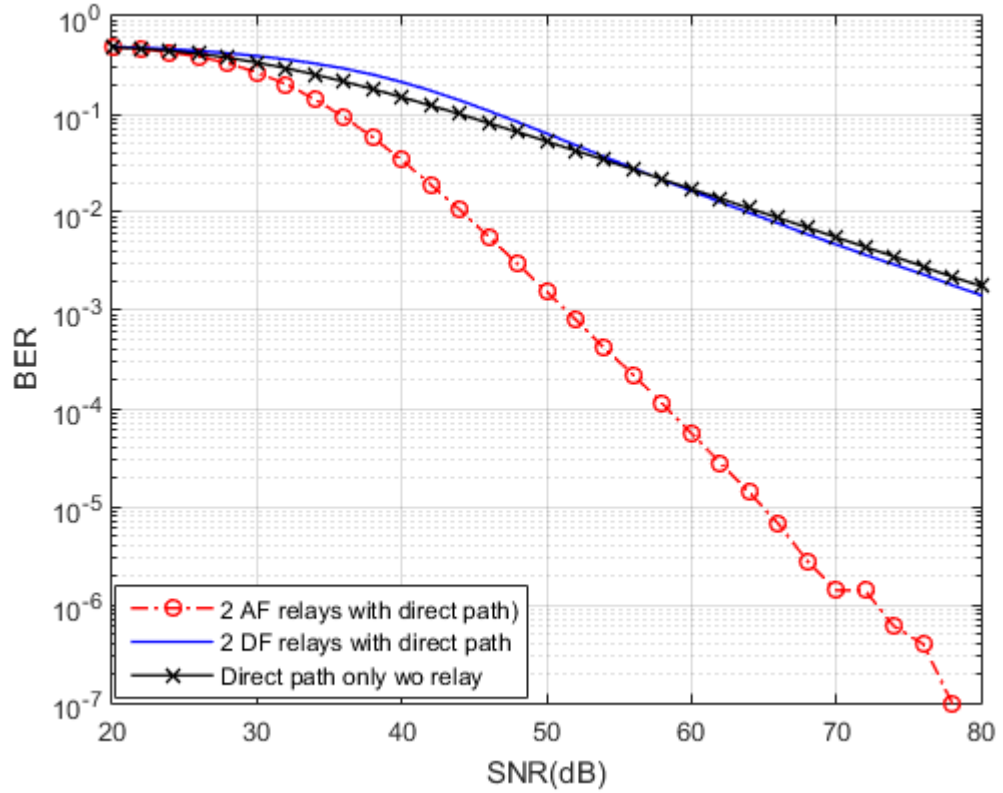


Figure 3.9 BER vs SNR for cooperative relaying for mmWaves using two AF and DF relays in parallel with the direct path over 28 GHz frequency at a distance ( $r_{SD}$ ) 10 m.

The error probability performance results of the types stated above over carrier frequency 38 GHz and distance 10 m between the source and destination are shown in Figure 3.10. This figure demonstrates that both types of relays and the direct path perform similarly at low SNR (34dB), as SNR increases, the diversity AF relays outperform the diversity DF relays and the direct path without relays, while the diversity DF relays and the direct path perform nearly identically at all SNR values.

At BER  $10^{-2}$ , the difference in performance between two DF relays and two AF relays is almost 20 dB.

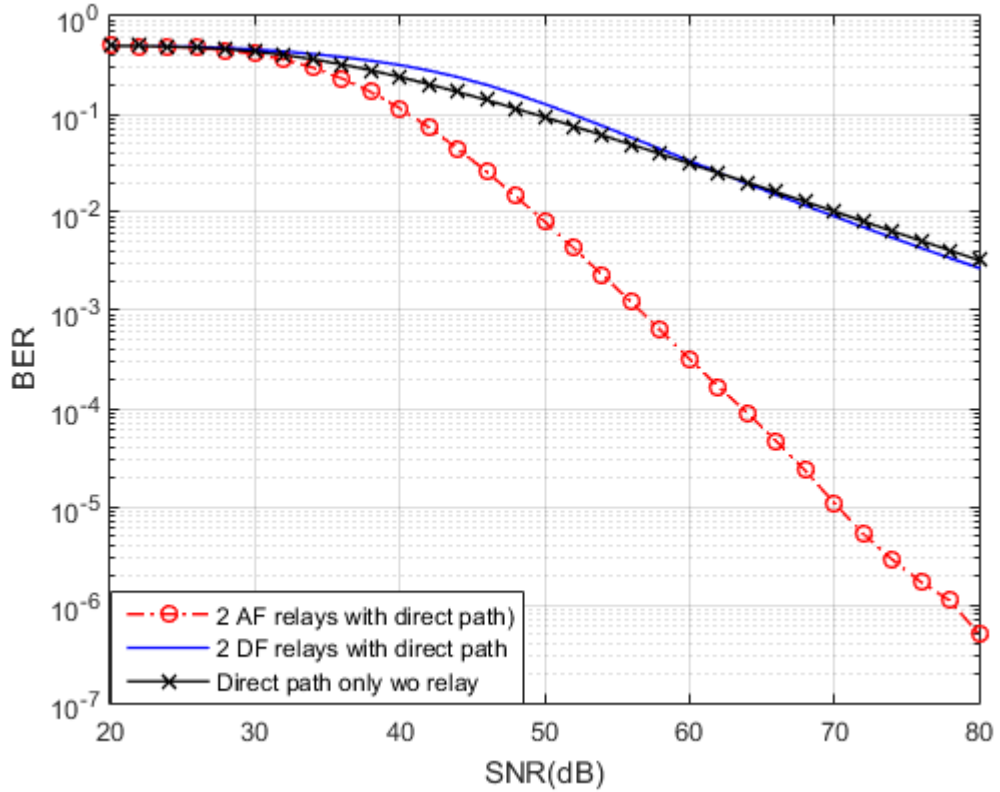


Figure 3.10 BER vs. SNR for cooperative relaying for mmWaves using two AF and DF relays in parallel with the direct path over 38 GHz frequency at distance ( $r_{SD}$ ) 10 m.

Figure 3.4 illustrates the error probability performance of the three types mentioned before but at a carrier frequency of 60 GHz and a distance of 10 m between the source and destination. The two types of relays and the direct path have error probability performance virtually identical before 40 dB SNR; however, as SNR increases, the diversity AF relays outperforms the diversity DF relays and the direct path without a relay. Furthermore, for all SNR values, the diversity DF relays and direct path perform nearly identically.

There are around 20 dB worth of variation in performance between two DF relays and two AF relays at BER  $10^{-2}$ .

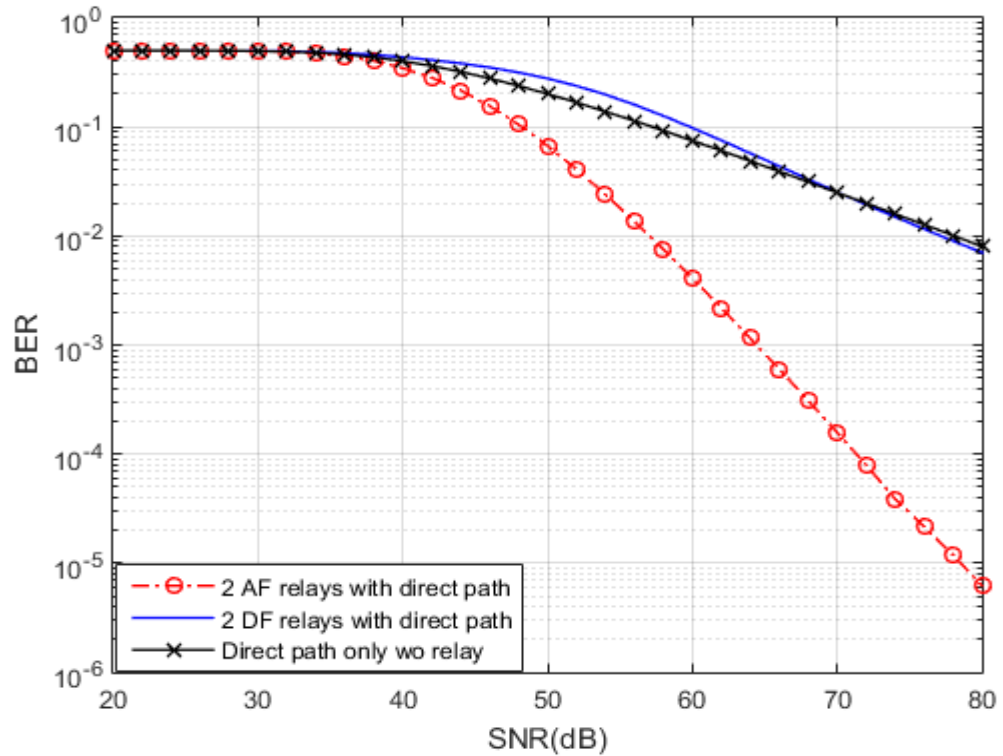


Figure 3.11 BER vs. SNR for cooperative relaying for mmWaves using two AF and DF relays in parallel with the direct path over 60 GHz frequency at a distance ( $r_{SD}$ ) 10 m.

Using a carrier frequency of 73 GHz and a distance of 10 m between the source and destination, Figure 3.5 shows the error probability performance of diversities AF and DF relays, and a direct path without relays.

In the figure, it can be seen that the performance of diversity AF relays, diversity DF relays, and the direct path is similar before 43 dB SNR. However, as SNR increases, the diversity AF relays outperforms the diversity DF relays and the direct path without relays.

It is nearly 20 dB between the performance of two DF relays and two AF relays at BER  $10^{-2}$ .

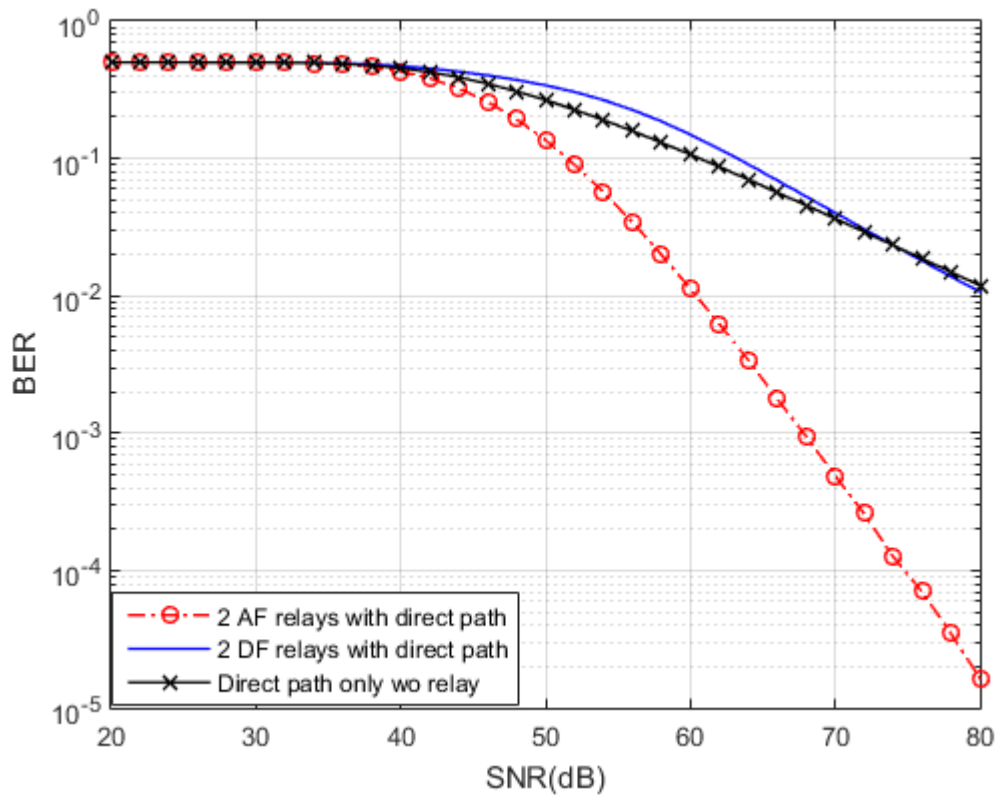


Figure 3.12 BER vs SNR for cooperative relaying for mmWaves using two AF and DF relays in parallel with the direct path over 73 GHz frequency at a distance ( $r_{SD}$ ) 10 m.

As seen in Figure 3.13, the error probability curves of two AF relay with the direct link increase with increasing frequency as a result of severe attenuation at high carrier frequencies.

The curves illustrate that at SNR 60 dB, the BER for 28 GHz is about than  $10^{-4.5}$ , but the BER for 73 GHz is approximately  $10^{-2}$ . This demonstrates that the performance of the 28 GHz frequency is superior to the performance of the other frequencies discussed previously.

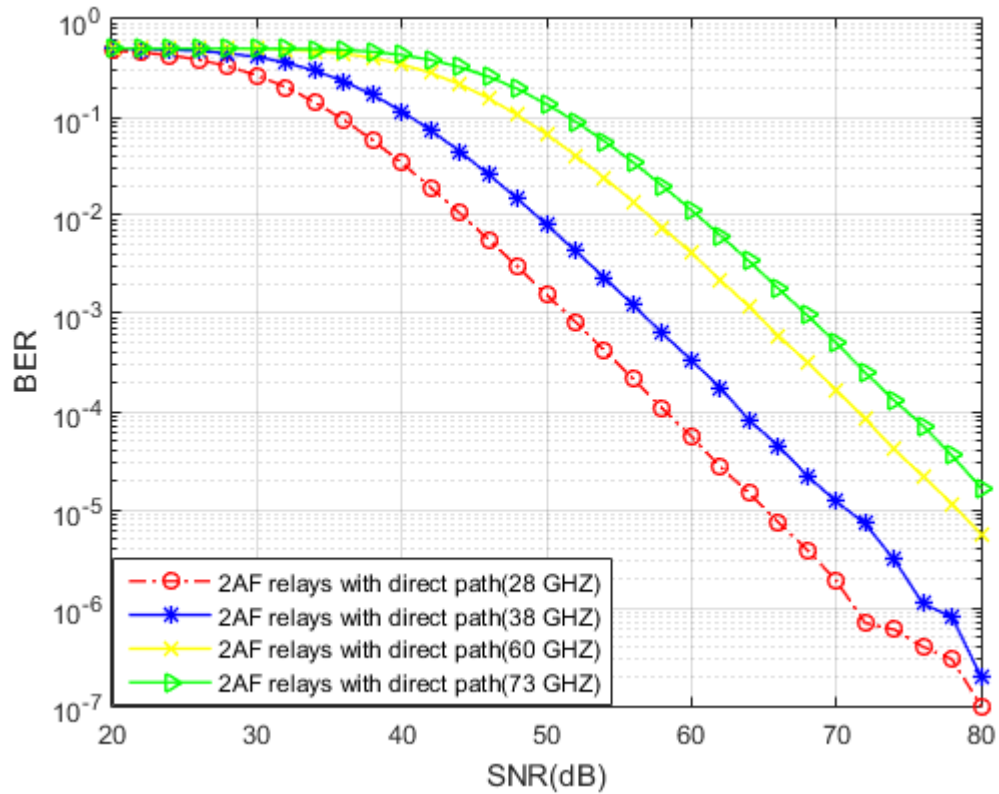


Figure 3.13 BER vs. SNR for two AF relays with direct path over different frequencies at distance 10 m.

The error probability performance of the two DF relaying protocols with the direct path at the four frequencies discussed before is depicted in Figure 3.14.

The figure illustrates that the difference in performance between 73 GHz and 28 GHz at BER  $10^{-2}$  is about 16 dB.

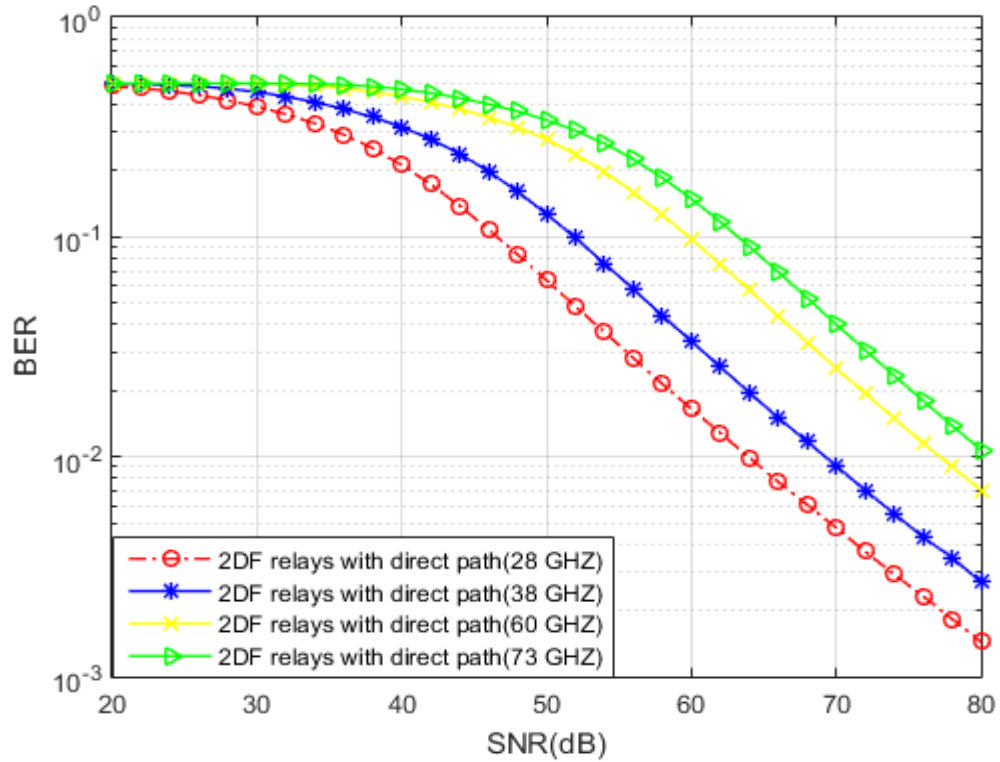


Figure 3.14 BER vs. SNR for two DF relays with direct path over different frequencies at distance 10 m.

Two cooperative communication systems with a single source, a single destination, and two relays (AF and DF) placed in parallel with the direct line have been assumed. When it comes to frequency, the first operates at 28 GHz while the second operates at 73 GHz; also, the source and destination distances for both systems are considered to be 10 m.

The error probability performance of these systems is illustrated in Fig. 3.15, which shows that two AF relays with the direct path outperform two DF relays with the direct path; additionally, the system operating at 28GHz has a higher BER-SNR than the system operating at 73 GHz. Furthermore, it demonstrates that the performance gap between 73GHz and 28GHz is

around 15 dB at BER  $10^{-3}$  for the same type of relaying protocol (AF relay with direct path) when comparing the two frequencies.

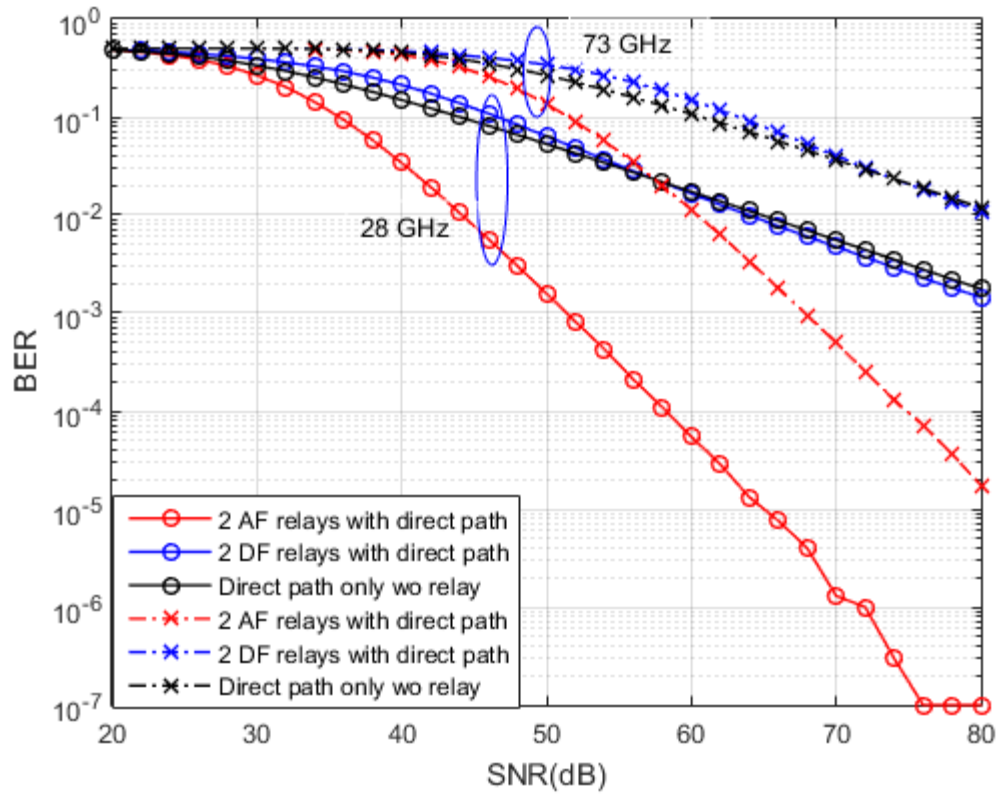


Figure 3.15 BER vs. SNR for cooperative relaying for mmWaves using two AF and DF relays with the direct path over 28 and 73 GHz at distance 10 m.

### **3.4 Comparison of the simulation results for the dual-hop systems that are using one and two parallel AF and DF relay over 28 GHz**

Comparisons have been made between the performance of the systems depicted in Figures 2.13 and 2.14, which each consist of one AF and DF relay located halfway between the source and destination, and the performance of those systems consisting of two relays located in parallel with the direct path shown in Figures 2.15 and 2.16.

The distance between the source and destination is 10 meters and the carrier frequency 28 GHz in both cases.

Figure 3.16 illustrates that the error probability for the system with two AF relays with a direct path is better than the error probability for the system with one AF relay with a direct path; additionally, the DF relays in both schemes did not add any significant compensation to the signals when compared to the AF relays. This is demonstrated by the curves, which show that the BER of two AF relays with a direct path is about  $10^{-4}$  at SNR 60 dB, whereas the BER of one AF relay with a direct path is  $10^{-2}$ ; and it is estimated that the performance difference between one AF relay and two AF relays at BER  $10^{-3}$  is roughly 8 dB.

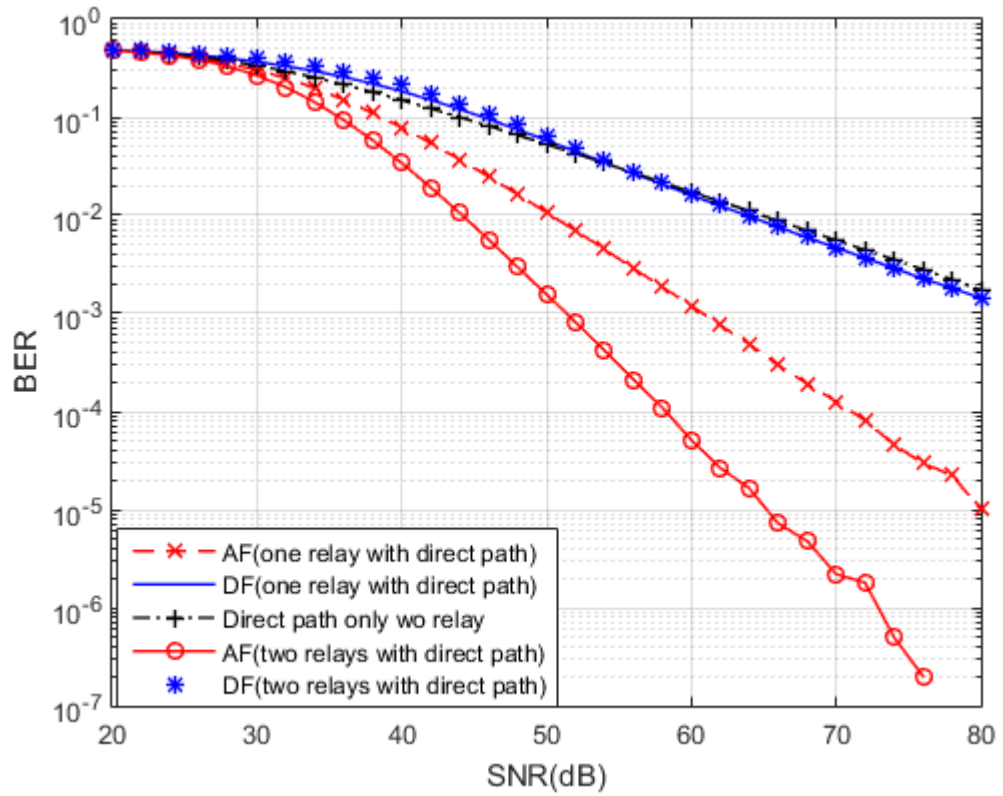


Figure 3.16 BER vs. SNR for cooperative relaying for mmWaves using one and two parallel AF and DF relays over 28 GHz in the presence of the direct path at a distance 10 m.

## Chapter Four

### Modeling of outdoor mmWave Channels

#### 4.1 Introduction

It is proposed in this thesis that the wireless system model under investigation is a dual-hop relay-based system with a single source (S), a single destination (D), and either one or two relays in parallel between the source and the destination in the presence of a direct path.

To facilitate the outdoor communication between the source and destination and to obtain higher data rates over 28, 38, and 73 GHz waves, the system model includes AF and DF relaying protocols, which has been classification in Figure 3.1. In the suggested systems, binary phase-shift keying (BPSK) is used as a modulation method.

The error probability and channel capacity performance for the proposed systems shown in Figures (2.13, 2.14, 2.15, 2.16) for the outdoor environments are analyzed through simulation by using Monte-Carlo simulations via MATLAB programming.

In Monte Carlo simulations, all channels from the source to relay/relays, relay/relays to destination, source to destination are generated using the reference path loss model (close-in free space reference distance (CI) model  $d_0 = 1\text{m}$ ) according to equation (2.3) that has been explained in chapter two.

The parameters (FSPL( $d_0$ ),  $n$ ,  $\sigma$ ) of this model are shown in Table 2.3. These parameters are the results of measurements made in different campaigns in New York City at frequencies 28, 38, 73 GHz [21][30]. Where the 28 GHz and 73 GHz outdoor propagation measurements were conducted in downtown Manhattan around the NYU campus, and 38 GHz outdoor propagation measurements in Austin. The parameters of the proposed path

loss model are adopted in this chapter to study the BER and capacity performance over outdoor mmWave channels.

The following paragraphs explain the comparison of the simulation results of dual-hop AF and DF relay systems over mm-wave frequencies (28 GHz, 38 GHz, and 73 GHz), comparison of the simulation results of dual-hop systems using two parallel AF and DF relays over mm-wave frequencies (28 GHz, 38 GHz, and 73 GHz), and comparison of the simulation results for the dual-hop systems that are using one and two parallel AF and DF relay over 28 GHz.

## **4.2 Comparison of the simulation results of dual-hop AF and DF relay systems over mm-wave frequencies (28 GHz, 38 GHz, 73 GHz)**

The error probability and channel capacity performance of the dual-hop schemes described in figures 2.13 and 2.14 have been compared in this part, which each employs one relay (AF and DF) located between the source and destination over mmWave frequencies 28 GHz, 38 GHz, 73 GHz. The distance from the source to the destination ( $r_{SD}$ ) is considered to be 200 m for all cases; and  $r_{SR}$ ,  $r_{RD}$  equal 110 m , 110 m, respectively.

Figure 4.1 shows the BER-SNR curves for the AF and DF cooperative communications with the direct path by using the MRC technique at the destination to achieve the diversity gain over 28 GHz operating frequency. The FSPL ( $d_0 = 1\text{m}$ ) at 28 GHz is 61.38 dB and the path loss exponent ( $n$ ) and shadow factor ( $\sigma$ ) parameters taken from the measurements performed in [21][30] for the outdoor LOS environment are 1.9 and 1.1 dB respectively.

At SNR values less than 68dB, all curves are relatively similar in performance, but as SNR increases, the performance of the AF relay with the direct path (denotes to diversity AF)outperforms both the DF relay with the direct path (diversity DF) and the direct path without a relay, with the difference in performance between diversity DF and direct path with AF is approximately 22 dB and 38 dB, respectively at BER  $10^{-3}$ . Furthermore, the diversity DF has better performance than the direct path without a relay with the difference of 16 dB at BER  $10^{-3}$ .

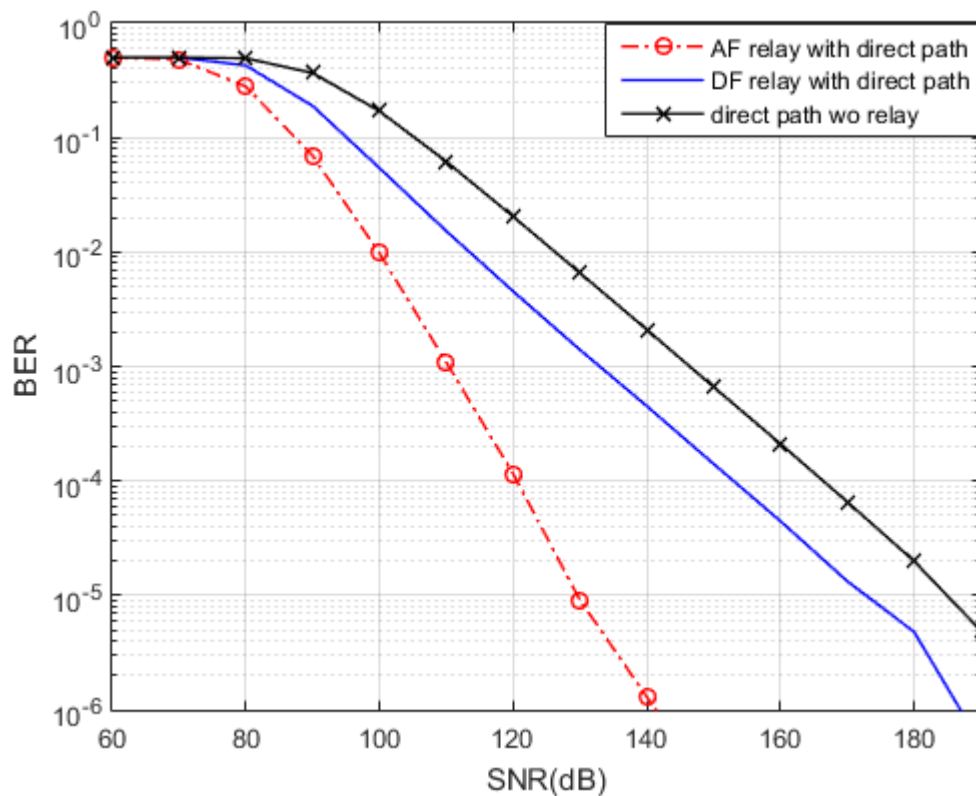


Figure 4.1 BER vs SNR for cooperative relaying for mmWaves using one AF and DF relays over 28 GHz in the presence of the direct path at a distance ( $r_{SD}$ ) 200 m.

The path loss exponent ( $n$ ) and shadow factor ( $\sigma$ ) values calculated from previous research's measurements at frequency 38 GHz are 1.9 and 4.6 dB, respectively, whereas the FSPL at the reference distance ( $d_0 = 1\text{m}$ ) is 64 dB.

The following figure illustrates the error probability performance results of the three categories discussed previously over carrier frequency 38 GHz and distance 200 m between the source and destination.

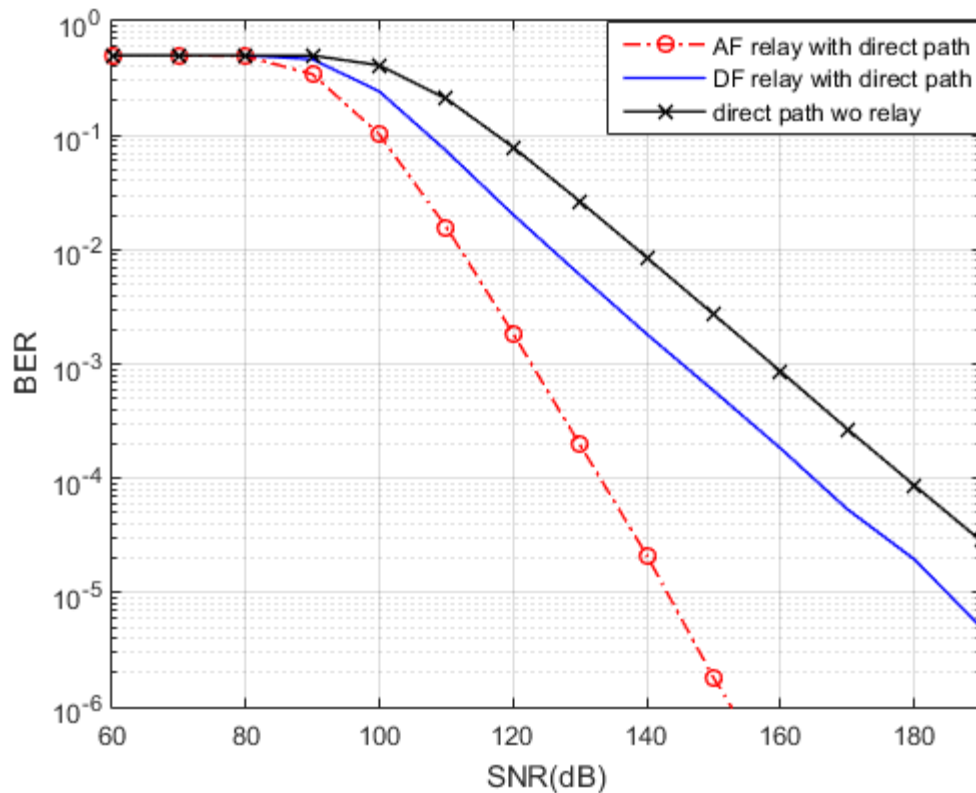


Figure 4.2 BER vs SNR for cooperative relaying for mmWaves using one AF and DF relays over 38 GHz in the presence of the direct path at a distance ( $r_{SD}$ ) 200 m.

The figure shows that at low SNR ( $< 80$  dB), both types of relays and the direct path have nearly identical error probability performance; however, as SNR rises, the diversity AF outperforms the diversity DF and the direct path, with the difference in performance between diversity DF and direct path with AF being approximately 24 dB and 37 dB respectively at BER  $10^{-3}$ . While the DF relay appears to perform better than the direct path with a difference of 13 dB at BER  $10^{-3}$ .

The error probability performance at 73GHz for three categories shown in Figure 4.3, where the FSPL, path loss exponent ( $n$ ), and shadow factor ( $\sigma$ ) are 69.7dB, 2.4, and 6.3dB, respectively.

The Figure illustrates that the three categories discussed previously have similar performance levels before 85 dB SNR; as SNR increases, the diversity AF also outperforms the diversity DF relay and the direct path without a relay in this band, with the performance difference between the diversity DF relay and the direct path with AF relay, is roughly 21 dB and 39 dB at BER  $10^{-3}$ , respectively.

On the other hand, the DF relay has better performance than the direct path, and at BER  $10^{-3}$  the difference in performance is almost 18 dB.

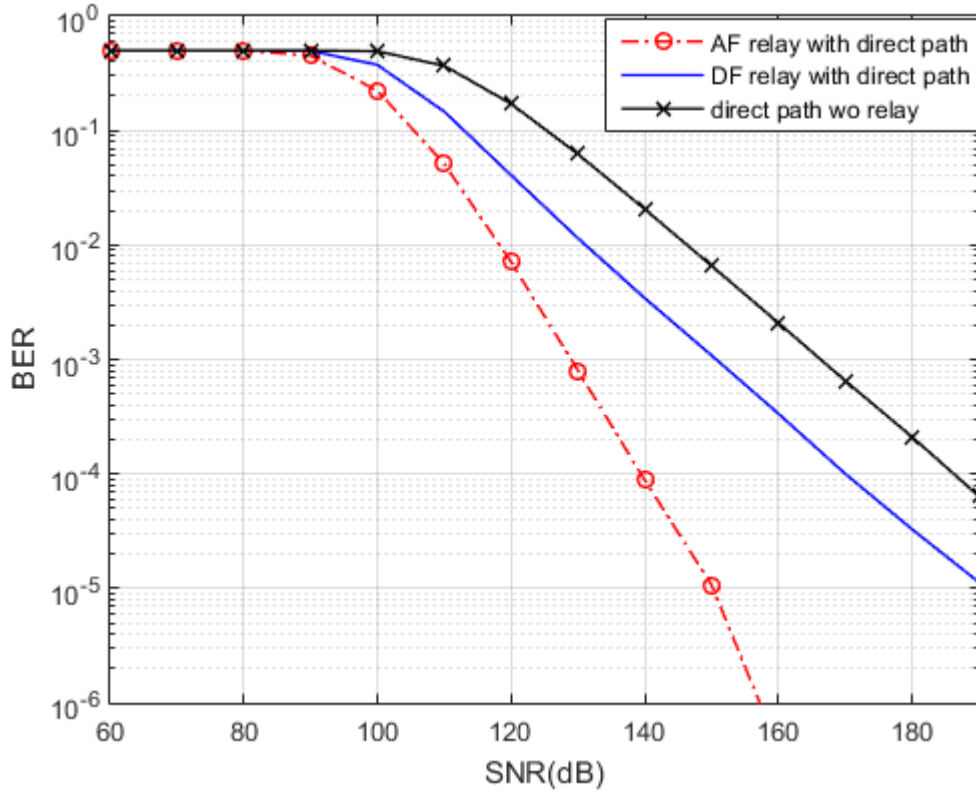


Figure 4.3 BER vs SNR for cooperative relaying for mmWaves using one AF and DF relays over 73 GHz in the presence of the direct path at a distance ( $r_{SD}$ ) 200 m.

The error probability curves for the AF relaying protocol with the direct link increase with increasing frequency due to significant attenuation at high carrier frequencies, as illustrated in Figure 4.4. It demonstrates that at SNR 120 dB, the BER for 28 GHz is  $10^{-4}$ , while it is about  $10^{-2}$  for 73 GHz. This indicates that the performance of the 28 GHz frequency is superior to that of the other frequencies mentioned.

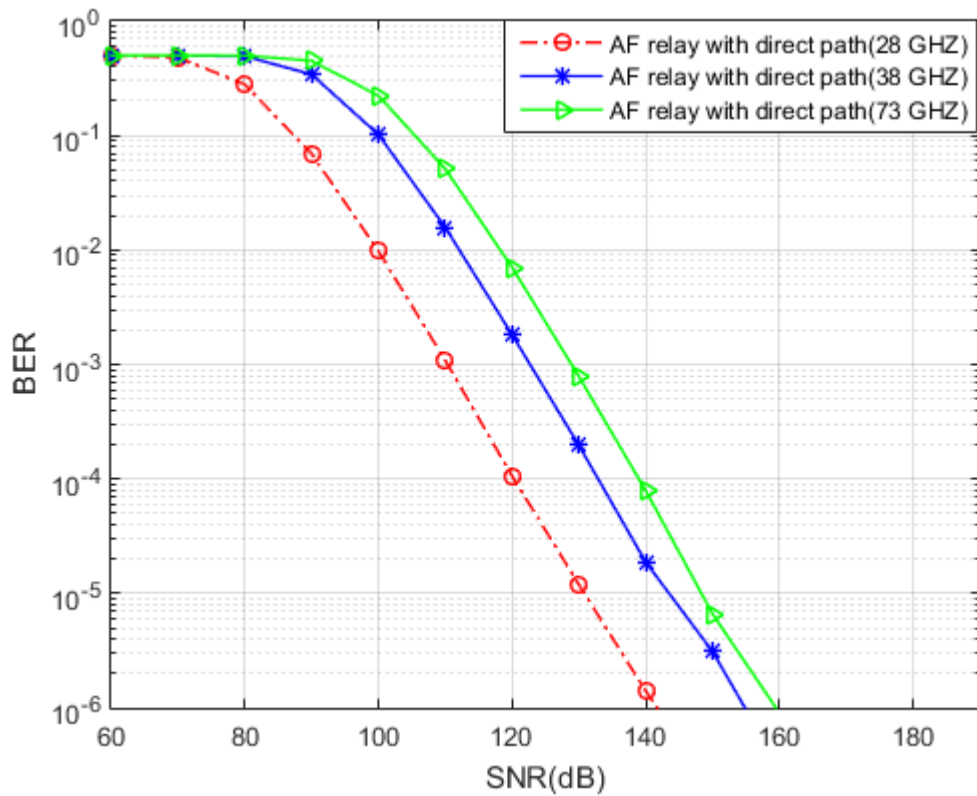


Figure 4.4 BER vs SNR for AF relay with a direct path over different frequencies at a distance of 200 m.

Figure 4.5 compares the error probability performance of the DF relaying protocol with the direct path at the four frequencies stated. At SNR 120 dB, the BER for 28 GHz is about  $10^{-2.5}$ , whereas it is about  $10^{-1.5}$  for 73 GHz. This means that as the carrier frequency increases, the error probability increase.

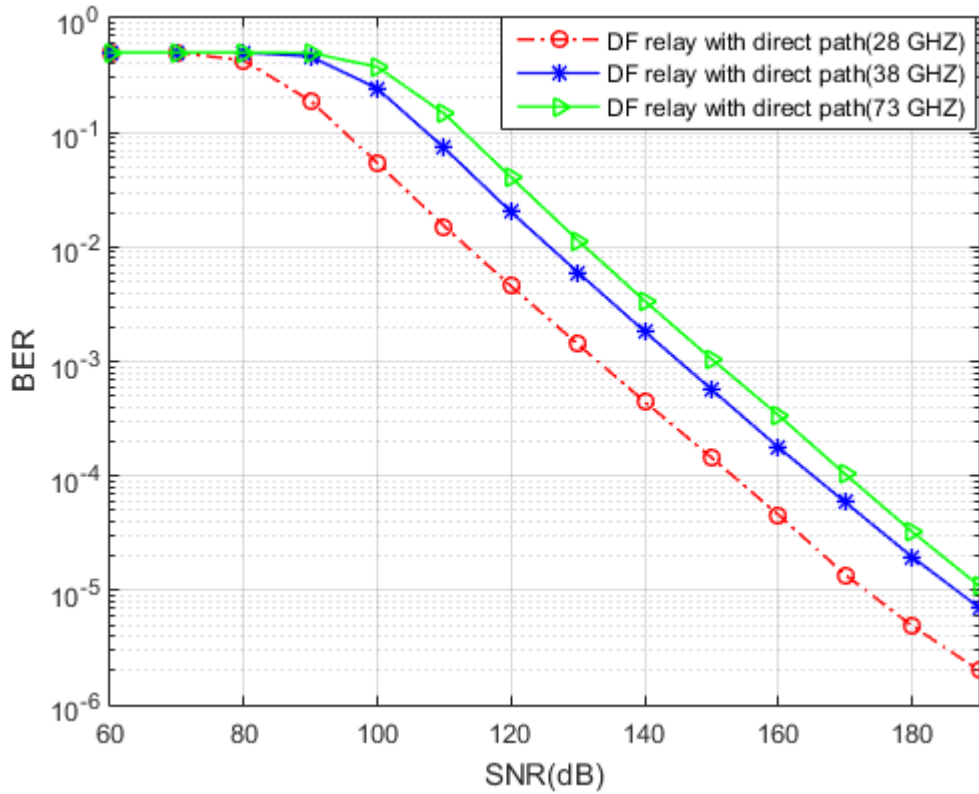


Figure 4.5 BER vs SNR for DF relay with a direct path over different frequencies at a distance of 200 m.

As demonstrated in Figure 4.6, the error probability curves for the direct path become higher as the frequency of the carrier increases. This is owing to the substantial attenuation at high carrier frequencies. It reveals that at SNR 120 dB, the BER for 28 GHz and 73 GHz is about  $10^{-2}$ ,  $10^{-1}$  respectively. This demonstrates that the performance of the 28 GHz frequency is superior to the performance of the other frequencies discussed previously.

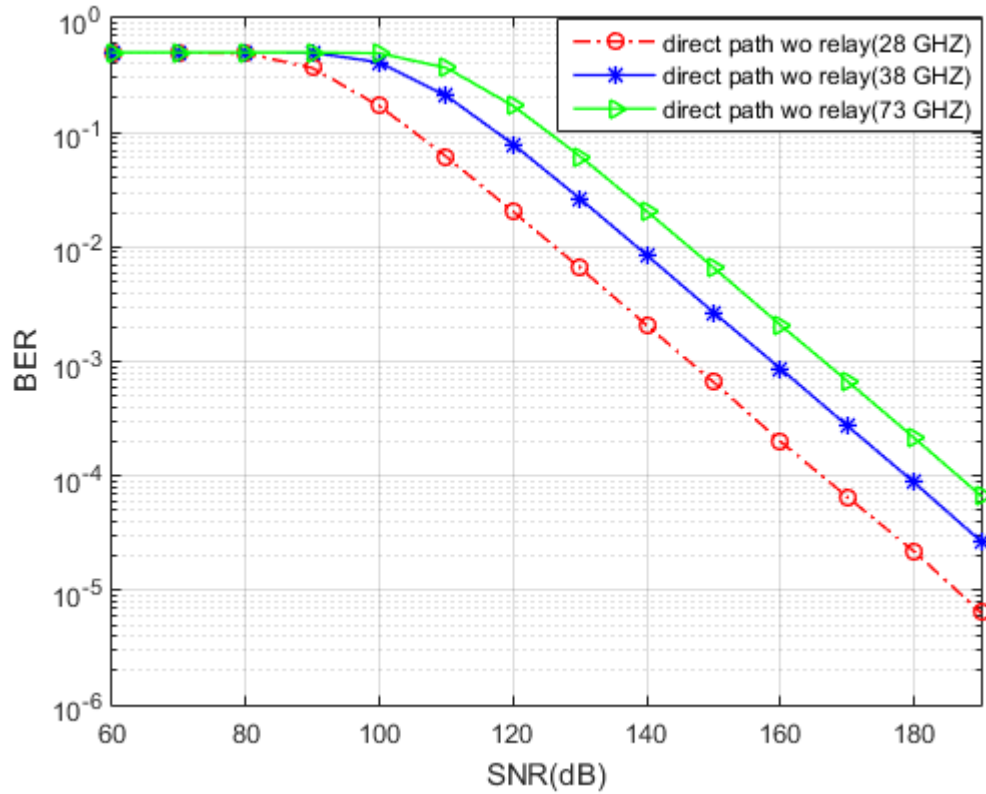


Figure 4.6 BER vs SNR for the direct path without relay over different frequencies at a distance of 200 m.

As previously stated, millimeter waves cannot pass long distances due to the substantial attenuation caused by their high frequency. As a result, cooperative communications via relays were used to compensate for attenuation and to shorten lengthy distances.

Several prior research revealed that the millimeter waves at 28 and 73 GHz could be detected at least 100 m to 200 m distance from source to destination [57][30].

The BER-SNR performance of cooperative communications systems operate at 28 GHz is illustrated in Figure 4.8 for source-destination separations of 100 meters and 200 meters. The figure shows that the BER-SNR performance is better at 100 meters than at 200 meters. Additionally, the

figure shows that all curves have similar BER-SNR performance before 60 dB SNR; then after this value, the curve of diversity AF for the distance 100m outperforms the other curves; also the difference in performance between AF relays, DF relays, and direct path for the distance 200m and 100 is about 12 dB, 12dB and 11dB respectively at BER  $10^{-3}$ .

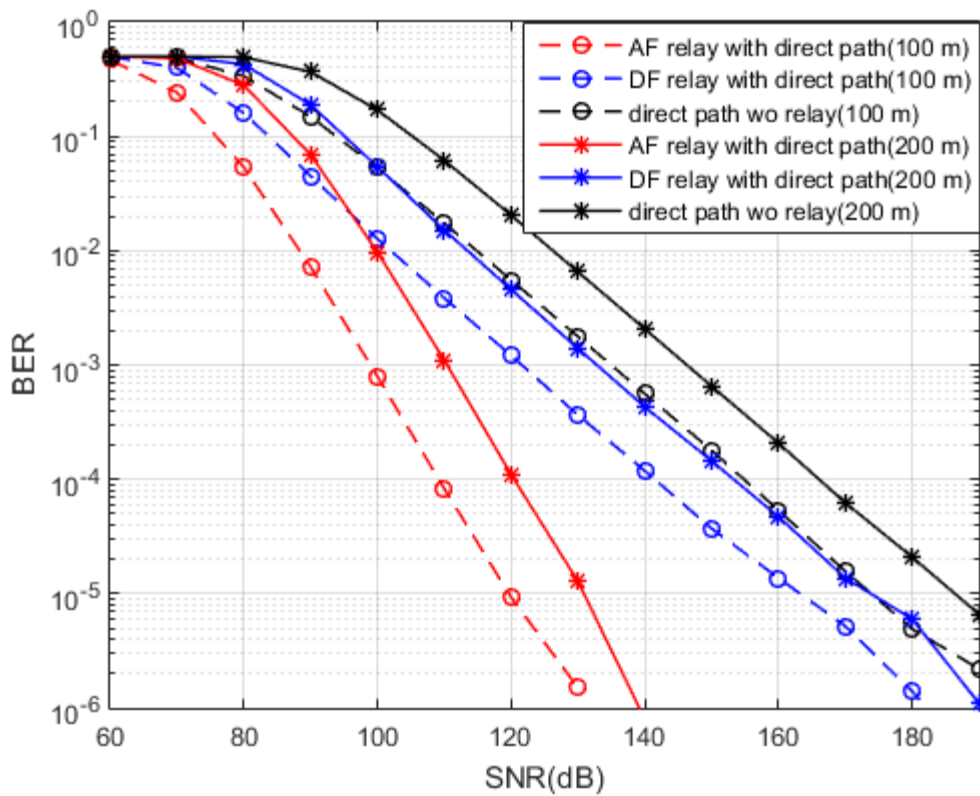


Figure 4.7 BER vs SNR for the two cooperative relaying systems for mm Waves using one AF and DF relays over 28 at a distance 100 m and 200 m.

As for other frequencies, such as the 73 GHz, the distance must be reduced to less than 200 meters, or the number of antenna elements should be increased to obtain results or performance close to the performance of systems operating at frequency 28 [30].

When the distance is reduced to 100 m (73 GHz), the error probability performance for three types (diversity AF, diversity DF, and direct path) is quite similar to that at 28 GHz when the distance 200 m, as shown in Figure 4.8.

At BER  $10^{-3}$ , the difference in performance between identical types but with different frequencies is approximately 6 dB, 5 dB, and 6 dB, respectively.

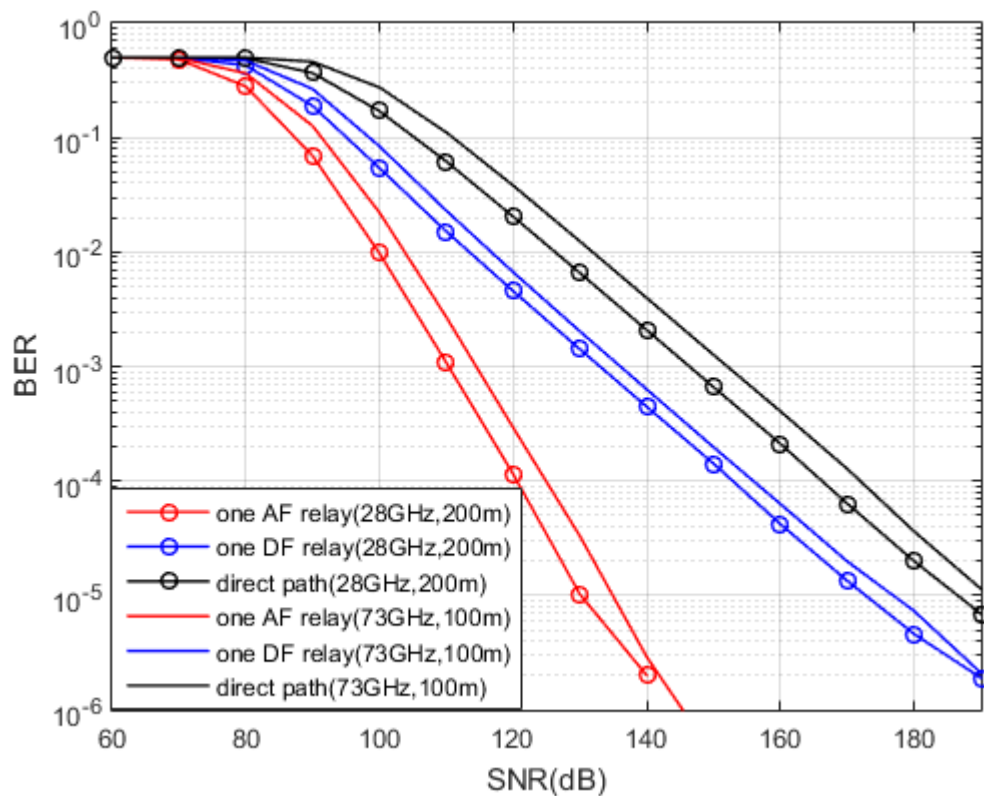


Figure 4.8 BER vs SNR for cooperative relaying for mmWaves using one AF and DF relays over 28 and 73 GHz at a distance 200 and 100 m, respectively.

The simulation results of AF relay, DF relay, diversity AF, diversity DF, and the direct path (without relay) in terms of channel capacity of BPSK as a function of SNR over 28 GHz frequency and distance ( $r_{SD}$ ) 200 m have been shown in figure 4.9.

From analyzing this graph, it is shown that the performance of all protocols is very close in low SNR ( $< 40$  dB), but with increasing SNR, diversity DF outperforms (DF relay with the direct path) the other protocols, i.e. one DF relay, diversity AF (AF relay with the direct path), one AF relay, and the direct path without a relay.

As illustrated in this figure, the difference in performance between the diversity AF and diversity DF relays at 3 bit/s/Hz capacity is around 6 dB SNR, while the direct path performance degrades with a difference of roughly 12 dB compared to the diversity DF relay at the same value of capacity. In contrast, the DF relay and diversity AF performance is relatively similar, and both have better performance than the direct path.

At 70 dB SNR the channel capacity for the direct path, AF relay, diversity AF, DF relay, and diversity DF are 3 bit/s/Hz, 3.3 bit/s/Hz, 3.8 bit/s/Hz, 4 bit/s/Hz, and 5 bit/s/Hz respectively.

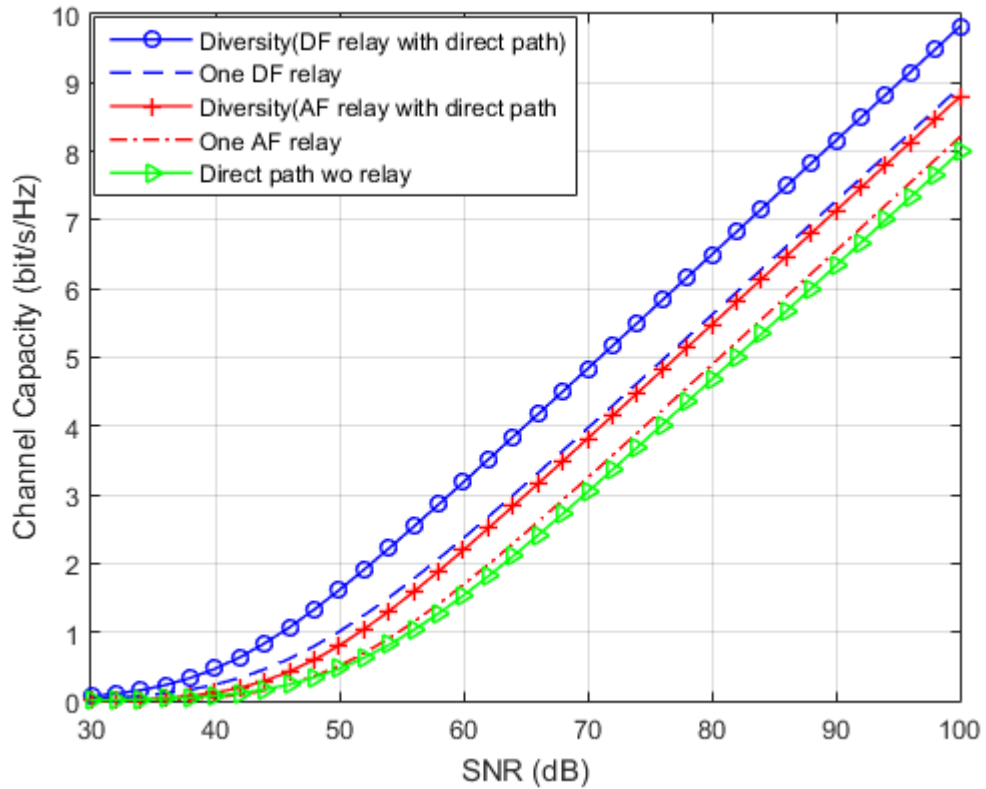


Figure 4.9 Channel capacity of cooperative diversity protocols at 28 GHz.

A comparison of the channel capacity of one AF relay, one DF relay, and the direct path without relay in terms of SNR values for mmWave frequencies of 28 and 73 GHz is shown in figure 4.10. The figure shows two outcomes, the first that 28GHz has better channel capacity performance than 73GHz due to an increase in the path loss exponent at 73 GHz, while the second shows the outperform of DF relay over AF relay and the direct path.

At 70 dB SNR, the channel capacities for the direct path, AF relay, and DF relay at the 73 GHz are 1.5 bit/s/Hz, 2 bit/s/Hz, 2.7 bit/s/Hz respectively, whereas the values at 28 GHz frequency are 3 bit/s/Hz, 3.3 bit/s/Hz, and 4 bit/s/Hz respectively.

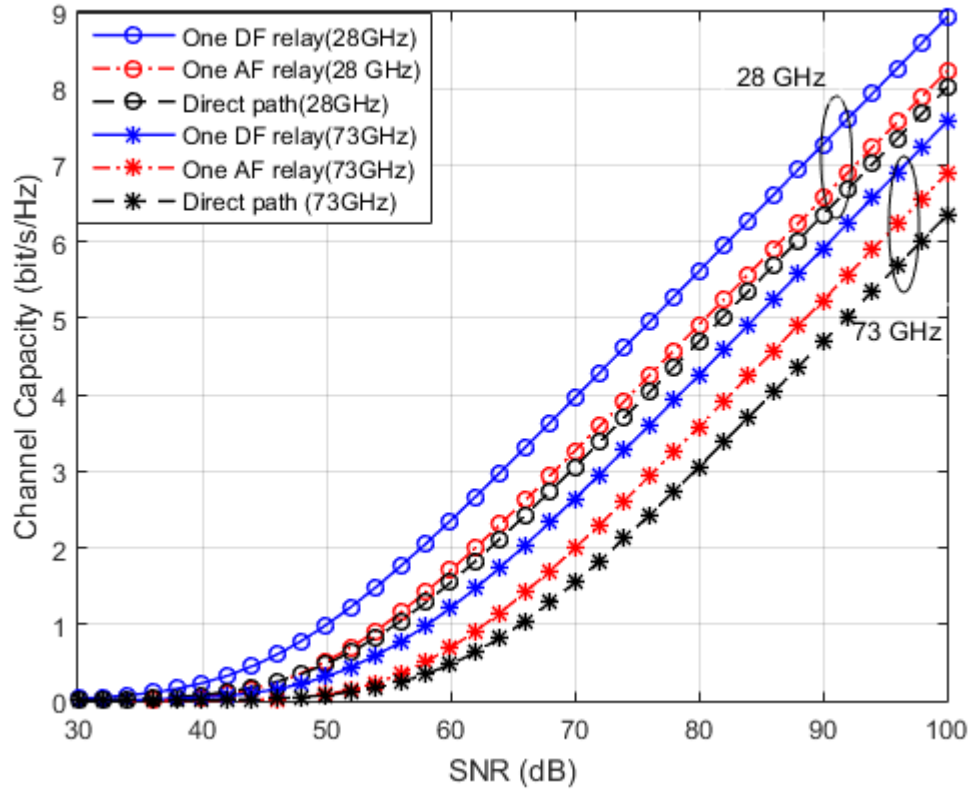


Figure 4.10 Comparison of channel capacity of one AF, one DF relay, and direct path over mm-wave frequencies 28 GHz and 73 GHz.

### 4.3 Comparison of the simulation results of dual-hop systems using two parallel AF and DF relays over mm-wave frequencies (28 GHz, 38 GHz, 73 GHz)

The error probability performance of cooperative communication systems consisting of two relays between the source and the destination in parallel with a direct path have been compared in this subsection over the mm-wave frequencies 28 GHz, 38 GHz, 73 GHz, as shown in figures 2.15 and 2.16. The relaying protocols are AF and DF, and the distance between the source and destination ( $r_{SD}$ ) assumed to be 200 m, and ( $r_{SR1}$ ), ( $r_{R1D}$ ),

$(r_{SR2}), (r_{R2D})$ , all of them have the same values equal to 110 m.

As illustrated in Figure 4.11, the BER-SNR curves for the two AF and two DF relays with the direct path using the MRC technique at the destination to achieve the cooperative diversity (diversity gain) over 28 GHz operating frequency.

The parameters of the reference path loss model for the outdoor LOS environment used to model the mmWave channels between the nodes are the same values used at frequency 28GHz in the previous subsection. i.e. The FSPL ( $d_0 = 1\text{m}$ ), path loss exponent ( $n$ ), and shadow factor ( $\sigma$ ) are 61.38 dB, 1.9 and 1.1 dB respectively.

At SNR values less than 68dB, all curves are relatively similar in performance, but as SNR increases, the performance of the two AF relays with the direct path (diversity AF relays) outperforms both the two DF relays with the direct path (diversity DF relays) and the direct path without a relay, with the difference in performance between diversity DF and direct path with diversity AF are approximately 34 dB and 50dB, respectively at BER  $10^{-3}$ . Furthermore, diversity DF relays with a direct path has better performance than the direct path without relays with the difference of 16 dB at BER  $10^{-3}$ .

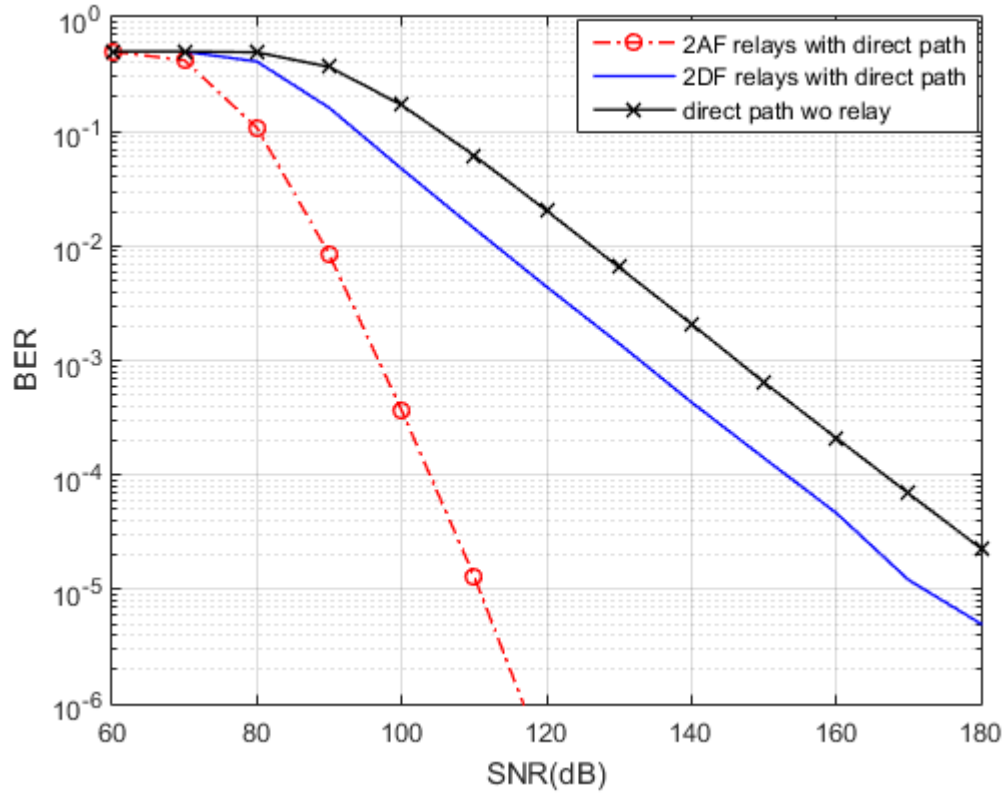


Figure 4.11 BER vs. SNR for cooperative relaying for mmWaves using two AF and DF relays in parallel with the direct path over 28 GHz frequency at a distance 200 m.

The parameters of the reference path loss model FSPL ( $d_0 = 1\text{m}$ ), path loss exponent ( $n$ ), and shadow factor ( $\sigma$ ) for the outdoor LOS environment at frequency 38 GHz are 64 dB, 1.9, and 4.6 dB respectively[21][30].

The following figure illustrates the BER comparison for the all types mentioned before at 38 GHz carrier frequency and distance 200 m between the source and destination. The figure shows that at low SNR ( $< 80\text{ dB}$ ), both types of relays and the direct path have nearly identical error probability performance; however, as SNR rises, diversity AF outperform the diversity DF and the direct path without a relay, with a difference in performance between diversity DF and direct path with diversity AF being approximately

37 dB and 51 dB respectively at BER  $10^{-3}$ . While diversity DF appear to perform better than the direct path with a difference of 14 dB at BER  $10^{-3}$ .

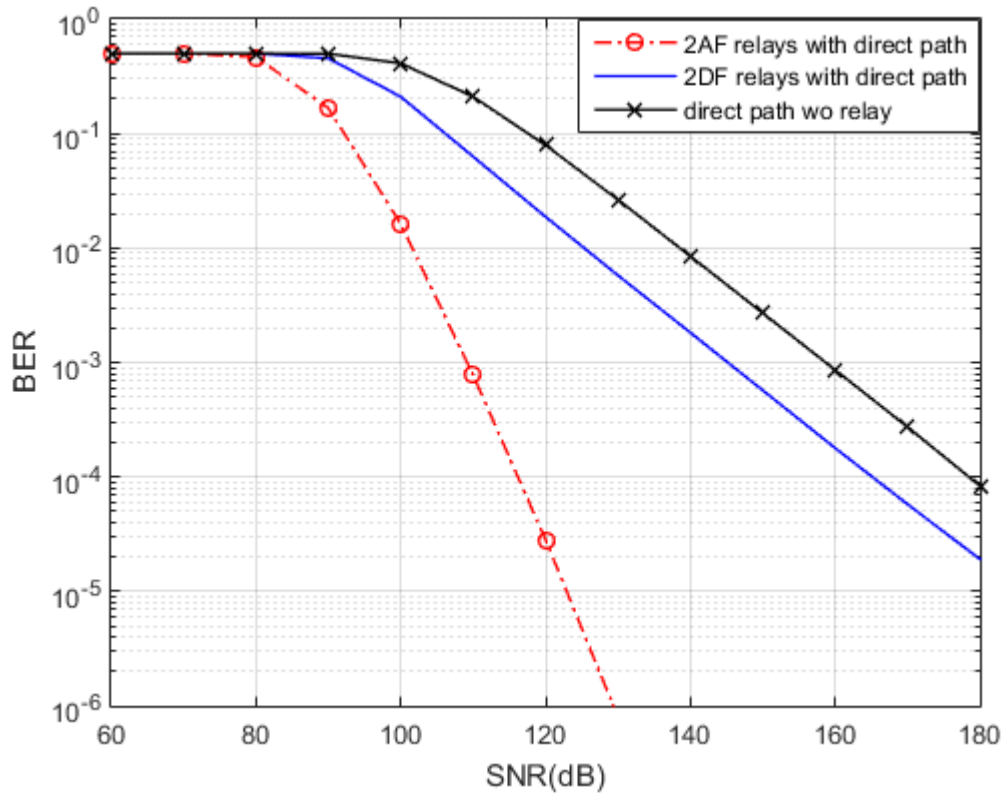


Figure 4.12 BER vs. SNR for cooperative relaying for mmWaves using two AF and DF relays in parallel with the direct path over 38 GHz frequency at a distance 200 m.

The comparison of the BER for two relaying protocols operating at 73GHz shown in Figure 4.13, where the FSPL ( $d_0 = 1m$ ), path loss exponent ( $n$ ), and shadow factor ( $\sigma$ ) are 69.7dB, 2.4, and 6.3dB, respectively.

The Figure illustrates that the three categories discussed previously have similar performance levels before 85 dB SNR; as SNR increases, the diversity AF outperform other types, with the performance differences are

roughly 33 dB and 51 dB at BER  $10^{-3}$ , respectively.

On the other hand, diversity DF have better performance than the direct path, and at BER  $10^{-3}$  the difference in performance is almost 18 dB.

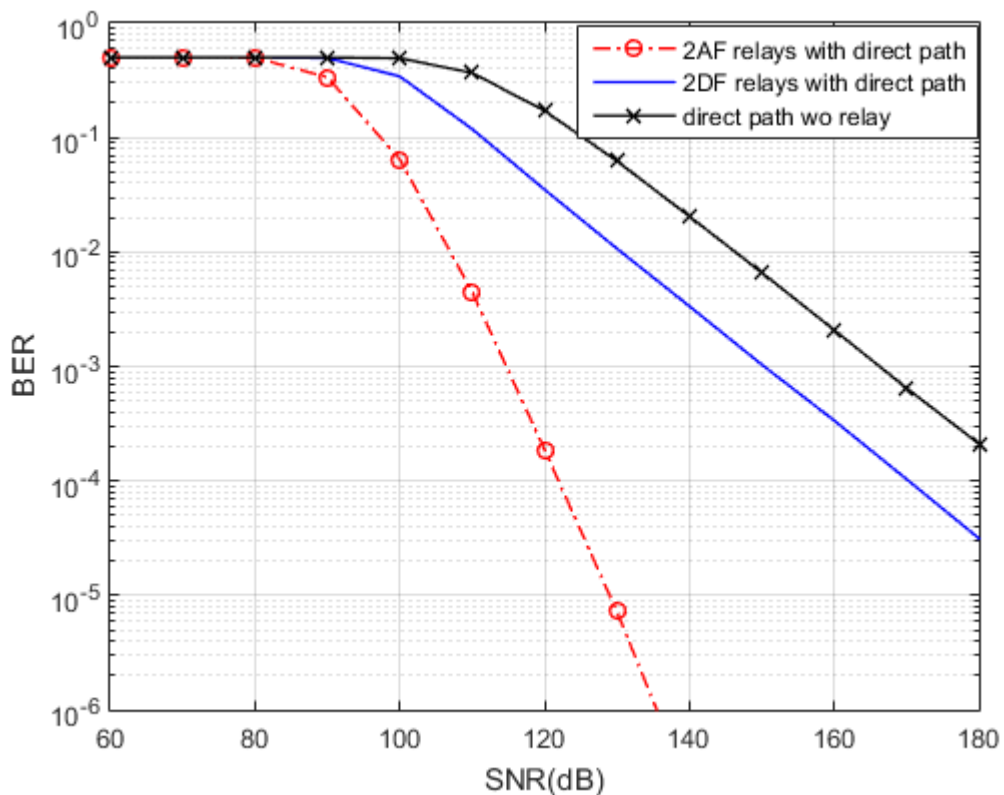


Figure 4.13 BER vs. SNR for cooperative relaying for mmWaves using two AF and DF relays in parallel with the direct path over 73 GHz frequency at a distance 200 m.

The error probability curves for two AF relaying protocols with the direct link increase with increasing frequency due to significant attenuation at high carrier frequencies, as illustrated in Figure 4.14. It demonstrates that the SNR about 98 dB, 110 dB, and 115 dB for the curves of 28GHz, 38GHz, and 73 GHz, respectively at BER  $10^{-3}$ . This indicates that the performance

of the 28 GHz frequency is superior to that of the other frequencies mentioned.

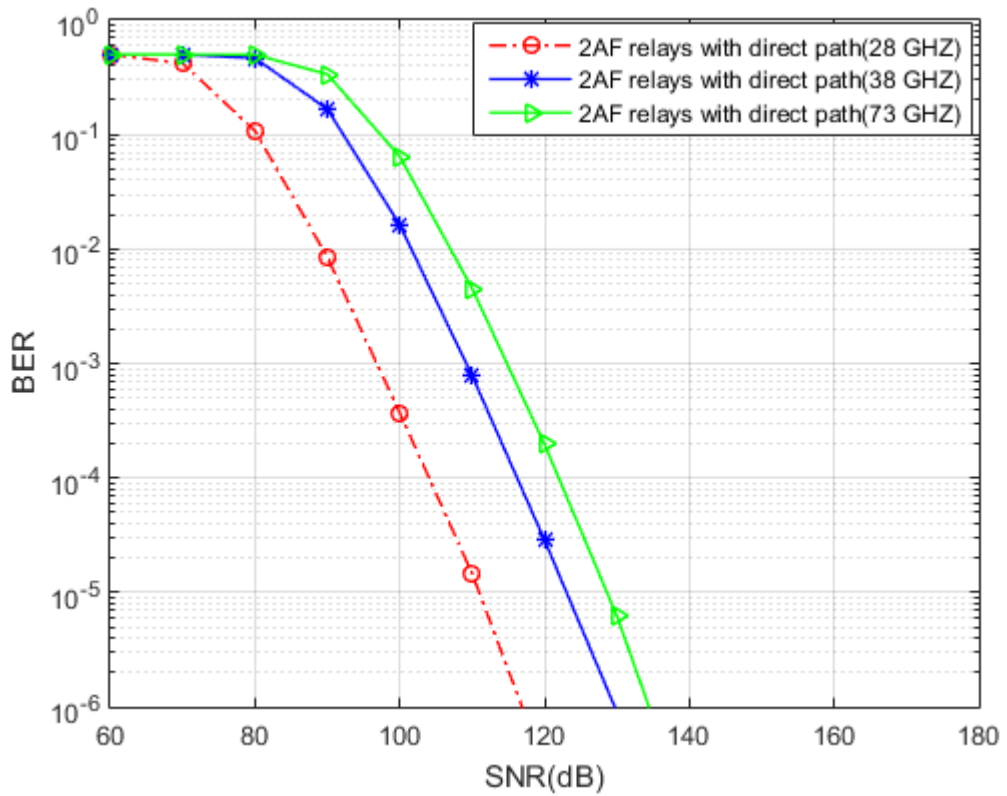


Figure 4.14 BER vs SNR for two AF relay with a direct path over different frequencies at a distance of 200 m.

Figure 4.15 compares the error probability performance of two DF relaying protocols with the direct path at the four frequencies stated. At BER  $10^{-3}$  the SNR values for all curves are 132 dB, 145 dB, and 150 dB.

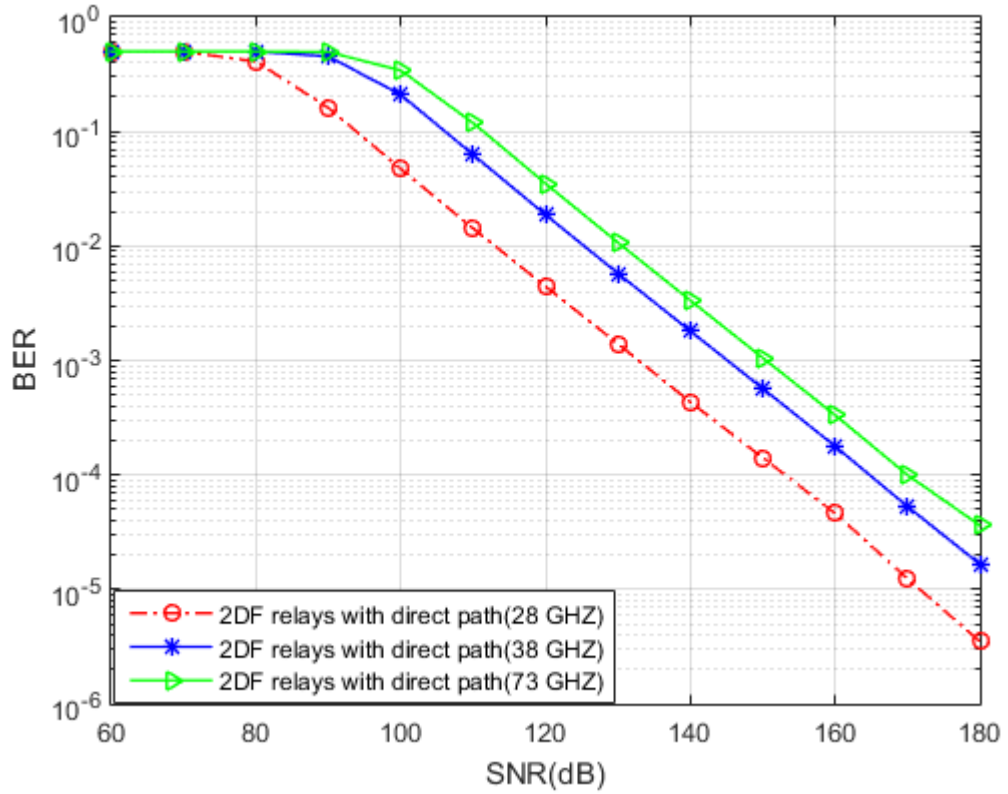


Figure 4.15 BER vs SNR for two DF relay with a direct path over different frequencies at a distance of 200 m.

Additionally, we compared the performance of low frequency (28 GHz) and high frequency (73 GHz) (i.e. the frequencies utilized in this work) in the outdoor environment at a distance of ( $r_{SD}$ ) 200 m to determine which one performs better in all cases. As seen in Fig. 4.16, the BER-SNR curves at 28 GHz are superior to those at 73 GHz for all cases. Moreover, it shows the difference in performance between 73GHz and 28GHz is approximately 19 dB at BER  $10^{-3}$  for the same type of relaying protocol (two AF relays with direct path).

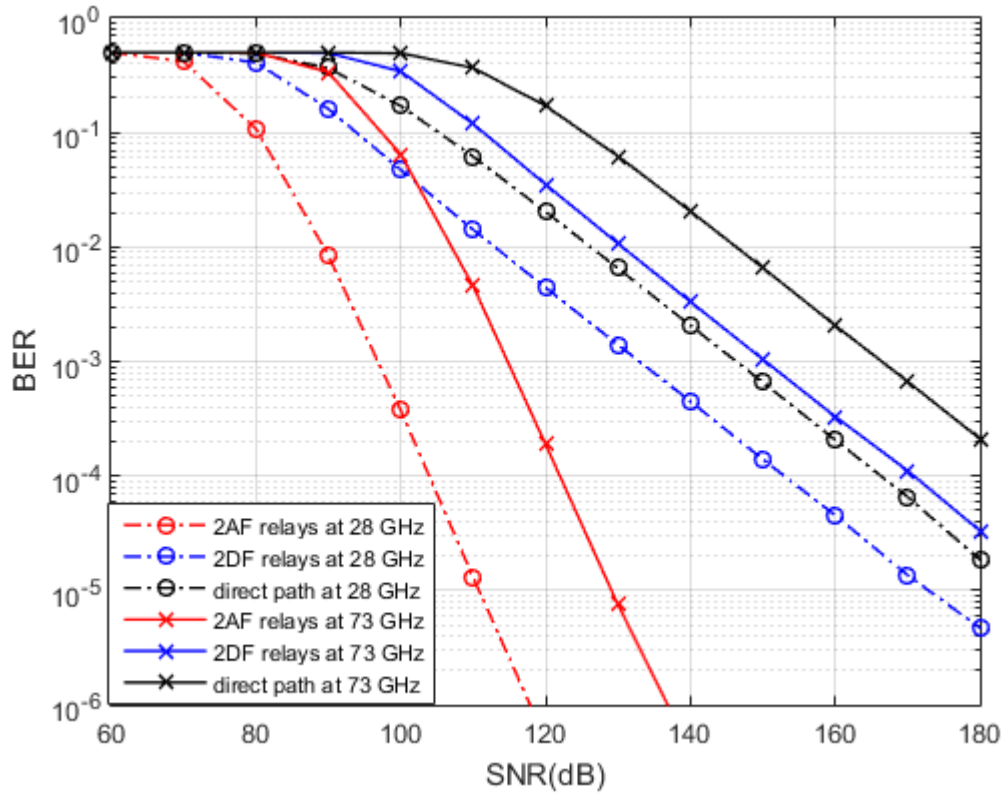


Figure 4.16 BER vs. SNR for cooperative relaying for mmWaves using two AF and DF relays with the direct path over 28 and 73 GHz at a distance 200 m.

The BER-SNR performance of cooperative communications systems operate at 28 GHz is illustrated in Figure 4.17 for source-destination separations of 100 meters and 200 meters. The figure shows that the error probability performance is better at 100 meters than at 200 meters. Additionally, the figure shows that all curves have similar performance before 60 dB SNR; then after this value, the curve of diversity AF for the distance 100 m outperforms the other curves. Also the difference in performance between the AF relays, DF relays, and direct path for the distance 200m and 100 is about 10dB, 14dB and 11dB respectively at BER  $10^{-3}$ .

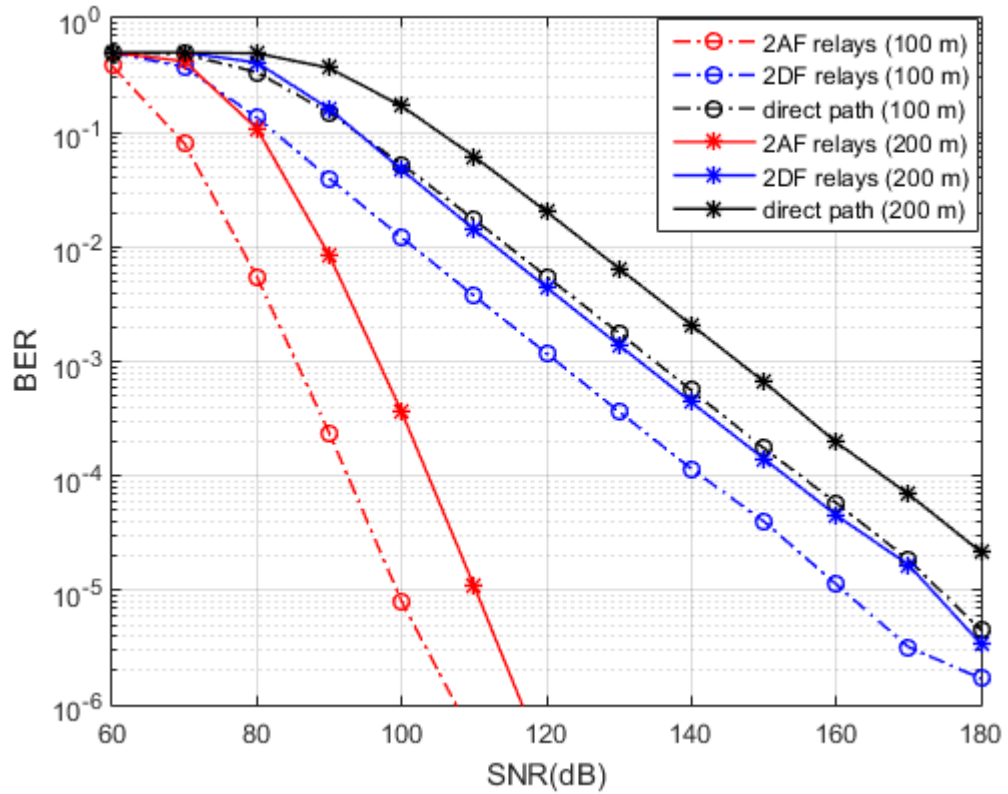


Figure 4.17 BER vs SNR for cooperative relaying for mm Waves using two AF and DF relays with the direct path over distance ( $r_{SD}$ ) 100 m and 200 m.

The previous data illustrate that, despite noise propagation, amplified relaying performs significantly better than decoded relaying, particularly in terms of diversity due to amplified and forward relaying with the direct path. This is a major and somewhat observation because amplified relaying channels do not suffer from the weakest-link problem that decoded relaying channels do, in which decoding problems on any single-hop spread along the channel.

#### **4.4 Comparison of the simulation results for the dual-hop systems that are using one and two parallel AF and DF relay over 28 GHz**

The error probability performance of the systems depicted in Figures 2.13 and 2.14, which consist of one AF and DF relays between the source and destination, have compared with those systems which are made up of two relays in parallel with the direct path shown in Fig. 2.15 and Fig. 2.16.

The distance between the source and destination is 200 meters, and the carrier frequency 28 GHz in both cases.

As shown in Figure 4.18, the error probability for the system with two AF relays with a direct path is better than those has one AF relay with the direct path due to the cooperative diversity; additionally, the DF relays in both schemes did not add valuable compensation to the signals comparing to the AF relay.

This is demonstrated by the curves, which show that the BER of two AF relays with a direct path is about  $10^{-3.6}$  at SNR 100 dB, whereas the BER of one AF relay with a direct path is  $10^{-2}$ ; and the difference in performance between one AF relay and two AF relays at BER  $10^{-3}$  is estimated to be approximately 13 dB.

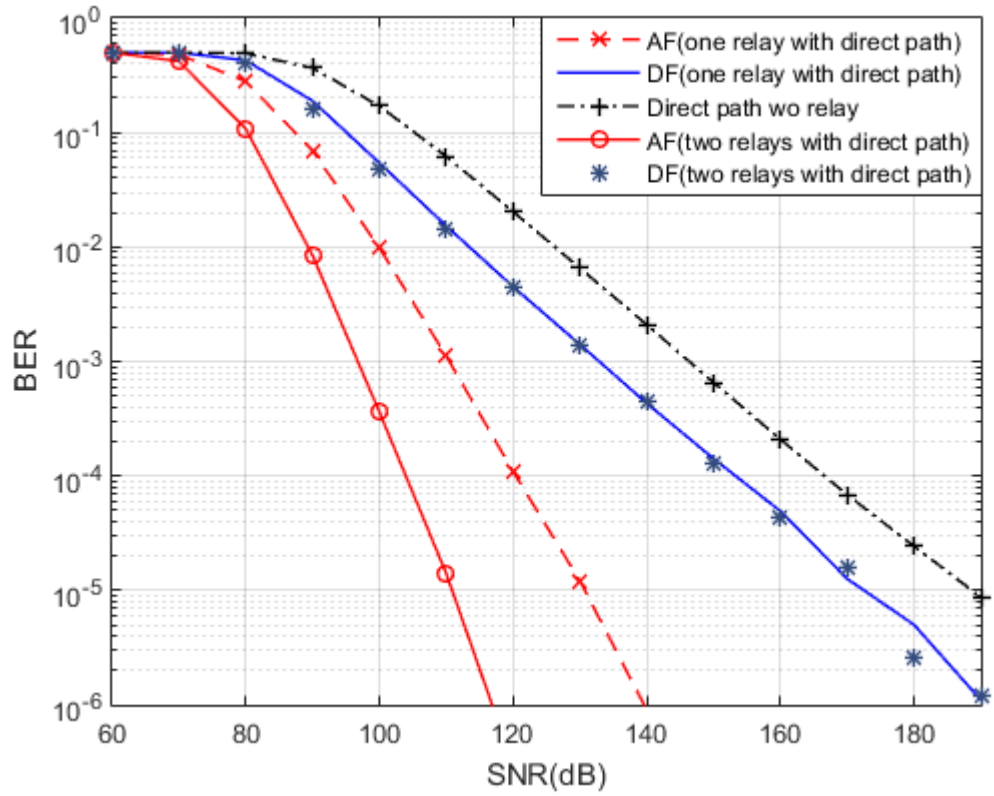


Figure 4.18 BER vs. SNR for cooperative relaying for mmWaves using one and two parallel AF and DF relays over 28 GHz in the presence of the direct path at a distance 200 m.

## Chapter Five

### Conclusions and Future Work

#### 5.1 Conclusions

In this dissertation, mmWave channels with different frequency bands have been investigated and characterized, in which the pass-loss inherent in these bands were calculated for channel modeling. Moreover, cognitive radio with two-way relaying networks (TWRN) has been considered and proposed over mmWave channels for the next generation of wireless communication. Furthermore, cooperative communications via relaying networks were considered in this thesis by assuming amplifying or decoding techniques, i.e. AF or DF relaying network. These mechanisms have been utilized to enhance the diversity gain and to overcome the degradation of signals due to the attenuation that has taken place in the mmWave bands.

The modulation scheme, which is considered in this research, was BPSK to represent the transmitted data over the assumed mmWave channels with different frequency bands, and in the presence of an additive AWGN channel.

Several simulations scenarios have been taken into account in this research, which was achieved by using Matlab programming, where the error probability represented by BER against different values of SNR showed outperforming of the AF relay comparing to DF type since the effect of error propagation in DF relay outweighs the noise amplification in the AF relaying mode. On the other hand, the capacity of the considered systems, in bit/sec/Hz, were evaluated and simulated, in which DF relay demonstrated better performance than AF type.

## 5.2 Future Work

Due to time constraints, the study undertaken and addressed in this thesis does not cover all facets of cooperative relaying for mmWaves systems, leaving the potential for more improvements and suggestions for future research. The following are possible extensions to this thesis work:

1. We would like to enhance our work in this field by implementing a dual-hop relay network using the compress-and-forward (CF) and Decode-Amplify and Forward (DAF) relaying protocols, rather than the AF and DF relays presented in this study.
2. Advanced modulation schemes such as Quadrature Phase Shift Keying (QPSK), Eight Phase Shift Keying (8 PSK), 16 Quadrature Amplitude Modulation (16 QAM), 64 Quadrature Amplitude Modulation (64QAM), would be used to get more realistic results and better performance.
3. The schemes described in this thesis have assumed a source node desiring to communicate with one destination node via a cooperative relay node. The issue can be generalized and extended to multi-user setups. This type of study would enable the system's throughput to be increased, which is a significant area of future research in real wireless systems.
4. Half-duplex transmission has been used in the proposed systems. While the usage of half-duplex enabled an examination of the cooperative scheme's performance, more studies can be conducted using the same system model with full-duplex capability.
5. It would be interesting to extend this study's research to multiple inputs multiple outputs (MIMO) systems rather than single input single output systems (SISO). Multiple-antenna relay systems can be used to take the advantage of the higher diversity. Therefore, this work

can be extended for multiple antennae in AF and DF relays cooperative systems to derive new exact expressions for the average error probability of the system.

6. In this work we have taken the effects of large-scale propagation fading on millimeter waves, it is possible in the future to take into consideration the effects of small-scale fading such as time dispersion due to multipath delays and random frequency modulation caused by the Doppler shifts on different signal versions. As well as the effects of rain, oxygen, and water vapor on mm-wave signals.

## References

- [1] R. Mesleh and A. Alhassi, *Space Modulation Techniques*. 2018.
- [2] G. Singh, “Generations of wireless Communications Technologies,” *Www.Academia.Edu*, 2016.
- [3] H. Elshaer, “Decoupled Cell Association Towards Device-Centric 5G Cellular Networks,” p. 188, 2017, [Online]. Available: <https://kclpure.kcl.ac.uk/portal/>.
- [4] S. Mondal, A. Sinha, and J. Routh, “A Survey on Evolution of Wireless Generations 0G to 7G,” *Int. J. Adv. Res. Sci. Eng.*, vol. 1, pp. 5–10, 2015.
- [5] A. Mathematics, “Analog wireless,” vol. 115, no. 6, pp. 427–435, 2017.
- [6] C. Diakhate, “Propagation channel modeling at centimeter – and – millimeter – wave frequencies in 5G urban micro – cellular context,” 2019.
- [7] S. Mukhopadhyay, V. Agarwal, S. Sharma, and V. Gupta, “A Study On Wireless Communication Networks Based On Different Generations,” *Int. J. Curr. Trends Eng. Res.*, vol. 2, no. 5, pp. 300–304, 2016.
- [8] T. S. Rappaport *et al.*, “Millimeter wave mobile communications for 5G cellular: It will work!,” *IEEE Access*, vol. 1, pp. 335–349, 2013, doi: 10.1109/ACCESS.2013.2260813.
- [9] B. Abdullah Al-mamun, S. Biswas, H. Bellal, and B. Saibba, “Past , Present and Future of Mobile Wireless Communication Past,” *IOSR J. Electron. Commun. Eng.*, vol. 12, no. 5, pp. 55–58, 2017, doi:

10.9790/2834-1205015558.

- [10] M. Telecommunication, “Guidelines for evaluation of radio Mobile Activites of ETRI interface technologies for,” vol. 1, pp. 1–55, 2009.
- [11] M. Sauter, *From GSM to LTE - Advanced Pro and 5G*. .
- [12] Z. Xiao, L. Dai, Z. Ding, J. Choi, P. Xia, and X. G. Xia, “Millimeter-wave communication with non-orthogonal multiple access for 5G,” *arXiv*, vol. 7, pp. 116123–116132, 2017, doi: 10.1109/access.2019.2935169.
- [13] M. De Ree, G. Mantas, A. Radwan, S. Mumtaz, J. Rodriguez, and I. E. Otung, “Key Management for beyond 5G Mobile Small Cells: A Survey,” *IEEE Access*, vol. 7, pp. 59200–59236, 2019, doi: 10.1109/ACCESS.2019.2914359.
- [14] M. H. A. Saada and R. A. Alhalabi, “Design of Efficient Millimeter Wave Planar Antennas for 5G Communication Systems المليمتر الأنظمة الجيل الخامس اتصالات تصميم هو اثبات ذات كفاءة على تردد موجات Assistant prof. of Electrical Engineering الج - امع — ”, 2017.
- [15] G. Gampala and C. J. Reddy, “Design of millimeter wave antenna arrays for 5G cellular applications using FEKO,” *2016 IEEE/ACES Int. Conf. Wirel. Inf. Technol. ICWITS 2016 Syst. Appl. Comput. Electromagn. ACES 2016 - Proc.*, pp. 6–7, 2016, doi: 10.1109/ROPACES.2016.7465426.
- [16] T. Kim, I. Bang, and D. K. Sung, “Design criteria on a mmWave-based small cell with directional antennas,” *IEEE Int. Symp. Pers. Indoor Mob. Radio Commun. PIMRC*, vol. 2014-June, no. September, pp. 103–107, 2014, doi: 10.1109/PIMRC.2014.7136141.
- [17] C. Seker, M. T. Guneser, and T. Ozturk, “A Review of Millimeter

- Wave Communication for 5G,” *ISMSIT 2018 - 2nd Int. Symp. Multidiscip. Stud. Innov. Technol. Proc.*, pp. 1–5, 2018, doi: 10.1109/ISMSIT.2018.8567053.
- [18] S. Kwon and J. Widmer, “Relay selection for mmwave communications,” *IEEE Int. Symp. Pers. Indoor Mob. Radio Commun. PIMRC*, vol. 2017-October, pp. 1–6, 2018, doi: 10.1109/PIMRC.2017.8292437.
- [19] N. Ojaroudiparchin, M. Shen, and G. F. Pedersen, “Multi-layer 5G mobile phone antenna for multi-user MIMO communications,” *2015 23rd Telecommun. Forum, TELFOR 2015*, no. November, pp. 559–562, 2016, doi: 10.1109/TELFOR.2015.7377529.
- [20] J. Lee, Y. Song, E. Choi, and J. Park, “MmWave cellular mobile communication for Giga Korea 5G project,” *2015 21st Asia-Pacific Conf. Commun. APCC 2015*, pp. 179–183, 2016, doi: 10.1109/APCC.2015.7412507.
- [21] T. S. Rappaport, G. R. MacCartney, M. K. Samimi, and S. Sun, “Wideband millimeter-wave propagation measurements and channel models for future wireless communication system design,” *IEEE Trans. Commun.*, vol. 63, no. 9, pp. 3029–3056, 2015, doi: 10.1109/TCOMM.2015.2434384.
- [22] R. W. Simons, “Guglielmo marconi and early systems of wireless communication,” *GEC Rev.*, vol. 11, no. 1, pp. 37–55, 1996.
- [23] O. Billström, L. Cederquist, M. Ewerbring, G. Sandegren, and J. Uddenfeldt, “Fifty years with mobile phones from novelty to no. 1 consumer product,” *Ericsson Rev. (English Ed.)*, vol. 83, no. 3, pp. 101–106, 2006.
- [24] E. G. Turitsyna and S. Webb, “Terahertz characterisation of building

- materials,” *Electron. Lett.*, vol. 41, no. 2, pp. 40–41, 2005, doi: 10.1049/el.
- [25] S. Geng, J. Kivinen, X. Zhao, and P. Vainikainen, “Millimeter-wave propagation channel characterization for short-range wireless communications,” *IEEE Trans. Veh. Technol.*, vol. 58, no. 1, pp. 3–13, 2009, doi: 10.1109/TVT.2008.924990.
- [26] V. K. Sakarellos, D. Skraparlis, A. D. Panagopoulos, and J. D. Kanellopoulos, “Optimum placement of radio relays in millimeter-wave wireless dual-hop networks,” *IEEE Antennas Propag. Mag.*, vol. 51, no. 2, pp. 190–199, 2009, doi: 10.1109/MAP.2009.5162063.
- [27] E. Torkildson, H. Zhang, and U. Madhow, “Channel modeling for millimeter wave MIMO,” *2010 Inf. Theory Appl. Work. ITA 2010 - Conf. Proc.*, pp. 300–307, 2010, doi: 10.1109/ITA.2010.5454109.
- [28] E. Torkildson, U. Madhow, and M. Rodwell, “Indoor millimeter wave MIMO: Feasibility and performance,” *IEEE Trans. Wirel. Commun.*, vol. 10, no. 12, pp. 4150–4160, 2011, doi: 10.1109/TWC.2011.092911.101843.
- [29] S. Akoum, O. El Ayach, and R. W. Heath, “Coverage and capacity in mmWave cellular systems,” *Conf. Rec. - Asilomar Conf. Signals, Syst. Comput.*, pp. 688–692, 2012, doi: 10.1109/ACSSC.2012.6489099.
- [30] M. R. Akdeniz *et al.*, “Millimeter wave channel modeling and cellular capacity evaluation,” *IEEE J. Sel. Areas Commun.*, vol. 32, no. 6, pp. 1164–1179, 2014, doi: 10.1109/JSAC.2014.2328154.
- [31] H. Abbas and K. Hamdi, “Full duplex relay in millimeter wave backhaul links,” *IEEE Wirel. Commun. Netw. Conf. WCNC*, no. Wcnc, 2016, doi: 10.1109/WCNC.2016.7565000.

- [32] S. Kwon and J. Widmer, "Relay selection for mmwave communications," in *IEEE International Symposium on Personal, Indoor and Mobile Radio Communications, PIMRC*, Feb. 2018, vol. 2017-October, pp. 1–6, doi: 10.1109/PIMRC.2017.8292437.
- [33] W. I. Kim, J. S. Song, and S. K. Baek, "Relay-assisted handover to overcome blockage in millimeter-wave networks," *IEEE Int. Symp. Pers. Indoor Mob. Radio Commun. PIMRC*, vol. 2017-October, pp. 1–5, 2018, doi: 10.1109/PIMRC.2017.8292574.
- [34] Y. Yan, Q. Hu, and D. M. Blough, "Path Selection with Amplify and Forward Relays in mmWave Backhaul Networks," in *IEEE International Symposium on Personal, Indoor and Mobile Radio Communications, PIMRC*, Dec. 2018, vol. 2018-September, doi: 10.1109/PIMRC.2018.8580768.
- [35] K. Belbase, C. Tellambura, and H. Jiang, "Two-Way Relay Selection for Millimeter Wave Networks," *IEEE Commun. Lett.*, vol. 22, no. 1, pp. 201–204, 2018, doi: 10.1109/LCOMM.2017.2759106.
- [36] K. Belbase, C. Tellambura, and H. Jiang, "Coverage, Capacity, and Error Rate Analysis of Multi-Hop Millimeter-Wave Decode and Forward Relaying," *IEEE Access*, vol. 7, pp. 69638–69656, 2019, doi: 10.1109/ACCESS.2019.2919099.
- [37] Y. Liu and D. M. Blough, "Analysis of Blockage Effects on Roadside Relay-Assisted mmWave Backhaul Networks," in *IEEE International Conference on Communications*, May 2019, vol. 2019-May, doi: 10.1109/ICC.2019.8761486.
- [38] M. Ibrahim, W. Hamouda, and S. Muhaidat, "Spectral Efficiency of Multi-Hop Millimeter Wave Networks Using NthBest Relay Routing Technique," *IEEE Trans. Veh. Technol.*, vol. 69, no. 9, pp. 9951–9959,

2020, doi: 10.1109/TVT.2020.3003867.

- [39] D. Singh, A. Chattopadhyay, and S. C. Ghosh, “Distributed relay selection in presence of dynamic obstacles in millimeter wave D2D communication,” *arXiv*, 2019.
- [40] M. Han, J. Du, Y. Zhang, X. Li, K. M. Rabie, and G. Nauryzbayev, “Efficient Hybrid Beamforming Design in mmWave Massive MU-MIMO DF Relay Systems with the Mixed-Structure,” *IEEE Access*, vol. 9, pp. 66141–66153, 2021, doi: 10.1109/ACCESS.2021.3073847.
- [41] G. Ancans, V. Bobrovs, A. Ancans, and D. Kalibatiene, “Spectrum Considerations for 5G Mobile Communication Systems,” *Procedia Comput. Sci.*, vol. 104, no. December 2016, pp. 509–516, 2016, doi: 10.1016/j.procs.2017.01.166.
- [42] T. S. Rappaport *et al.*, “Wireless communications and applications above 100 GHz: Opportunities and challenges for 6g and beyond,” *IEEE Access*, vol. 7, pp. 78729–78757, 2019, doi: 10.1109/ACCESS.2019.2921522.
- [43] Berenguer Antonio, “Analysis and design of efficient passive components for the millimeter-wave and THz bands,” no. May, 2017.
- [44] J. Wells, “Faster than fiber: The future of multi-G/s wireless,” *IEEE Microw. Mag.*, vol. 10, no. 3, pp. 104–112, 2009, doi: 10.1109/MMM.2009.932081.
- [45] M. G. Sidelel, “Simulation-Based Stochastic Blockage Model for Millimeter-wave Communication,” 2020.
- [46] H. Zhang, S. Venkateswaran, and U. Madhow, “Channel modeling and MIMO capacity for outdoor millimeter wave links,” *IEEE Wirel. Commun. Netw. Conf. WCNC*, pp. 8–13, 2010, doi:

10.1109/WCNC.2010.5506714.

- [47] I. A. Hemadeh, K. Satyanarayana, M. El-Hajjar, and L. Hanzo, “Millimeter-Wave Communications: Physical Channel Models, Design Considerations, Antenna Constructions, and Link-Budget,” *IEEE Commun. Surv. Tutorials*, vol. 20, no. 2, pp. 870–913, 2018, doi: 10.1109/COMST.2017.2783541.
- [48] R. Koirala, “Joint localization and communication in 5G millimeter Remun Koirala To cite this version : HAL Id : tel-02998404 Remun KOIRALA Fonctions conjointes de localisation et de communication,” 2020.
- [49] M. N. Ghani *et al.*, “Initial Beam Access Schemes for Millimeter Wave Cellular Networks by Mohammed Jasim A dissertation submitted in partial fulfillment of the requirements for the degree of Doctor of Philosophy Department of Electrical Engineering College of Engineering Univ,” 2018.
- [50] H. H. Abbas, “Beamforming Techniques for Millimeter Wave Relay Networks,” 2017.
- [51] S. Hur *et al.*, “Proposal on millimeter-wave channel modeling for 5G cellular system,” *IEEE J. Sel. Top. Signal Process.*, vol. 10, no. 3, pp. 454–469, 2016, doi: 10.1109/JSTSP.2016.2527364.
- [52] S. Deng, M. K. Samimi, and T. S. Rappaport, “28 GHz and 73 GHz millimeter-wave indoor propagation measurements and path loss models,” *2015 IEEE Int. Conf. Commun. Work. ICCW 2015*, pp. 1244–1250, 2015, doi: 10.1109/ICCW.2015.7247348.
- [53] S. Sun *et al.*, “Propagation path loss models for 5G urban micro-and macro-cellular scenarios,” *IEEE Veh. Technol. Conf.*, vol. 2016-July, no. May, 2016, doi: 10.1109/VTCSpring.2016.7504435.

- [54] M. Peter, “Measurement , Characterization and Modeling of Millimeter-Wave Channels : From 60 GHz to 5G,” 2017.
- [55] J. Kim, “Millimeter-wave (mmWave) radio propagation characteristics,” *Oppor. 5G Networks A Res. Dev. Perspect.*, pp. 461–479, 2016.
- [56] J. Kim and A. F. Molisch, “Quality-aware millimeter-wave device-to-device multi-hop routing for 5G cellular networks,” *2014 IEEE Int. Conf. Commun. ICC 2014*, pp. 5251–5256, 2014, doi: 10.1109/ICC.2014.6884155.
- [57] Y. Niu, Y. Li, D. Jin, L. Su, and A. V. Vasilakos, “A survey of millimeter wave communications (mmWave) for 5G: opportunities and challenges,” *Wirel. Networks*, vol. 21, no. 8, pp. 2657–2676, 2015, doi: 10.1007/s11276-015-0942-z.
- [58] M. Asshad, S. A. Khan, A. Kavak, K. Küçük, and D. L. Msongaleli, “Cooperative communications using relay nodes for next-generation wireless networks with optimal selection techniques: A review,” *IEEJ Trans. Electr. Electron. Eng.*, vol. 14, no. 5, pp. 658–669, 2019, doi: 10.1002/tee.22852.
- [59] R. Kumar and A. Hossain, “Survey on half- and full-duplex relay based cooperative communications and its potential challenges and open issues using Markov chains,” *IET Communications*, vol. 13, no. 11. Institution of Engineering and Technology, pp. 1537–1550, Jul. 16, 2019, doi: 10.1049/iet-com.2018.5823.
- [60] F. Gharari, T. M. C. Chu, and H. J. Zepernick, “Performance analysis of a piecewise-and-forward relay network on Rayleigh fading channels,” *2015, 9th Int. Conf. Signal Process. Commun. Syst. ICSPCS 2015 - Proc.*, no. March, 2015, doi: 10.1109/ICSPCS.2015.7391753.

- [61] G. D. Mandyam, “Third-generation cellular communications: An air interface overview,” *Mobile Communications Handbook, Third Edition*. pp. 429–450, 2017, doi: 10.1201/b12494.
- [62] X. Bao, J. Li, and ( Tiffany, “Decode-Amplify-Forward (DAF): A New Class of Forwarding Strategy for Wireless Relay Channels.”
- [63] J. Feldman, M. J. Wainwright, and D. R. Karger, “Using linear programming to decode binary linear codes,” *IEEE Transactions on Information Theory*, vol. 51, no. 3. pp. 954–972, 2005, doi: 10.1109/TIT.2004.842696.
- [64] M. M. Tahseen, “Analysis of OSTBC in Cooperative Cognitive Radio Networks using 2-hop DF Relaying Protocol,” *Network*, no. May, 2011.
- [65] T. Abadi, “DESIGN AND PERFORMANCE ANALYSIS OF COOPERATIVE RELAY SYSTEMS,” 2015.
- [66] P. Lu, *Decoding and lossy forwarding based multiple access relaying*. 2015.
- [67] I. Repository, “Novel transmission schemes for application in two-way cooperative relay wireless communication networks Novel Transmission Schemes for Application in Two-way Cooperative Relay Wireless Communication Networks,” 2019.
- [68] X. Wu *et al.*, “60-GHz Millimeter-Wave Channel Measurements and Modeling for Indoor Office Environments,” *IEEE Trans. Antennas Propag.*, vol. 65, no. 4, pp. 1912–1924, 2017, doi: 10.1109/TAP.2017.2669721.
- [69] N. A. Muhammad, P. Wang, Y. Li, and B. Vucetic, “Analytical Model for Outdoor Millimeter Wave Channels Using Geometry-Based

- Stochastic Approach,” *IEEE Trans. Veh. Technol.*, vol. 66, no. 2, pp. 912–926, 2017, doi: 10.1109/TVT.2016.2566644.
- [70] M. Kyrö *et al.*, “Measurement based path loss and delay spread modeling in hospital environments at 60 GHz,” *IEEE Trans. Wirel. Commun.*, vol. 10, no. 8, pp. 2423–2427, 2011, doi: 10.1109/TWC.2011.062211.101601.
- [71] V. Va, T. Shimizu, G. Bansal, R. H. J.-F. and T. in, and undefined 2016, “Millimeter wave vehicular communications: A survey,” *dl.acm.org*, Accessed: Jun. 04, 2021. [Online]. Available: <https://dl.acm.org/doi/abs/10.1561/13000000054>.
- [72] C. Hansen, “INDUSTRY PERSPECTIVES WIG Ig : Multi -G Gabit W Ireless C Ommunications in the 60 Gh Z B and,” no. December, pp. 60–61, 2011.
- [73] T. S. Rappaport, J. N. Murdock, and F. Gutierrez, “State of the art in 60-GHz integrated circuits and systems for wireless communications,” *Proceedings of the IEEE*, vol. 99, no. 8. pp. 1390–1436, 2011, doi: 10.1109/JPROC.2011.2143650.
- [74] Y. Tan and Y. Tan, “Statistical Millimeter Wave Channel Modelling For 5G and Beyond by,” no. December 2019, 2020.
- [75] T. Baykas *et al.*, “IEEE 802.15.3c: The first IEEE wireless standard for data rates over 1 Gb/s,” *IEEE Commun. Mag.*, vol. 49, no. 7, pp. 114–121, 2011, doi: 10.1109/MCOM.2011.5936164.
- [76] V. Lochan, M. Fakharzadeh, and S. Choi, “Wi-Fi on Steroids : 802.11 ac and 802.11 ad,” *IEEE Wirel. Commun.*, vol. 20, no. 6, pp. 30–35, 2013.
- [77] “Indoor Millimeter Wave MIMO.pdf.” .

- [78] “Channel Modeling for Millimeter Wave MIMO.pdf.” .
- [79] R. Mesleh and A. Alhassi, “SMTs for Millimeter-Wave Communications,” in *Space Modulation Techniques*, John Wiley & Sons, Inc, 2018, pp. 167–183.
- [80] A. N. Uwaechia and N. M. Mahyuddin, “A comprehensive survey on millimeter wave communications for fifth-generation wireless networks: Feasibility and challenges,” *IEEE Access*, vol. 8, pp. 62367–62414, 2020, doi: 10.1109/ACCESS.2020.2984204.
- [81] S. Hur *et al.*, “Wideband spatial channel model in an urban cellular environments at 28 GHz,” *2015 9th Eur. Conf. Antennas Propagation, EuCAP 2015*, pp. 1–5, 2015.
- [82] S. Nie, G. R. MacCartney, S. Sun, and T. S. Rappaport, “28 GHz and 73 GHz signal outage study for millimeter wave cellular and backhaul communications,” *2014 IEEE Int. Conf. Commun. ICC 2014*, pp. 4856–4861, 2014, doi: 10.1109/ICC.2014.6884089.

## الخلاصة

نظرًا لمتطلبات معدل البيانات العالية للغاية وندرة طيف نطاق الموجات الدقيقة ، فإن نطاق موجات المليمترية هو بديل محتمل لتلبية متطلبات معدل البيانات المرتفع في الشبكات اللاسلكية. إن توفر عرض النطاق الهائل هو الفائدة الأساسية للانتقال إلى ترددات موجات المليمترية. ومع ذلك ، بسبب خسائر الانتشار التي تحدث عند الترددات العالية ، من المعروف أن شبكات الموجات المليمترية لها مدى تغطية قصير. بعض الحلول المقترحة لمعالجة مشاكل الإرسال هي استخدام صفائف كبيرة ذات توجيه أكبر ، واستخدام خلايا أصغر ، واستخدام شبكات الترحيل التعاونية لجعل مسارات المليمترية تصل لمسافات أبعد وتجنب مناطق التظليل.

في هذه الرسالة ، تم النظر في شبكات الترحيل ثنائية الاتجاه واقتراحه عبر قنوات موجات المليمتر للجيل التالي من الاتصالات اللاسلكية. يتم التحقيق من نوعين من شبكات الترحيل ثنائية الاتجاه وهما الترحيل عبر تقنيات التضخيم وإعادة التوجيه وفك التشفير وإعادة التوجيه.

يتم فحص وتوصيف قنوات الموجة المليمترية ذات نطاقات التردد المختلفة ، حيث يتم نقل البيانات من المصدر إلى الوجهة عبر نظام الاتصال التعاوني هذا إما باستخدام مرحلات التضخيم وإعادة التوجيه أو فك التشفير وإعادة التوجيه. لتعزيز كسب التنوع والتغلب على خسارة المسير الموجودة في النطاق قيد النظر.

تُستخدم مخططات تشكيل مفتاح إزاحة الطور الثنائي لتمثيل البيانات المرسله في هذا المشروع عبر هذه القناة وفي وجود قناة غاوسية بيضاء مضافة.

يتم أخذ العديد من سيناريوهات المحاكاة في الاعتبار في هذا البحث ، والتي يتم تحقيقها باستخدام برمجة الماتلاب ، حيث يتم الحصول على معدلات خطأ البت وإنتاجية النظام مقابل القيم المختلفة لنسبة الإشارة إلى الضوضاء من أجل المقارنة بين هذين النوعين.

تُظهر النتائج تفوقًا في أداء مرحل التضخيم وإعادة التوجيه على مرحل فك التشفير وإعادة التوجيه في مقياس أداء احتمالية الخطأ بينما في مقياس الإنتاجية أو سعة القناة يكون الترحيل باستخدام تقنية فك التشفير وإعادة التوجيه أفضل من مرحل التضخيم وإعادة التوجيه.



### إقرار المشرف

اشهد بان الرسالة الموسومة ب " إستقصاء أداء الأجيال القادمة من الاتصالات اللاسلكية عبر قنوات الموجات المليمترية" تمت تحت اشرافي وهي جزء من متطلبات نيل شهادة الماجستير في هندسة الاتصالات.

التوقيع:

المشرف: أ.م.د. محمود أحمد محمود الزبيدي

أ.م.د. محمد عبدالرحمن أحمد الحبار

التاريخ: / / 2021

### إقرار المقيم اللغوي

اشهد بانني قمت بمراجعة الرسالة الموسومة ب " إستقصاء أداء الأجيال القادمة من الإتصالات اللاسلكية عبر قنوات الموجات المليمترية" من الناحية اللغوية وتصحيح ما ورد فيها من أخطاء لغوية وتعبيرية وبذلك أصبحت الرسالة مؤهلة للمناقشة بقدر تعلق الامر بسلامة الأسلوب وصحة التعبير.

التوقيع:

المقوم اللغوي:

التاريخ: / / 2021

### إقرار رئيس لجنة الدراسات العليا

بناء على التوصيات المقدمة من قبل المشرف والمقوم اللغوي أرشح هذه الرسالة للمناقشة.

التوقيع:

الاسم:

التاريخ: / / 2021

## إقرار رئيس القسم

بناء على التوصيات المقدمة من قبل المشرف والمقوم اللغوي ورئيس لجنة الدراسات العليا أرشح هذه الرسالة للمناقشة.

التوقيع:

الاسم:

التاريخ: 2021 / /

إستقصاء أداء الأجيال القادمة من الإتصالات

اللاسلكية عبر قنوات الموجات المليمترية

رسالة تقدم بها

ريام حافظ علي العشو

إلى

مجلس كلية هندسة الالكترونيات

جامعة نينوى

كجزء من متطلبات نيل شهادة الماجستير

في

هندسة الاتصالات

بإشراف

أ.م.د. محمود أحمد محمود الزبيدي

أ.م.د. محمد عبدالرحمن أحمد الحبار



جامعة نينوى

كلية هندسة الالكترونيات

قسم هندسة الاتصالات

إستقصاء أداء الأجيال القادمة من الإتصالات

اللاسلكية عبر قنوات الموجات المليمترية

ريام حافظ علي العشو

رسالة ماجستير علوم في هندسة الاتصالات

بإشراف

أ.م.د. محمود أحمد محمود الزبيدي  
أ.م.د. محمد عبدالرحمن أحمد الحبار